Etude théorique et expérimentale de transformations de phase par diffusion dans des aciers sous champ magnétique intense

Yudong Zhang

UNIVERSITÉ DE METZ

NORTHEASTERN UNIVERSITY

DISSERTATION

Presented at

University of Metz and Northeastern University

ZHANG Yudong

To obtain the doctor's degree of
University of Metz and Northeastern University

SPECIAL FIELD: Engineering Sciences
OPTION: Materials Science

Theoretical and Experimental Study on Diffusion-Controlled Phase Transformations in Steels under High Magnetic Field

Defended on the 7th of February 2004 in front of the jury:

G. CHALANT	Professor:	Science and technology Attaché French Embassy in China, Beijing	Reviewer
Z. Q. HU	Professor Academician:	Institute of Materials Research Chinese Academy of Sciences	Reviewer
C. ESLING	Professor:	Université de Metz, France	Supervisor
L. ZUO	Professor:	Northeastern University, PR China	Supervisor
X. ZHAO	Professor:	Northeastern University, PR China	Co-Supervisor
G. BECK	Research Director	CNRS, INPL, Nancy, France	Jury member
J. Z. CUI	Professor:	Northeastern University, PR China	Jury member
K. E. HENSGER	Professor:	SMS Demag Aktiengesellschaft, Germany	Jury member
M. J. PHILIPPE	Professor:	Université de Metz, France	Jury member

Laboratoire d'Etude des Textures et Application aux Matériaux CNRS UMR 7078
Ile du Saulcy 57045 Metz Cedex 1

谨以此论文献给我的家人！

七　绝

女儿留学

孤身飘扬西欧行，
异国寒窗索真经。
孜孜不倦高峰攀，
风雨过后现彩虹。

—— 父亲，张润秋，2004 年 2 月于沈阳

Dedication poetry by my Dear Father, ZHANG Runqiu, Shenyang, February 2004
(English translation)

Far away overseas, in a land of the West

Looking for the Truth and after this long quest

Overcoming the storm of tense difficulty

THERE came the rainbow fraught with serenity

Poème-dédicace de mon Cher Papa ZHANG Runqiu, Shenyang, Février 2004
(Traduction française)

Toute seule outremer, très loin en Occident

En quête de vérité, traversant les orages

Après toutes ces épreuves, ce labeur épuisant

L'arc-en-ciel apparut, la fin du pèlerinage

Contents

Abstract

In this work, the influence of magnetic field on phase equilibrium in Fe-C binary system is theoretically simulated. The new diffusion-controlled phase transformation characteristics occurring in a medium carbon content low alloyed steel, 42CrMo, under magnetic field is systematically studied experimentally and theoretically.

During simulation, the Weiss model is corrected by substituting the molecular field coefficient λ with a short-range-ordering coefficient valid around and above Curie temperature Tc, so that the accurate temperature variations of magnetization of ferrite are obtained. The calculated susceptibilities based on the corrected model are in good agreement with the measured ones at temperatures above T_C. The magnetic susceptibility of austenite is calculated on the basis of band model. The confusion in expressing the energy change resulted from the magnetic field is also clarified. The influence of magnetic field is introduced as an extra driving force. On this basis, the ferrite/austenite and austenite/ferrite phase equilibrium boundaries in Fe-C diagram under magnetic field are simulated. Results show that magnetic field can impose remarkable influence on phase equilibrium by enlarging the ferritic and shrinking the austenitic phase area, hence obviously enhance the Ae_3 temperatures of steels and shift the eutectoid point to the higher carbon concentration and higher temperature sides.

Magnetic field can considerably increase the amount of product ferrite and accelerate the transformation speed from austenite to ferrite. Finally, a fine, randomly distributed ferritic and pearlitic microstructure, with equilibrium amount of ferrite is obtained under a fast cooling rate (46°C/min) owing to the combination of the thermodynamic and kinetic effects. A new rapid annealing method under high magnetic field has been worked out and put forward.

The magnetic field can obviously lower the nucleation barrier of ferrite from austenite. Together with its kinetic effect, the high temperature nucleation of ferrite on austenite boundaries is dominant at a medium slow cooling rate (10°C/min). Together with the inhomogeneous deformation of previous hot rolling, a microstructure of aligned ferrite and pearlite distributed alternately along the hot rolling direction is obtained when the magnetic field is applied in the same hot-rolling direction.

During high temperature tempering, magnetic field can effectively prevent cementite from growing directionally along the martensite plate boundaries and the inner twin boundaries through increasing cementite/ferrite interfacial energy and magnetostrictive strain energy and hence shows an effect of spheroidization. Meanwhile, it obviously postpones the process of recovery of the matrix but shows no obvious effect on the orientation distribution of the 'distortion-free' regions. The influence of magnetic field on low temperature tempering is that it changes the precipitation sequence of transition carbides, which makes the relatively high temperature monoclinic χ-Fe_5C_2 carbide precipitate with a denser distribution and smaller sizes, instead of the normal orthorhombic η-Fe_2C carbide. As a result, the toughness of the material is increased by 9%.

Insight into the effects of magnetic field on diffusion-controlled phase transformations contributes to the development of this research area and is of both theoretical significance and technical interest.

Résumé

Dans ce travail, l'influence du champ magnétique sur l'équilibre de phase est théoriquement simulée dans le système binaire Fe-C. Les nouvelles caractéristiques de la transformation de phase diffusive se produisant sous champ magnétique dans l'acier, 42CrMo, à moyen carbone allié sont systématiquement étudiées du point de vue expérimental et théorique.

Au cours de la simulation, le modèle de Weiss est corrigé en substituant au coefficient moléculaire de champ λ un coefficient d'ordre à courte distance valide autour et au-dessus de la température de curie *Tc*, de sorte que les variations précises de la magnétisation de la ferrite en fonction de la température sont obtenues. Les susceptibilités calculées basées sur le modèle corrigé sont en bon accord avec celles mesurées aux températures au-dessus de *Tc* La susceptibilité magnétique de l'austenite est calculée sur la base du modèle de bandes. La confusion dans l'expression du changement d'énergie qui résulte du champ magnétique est également clarifiée. L'influence du champ magnétique est présentée comme une force d'entraînement supplémentaire. Sur cette base, les lignes d'équilibre α/γ et γ/α dans le diagramme de phase Fe-C sous le champ magnétique sont simulées. Les résultats prouvent que le champ magnétique peut imposer une influence remarquable sur l'équilibre de phase en agrandissant le domaine d'existence de la ferrite et en rétrécissant celui de l'austénite, par conséquent pour augmenter évidemment les températures Ae3 des aciers et pour déplacer le point eutectoïde vers les concentrations en carbone plus élevées ou les températures plus élevées.

Le champ magnétique peut considérablement augmenter la quantité de ferrite produite et accélérer la vitesse de transformation de l'austenite en ferrite. Enfin, une microstructure de ferrite et perlite fine et homogène au taux d'équilibre est obtenue avec une vitesse de refroidissement rapide (46 °C/min) grâce à la combinaison des effets thermodynamiques et cinétiques. Une nouvelle méthode de recuit rapide sous le champ magnétique a été développée et proposée.

Le champ magnétique peut manifestement abaisser la barrière de nucléation de la ferrite à partir de l'austenite. Avec son effet cinétique, la nucléation à hautes températures de la ferrite sur les frontières de l'austenite est dominante à un taux de refroidissement moyennement lent (10 °C/min). Avec la déformation inhomogène du laminage à chaud précédent, une microstructure de ferrite et de pearlite alignées et distribuées alternativement le long de la direction du laminage à chaud est obtenue quand le champ magnétique est appliqué dans la même direction que celle du laminage à chaud.

Pendant le recuit à hautes températures, le champ magnétique peut efficacement empêcher la croissance directionnelle de la cementite le long des frontières des platelets de martensite et des joints des macles intérieures en augmentant l'énergie interfaciale cementite/ferrite et l'énergie magnétostrictive et par conséquent démontrer un effet de spheroidization. En attendant, il retarde manifestement le processus de restauration de la matrice mais ne démontre aucun effet manifeste sur la distribution des orientations des domaines libres de distorsions de réseau. L'influence du champ magnétique sur le recuit à basse température modifie la séquence de précipitation des carbures de transition, ce qui provoque la précipitation du carbure monoclinique χ-Fe_5C_2 typique de températures relativement hautes avec une distribution plus dense et de plus petites tailles, au lieu du carbure orthorhombique η- Fe2C habituel. Ainsi la dureté du matériau est augmentée de près de 9%.

L'étude des effets du champ magnétique sur des transformations de phase diffusives contribue au développement de ce secteur de recherches et présente à la fois une portée théorique et un intérêt technique.

摘　　要

本文对 Fe-C 二元系统，磁场作用下的相平衡特点进行了理论模拟；对 42CrMo 中碳合金结构钢，磁场作用下的扩散型相变的新特点进行了系统的实验与理论研究。

在理论模拟过程中，对 Weiss 分子场模型进行了修正，在居里点附近及以上温度以短程有序参数替代原分子场系数，据此计算的铁素体的磁化率在居里温度以上与实测值十分吻合。以电子能带模型为基础，对奥氏体的磁化率进行了计算。此外， 对各种磁化能的混乱使用予以澄清。磁场对相平衡的影响以附加相变驱动力的形式引入。由此，模拟了磁场作用下，Fe-C 相图中$\alpha/\alpha+\gamma$和$\gamma/\gamma+\alpha$相界线的新位置。结果表明：磁场使铁素体区增大；奥氏体区缩小，致使钢的 Ae_3 温度升高，共析点移向高碳及高温区。

磁场可显著增加转变产物中铁素体的相对百分含量，加快奥氏体向铁素体的转变速度。即使是快冷时(46°C/min)，磁场的热力学与动力学作用的综合影响，使转变产物仍为平衡态的铁素体与珠光体，但组织更细小、弥散。据此，本研究首次提出了强磁场快速退火工艺方法，并已申请专利。

磁场可明显降低奥氏体向铁素体转变时的形核能垒、加快转变速度，因此，即使是中慢速冷却时(10°C/min)，铁素体形核仍然发生在高温。由于高温形核过冷度低，故此奥氏体晶界为形核的主要位置。加之该材料热轧成型时的不均匀变形，使奥氏体以粗、细晶区的形式沿轧制方向交替分布。于是，当磁场的施加方向与原轧制方向一致时，磁场与不均匀变形的共同影响使中慢速冷却后得到的铁素体晶核和珠光体晶团仍成链状沿磁场方向交替分布。

高温回火时，磁场可通过提高渗碳体/铁素体界面能及磁致伸缩应变能有效地防止渗碳体沿马氏体晶界及马氏体晶内孪晶界的定向生长，显示出较强的球化作用。与此同时，磁场可明显地抑制基体相的回复进程；但对回复过程中形成的‘无畸变’区的晶体取向无明显作用。

低温回火时，磁场明显地改变‘过渡’碳化物（transition carbide）的析出顺序，它使具有单斜结构的χ-Fe_5C_2 较具有正交结构的η-Fe_2C 先沉淀析出。χ-Fe_5C_2 的低温析出使其形核率升高，长大受到抑制，因此，最终得到的χ-Fe_5C_2 分布更弥散，尺寸更细小。最终导致材料的冲击韧性增加 9%。

磁场下的扩散型相变的探索与研究将会对材料科学领域的不断发展做出有益的贡献，既具理论研究价值，又有实际应前景。

Conversion factors for magnetic quantities

Magnetic term	Symbol	SI unit	CGS unit	Conversion factor
Magnetic induction	B	Tesla (T)	Gauss (G)	1 T=10^4 G
Magnetic field (force)	H	Am^{-1}	Oersted (Oe)	1 Am^{-1}=$4\pi\times10^{-3}$ Oe
Magnetization per unit volume	M	Am^{-1} or $JT^{-1}m^{-3}$	emu cm^{-3} or erg Oe^{-1} cm^{-1}	1 Am^{-1}=10^{-3} emu cm^{-3}
Magnetization per unit mass	σ	J T^{-1} kg^{-1}	erg Oe^{-1} g^{-1}	1 J T^{-1} kg^{-1}=1 erg Oe^{-1} g^{-1}
Susceptibility per unit Volume	κ	J T^{-2} m^{-3}	erg Oe^{-2} cm^{-3}	1 J T^{-2} m^{-3}= 10^{-6}ergOe^{-2} cm^{-3}
Susceptibility per unit Mass	χ	J T^{-2} kg^{-1}	erg Oe^{-2} g^{-1}	1J T^{-2} kg^{-1} =10^{-4} erg Oe^{-2} g^{-1}
Susceptibility per mole	χ_m	J T^{-2} $mole^{-1}$	erg Oe^{-2} $mole^{-1}$	J T^{-2} $mole^{-1}$= 10^{-1} erg Oe^{-2} $mole^{-1}$
Magnetic flux	Φ	Weber (Wb)	Maxwell (Mx)	1 Wb=10^8 Mx
Permeability of free Space	μ_0	H m^{-1}	G Oe^{-1}	H m^{-1}=$10^7/4\pi$ G Oe^{-1}
Bohr magneton	μ_B	=9.2732×10^{-24} J T^{-1}	9.2732×10^{-21} erg Oe^{-1}	

A=ampere; H=Henry=Newton/Ampere; Tesla=Weber/m^2; J=Joule. The symbols for the above magnetic terms from different references may be different but the units and the conversion factors remain the same.

Reference

J. Crangle, The Magnetic Properties of Solids, Edward Arnold (Publishers) Ltd., London, 1977, p. 16

Acknowledgments

This work is financially supported by the key project of National Natural Science Foundation of China (Grant No. 50234020), the National High Technology Research and Development Program of China (Grant No. 2002AA336010) and the TRAPOYT in Higher Education Institutions of MOE, P.R.C. The work also obtains the support from Chinese-French Cooperative Research Project (PRA MX00-03). I would like to give my sincere thanks to these institutions.

The work is completed in EPM Key Laboratory (Northeastern University), Ministry of Education, China and the Laboratoire d'Etude des Textures et Application aux Materiaux of Université de Metz, France. I would like to give my hearted thanks to all the members for their kind help. I am also grateful to the High Magnetic Field Laboratory for Superconducting Materials, Institute for Materials Research, Tohoku University for their kind offer for all magnetic field experiments in this study.

I would like to express my special thanks to Professor G. Chalant who is the specialist in mechanics and materials science and is currently the science and technology attaché at the French Embassy in Beijing for reviewing my dissertation. I would also like to express my special gratitude to Professor Z. Q. Hu, the member of Chinese Academy of Engineering, the expert at materials sciences, for reviewing my dissertation.

Professor Claude Esling, Professor Liang Zuo and Professor Xiang Zhao have given careful instructions to this work. Every progress in this work coagulated their care and enlightenment. They are learnt, modest, serious and kind supervisors. From them, I have not only learnt knowledge but also setup precise scientific attitude towards work and persistence to overcome difficulty. I would like to give my hearted acknowledgements to them.

I would like to express my special acknowledgements to Professor F. Wagner, the director of LETAM. He accepted me to his laboratory and have taken care of the progress of my study.

I would like to avail of this opportunity to give my special thanks to Professor Z. D. Liang, Professor A. Hazotte, Professor M. Humbert, Professor J. Z. Xu, Professor F. Wang, Senior Engineer G. Q. Chen, Associate Professor Y. H. Sha, Associate Professor Y. D. Liu, N. Bozzolo, N. Gey, A. Tidu, N. Maloufi, J-S Lecomte, C. Leruelle, A. Thil, N. Niclas, A. Henry and other related staff members in NEU and LETAM for their kind help for my study. I would also like to express my special thanks to Hudde for her kind offer of ab initio calculation for my work.

During my study, I have always received direct helps from my co-Ph. D and former Ph. D students. Dr C. S. He, Dr. Q. W. Jiang, Dr E. Suzon, Z. C. Hu, N. Dewobroto, S. R. Dey, B. Gardiola, L. Germain, G. Vincent, E. Lenarduzzi and other students, their kind care, selfless helps and deep friendship have made up of large part of the support to and enjoyment of my

study. I will cherish all of these deep in my mind.

I would also like to give my special thanks to Professor B. L. Wu, Associate Professor J. H. Shi, Engineer H. S. Wang, Associate Professor Y. H. Zhao, Q. H. Meng and other colleagues in Shenyang Institute of Aeronautical Engineering for their kind support and understanding to my Ph. D study.

Last, I would like to give my hearted thanks to all my family members for their deep understanding and hearted support to my live during my study.

Introduction

1. Outline

Efforts on understanding the origin of magnetism of matters and its mystical powers of force at distance have been made by mankind for over 2000 years. From puzzled, starting to learn, to establishing theory to explain it and to deliberately applying it to almost every area of science and technique, man has experienced a long and an uneven developing process. It first led to the compass in China 2200 years ago. Then came the electrical age marked by the first electrostatic generator in 1660 by Otto von Grericke. The quest to make clear the essence of magnetism certainly helped drive the development of electromagnetic devices and equipment. It was the work of Hans Christian Oersted, who demonstrated that electrical current generated magnetic field, and André-Marie Ampere, the discoverer of the solenoid, who established that magnetism was due to circulating currents, that the era of electromagnetism was born. Just as Brooks has summarized [1]: Magnetism has been a part of science and technology for over 2000 years and it remains today a critical component of scientific discoveries and the cornerstone of nearly all technologies.

As a new technique, magnetic field, now, has been applied to biology, chemistry, information, traffic and transportation, materials and metallurgy and many other areas. Especially, in recent 5 years, with the advances in superconducting materials manufacture and cryocooling technique, high magnetic field generating technique has made big break through which certainly provides plenty of opportunities for expanding scope and depth of many of magnetic field related researches. That can be easily perceived from the amount of scientific reports surging in all kinds of academic journals and conference proceedings. And then comes an impetus of even rapid and powerful development.

As an important branch of science, materials and metallurgy field did not let it wait and look upon, instead, made it one of the earliest ones to be actively involved in. Having gone through a development of nearly 50 years, electromagnetic stirring, inductive heating and electromagnetic casting have well been put into practice. Impulsive, pulsed and traveling-wave magnetic fields and magnetic current casting are in the ascendant, which represents that the application of magnetic field is showing a strong tendency of broadening and deepening its development scope.

In 1980s with the maturity of superconducting technique, the generation of direct current high magnetic field was available [2, 3]. Unlike common electromagnetic field that affects matters in a macroscopic scale, high magnetic field as a clean, non-contacting and powerful

source of energy can act on atomic behaviors, such as atom arrangement, matching and migration and thus exert powerful influence on microstructures and properties of materials. Initially, the purpose to introduce the energies of electricity and magnetism to materials treatment was to mitigate the restriction in producing high performance and high quality materials and it was first introduced to smelting and casting processes of metals. The large economic profits achieved stimulated the strong desire to apply electromagnetic energy to other materials processing processes. Encouraged by the achievements acquired in smelting and casting of metallic materials, more and more materials researchers have joined themselves into the attempts of applying magnetic field, especially high magnetic field, to solid state phase transformation area. With the widening and deepening of the research in this area, more and more new important phenomena have been spotted. Many transformations showed new behaviors and regulations.

2 Solid state phase transformations in magnetic field

2. 1 Introduction

For ferrous alloys with phase transformations, the final strengthening is resulted from the transformation from austenite to martensite. The amount of martensite obtained from the transformation directly affects the strengthening effect. As austenite is paramagnetic and martensite is ferromagnetic, the introduction of the applied magnetic field will certainly promote the transformation and, in turn, enhance the effect of strengthening. Therefore, applying magnetic field to heat treatment started from quenching process in the late 50s and the 60s last century [4-11]. The representative investigations were conducted by the research group of Sadovsky et al. [4-7]. They carried out a series of researches on the effect of magnetic field on martensitic starting point, the amount of martensite obtained and microstructure morphologies appearing during martensitic transformation in some ferroalloys. It was found that the magnetic field can obviously increase the transformation temperature and promote transformation amount. As there was no powerful superconducting magnet, the intensity of magnetic field obtained was limited and hence further investigations were restricted. Until 1980s with the progress in high field generating technique, study on this aspect started to go deeper and wider. Japanese researchers, Kakeshita et al. [12-26] carried out a relatively thorough researches on effects of composition, grain boundary, crystallographic orientation, Invar character, thermal elastic nature and magnetism of austenite on magnetic field induced martensitic transformation under high magnetic field. Many useful results were obtained on influence of magnetic field on *Ms* temperature, the

amount of martensite obtained, morphology and TTT diagram of the transformation. As there were technical difficulties in operation, the above researches mainly dealt with limited materials with ultra-low *Ms* temperatures. With further progress in cryocooling technique and manufacture of superconducting magnet, installation of high temperature heat treatment equipment inside superconducting magnet has been available. Therefore, researches on high temperature phase transformations under high magnetic field of more than 10 Teslas are possible. From 1990s, high magnetic field has been introduced into various solid-state phase transformations, such as transformation from austenite to ferrite and its reverse, recrystallization, and ordering transition. Many valuable microstructure phenomena and their evolution under magnetic field have been revealed. On the basis of experimental investigations, researchers have also been conducting theoretical simulation to describe quantitatively the effect of magnetic field. Now materials science research under high magnetic field is undergoing a new expansion both in developing new theory and technical applications.

2. 2 Martensitic transformation in magnetic field

2.2.1 Effect of magnetic field on the nature of martensitic transformation and its starting temperature *Ms*

Like temperature or pressure, the magnetic field is one of the important thermodynamic parameters that are used to change the internal energies of materials. In the case of transformation from austenite to martensite, the Gibbs free energy of martensite would be greatly lowered as it has higher magnetization compared with that of austenite. The latter is paramagnetic and its Gibbs free energy does not change much with the applied magnetic field. Therefore the ferromagnetic martensite becomes much more stable in the field. As shown in Fig. 1-1, since magnetic field lowers the Gibbs free energy of martensite G_α to G_α^M and that of austenite changes only a little from G_γ to G_γ^M, the equilibrium temperature of the two phases T_0 is thus be elevated to T_0^M and then the *Ms* will go up in the same direction. As the driving force of the transformation is determined by the Gibbs free energy difference between the two phases, the transformation can be greatly enhanced by the application of the magnetic field.

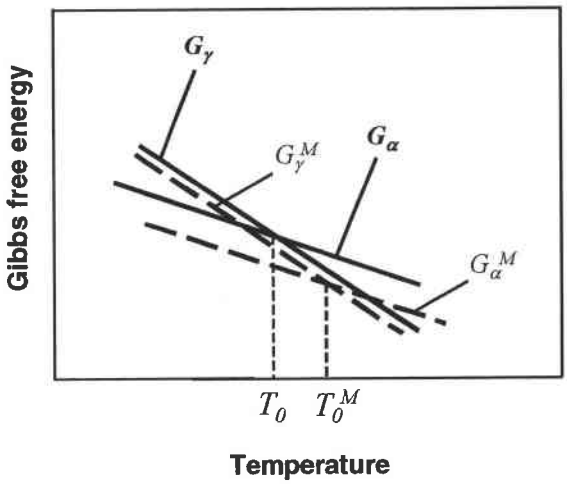

Figure 1-1 Changing of Gibbs free energy of austenite and martensite with temperature in the case without and with magnetic field, α – *martensite*; γ – *austenite*; M – *magnetic field*

Most early researches on field effects dealt with this issue. Bernshteyn et al. [8] applied a magnetic field of 4000 Oersted to the martensitic transformation in some iron-nickel-carbon steels and found the transformation was greatly accelerated which resulted in an increases of yield point of the steel by 10-15%. But they failed to observe the increase of *Ms* under the field and attributed it to the insufficiency of field strength to give perceptible effect on the transformation temperature. Estrin [9] investigated the influence of a pulsating magnetic field on different martensitic transformations with athermal and isothermal natures in Nickel steels and Fe-Ni-Mn alloys, respectively. They observe an average 6°C increase under a field of 18.6 k oersted and a sudden increase in the amount of athermal martensite in steels. The effect is that a magnetic field would shift the martensitic point and the entire martensitic transformation curve to a high temperature. But the result from the alloy with isothermal nature was different. Although there was also an increase of *Ms*, no sudden increase in the amount of martensite was spotted when the field was switched on, however, the rate of transformation was increased. These effects of magnetic field showed a completely thermodynamic nature of the influence on the transformation. Estrin [9] suggested that a pulsating magnetic field be successfully applied only to activate the martensitic transformation in materials with an athermal type of transformation at temperatures within the martensitic range or slightly above *Ms*. But the use of a pulsating field for materials with an isothermal martensitic transformation is not recommended. Similar results of enhancement of martensitic transformation by magnetic field were also found in other Fe-Ni alloys [4, 10]. There are also other researches conducted on the influence on magnetic field on reverse transformation from martensite to austenite [7] and transformation on tempering [8]. Results

showed that in both cases magnetic field can obviously slow down the decomposition of martensite. But the decomposition of retained austenite at high temperatures can be greatly accelerated, which further proved the thermodynamic nature of the influence of the field.

Krivoglaz et al. [5] conducted the thermodynamic analyses of the influence. They suggested that the effect of magnetic field on martensitic transformations be due only to the magnetostatic (Zeeman) energy. They proposed following formula to estimate the shift of *Ms*:

$$\delta T = \delta M \cdot H \cdot \delta V \cdot T_0 / q \tag{1-1}$$

where δM is the magnetization difference between the product and the parent phases, H the strength of applied magnetic field, δV volume change between the two phases and q the latent heat of transformation. The calculated shift of *Ms* for Fe-Ni alloys fitted well the experimental results [4, 6].

On this basis, Kakeshita et al. [12-26] have enlarged and deepened the scope of the research in this area since 1980s. They applied a pulsed magnetic field up to 31.75MA/m to the martensitic transformation in some ferroalloys. They noticed that there existed a critical strength of magnetic field to effectively induce martensitic transformation at the temperatures above *Ms*, and the higher the temperature was, the stronger the critical strength became. They also found that the experimentally measured increases in *Ms* temperature of the Fe-Pt ordered and disordered alloys [12, 25], Fe-Ni-Co-Ti thermoelastic alloy [13] and Fe-Ni alloys [14,16] were not in agreement with the calculated results using Krivoglaz's formula (Eq. (1-1)). They proposed a more accurate expression for the magnetic Gibbs free energy change by clarifying the unknown effects which Krivoglaz et al. did not find under low field as the high field susceptibility and forced volume magnetostriction effects and gave the estimation formula of the increase of *Ms* as follows [22]:

$$\Delta G(Ms) - \Delta G(Ms') = -\Delta M(Ms') \cdot H_c - (1/2) \cdot \chi_h^p \cdot H_c^2 + \varepsilon_0 \cdot (\partial w / \partial H) \cdot H_c \cdot B \tag{1-2}$$

in which $\Delta G(Ms)$ and $\Delta G(Ms')$ represent the difference in the Gibbs chemical free energy between the austenitic and martensitic phases at temperatures *Ms* and *Ms'* (*Ms'* the martensitic transformation start temperature under magnetic field) $\Delta M(Ms')$ the difference in spontaneous magnetization (magnetic moment) between the austenitic and martensitic states,

H the strength of magnetic field, H_c the critical magnetic field to induce martensitic transformation, χ_h^p the high field susceptibility of the parent austenite, ε_0 the transformation strain, $(\partial w / \partial H)$ the forced volume magnetostriction and B the bulk modulus. The relations between $\Delta Ms(=Ms'-Ms)$ and H_c have been calculated for Fe-Pt [12] alloys, Invar Fe-Ni [14], non-Invar Fe-Ni-C [15] and Invar Fe-Mn-C [17] alloys, which are in good agreement with the experimental ones, as shown in Fig. 1-2. The authors also clarified the influence of composition [14], grain boundaries, crystal orientations [16], Invar characteristics [15], thermoelastic nature [13, 25] and austenitic magnetism [20] on the magnetic field-induced martensitic transformations. Results showed that Eq. (1-2) suited well under the above conditions. Thus, the propriety of the newly derived equation is quantitatively verified.

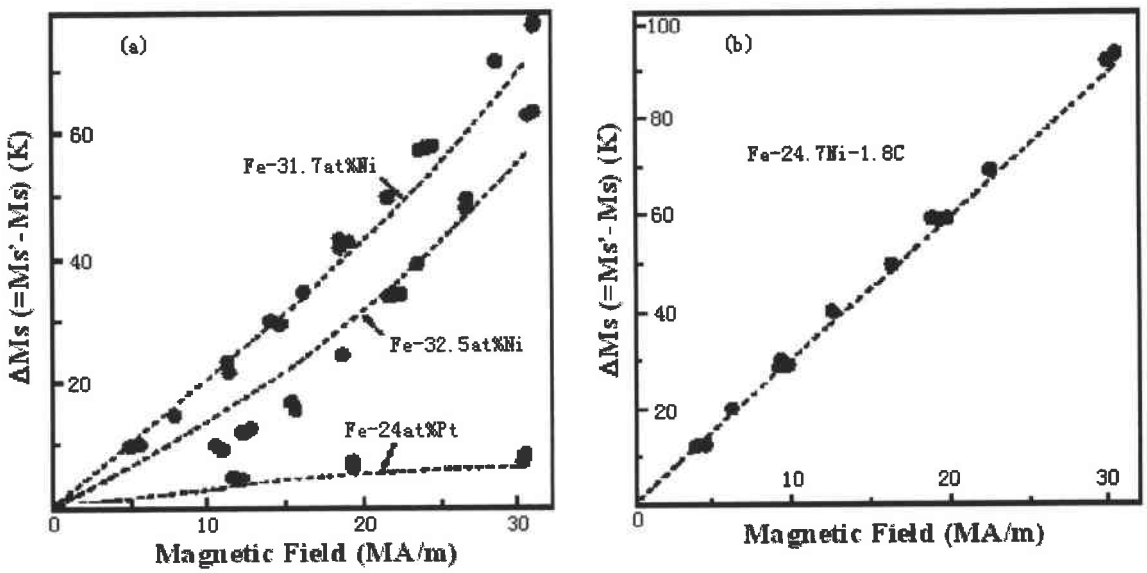

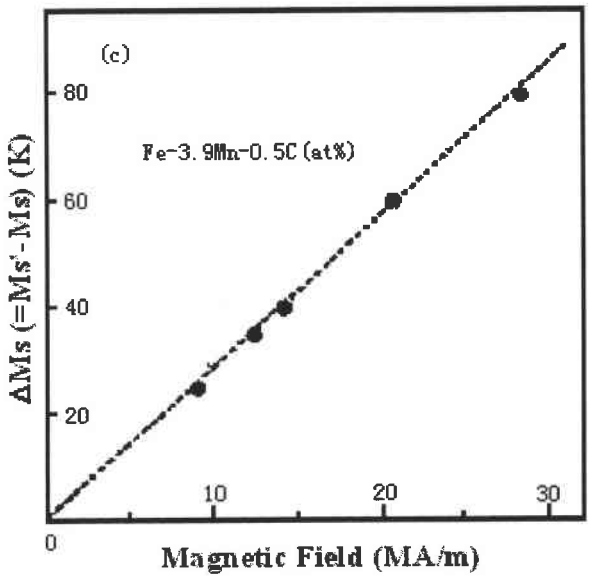

Figure 1-2 Comparison between calculated (dash line) and measured (dots) martensitic start temperature increase vs H_C for several ferroalloys [22]

They also tried to identify if there exists a maximum temperature above which martensite cannot be induced even though a magnetic field of any strength is applied. They found the third term on the right side of Eq. (1-2) is the controlling item. For different alloys, the energy due to the forced volume magnetostriction has either positive (Fe-Ni alloys) [14] or negative (Fe-Pt alloys) [12] volume change associated with the transformation and thus brings about an increase or a decrease to *Ms* temperature; while the other two terms in Eq. (1-2) are always positive and bring about increases to the *Ms* temperature. When the forced volume magnetostriction is negative, the increase of *Ms* temperature may possibly be saturated at certain *ΔMs*. However, when it is positive, under the field strength used in their researches, there was no evidence to show saturation and further investigation at higher field strength is needed.

2.2.2 Kinetics of martensitic transformation in magnetic field

It is known that there are two groups of martensitic transformations. One is athermal and the other is isothermal. The amount of martensite is only a function of temperature in the former group and a function of both temperature and time in the latter group. There has been a view that the isothermal transformation is rather general and the athermal one is its special case, considering that the incubation time needed for the athermal transformation might be

undetectably short. However, there is no direct proof of this idea. Aiming at clarifying this point, Kekeshita et al. [20] conducted the investigation on kinetics of martensitic transformation under static magnetic field. They identified that the isothermal kinetics of martensitic transformation was changed to an athermal one under magnetic field and proved that the equation to estimate the shift of *Ms* held for both situations. This suggested the difference between the athermal and isothermal kinetics be not intrinsic but could be explained by one basic rule. They also found [21] that the TTT diagram under static magnetic fields showed a C-shape, whose nose temperature was lower and incubation time was shorter, respectively, than those without the external field. Another characteristic feature was that the shifts of nose temperature and incubation time increase with increasing magnetic field as shown in Fig. 1-3. The results offered important information on the origin of martensitic transformation.

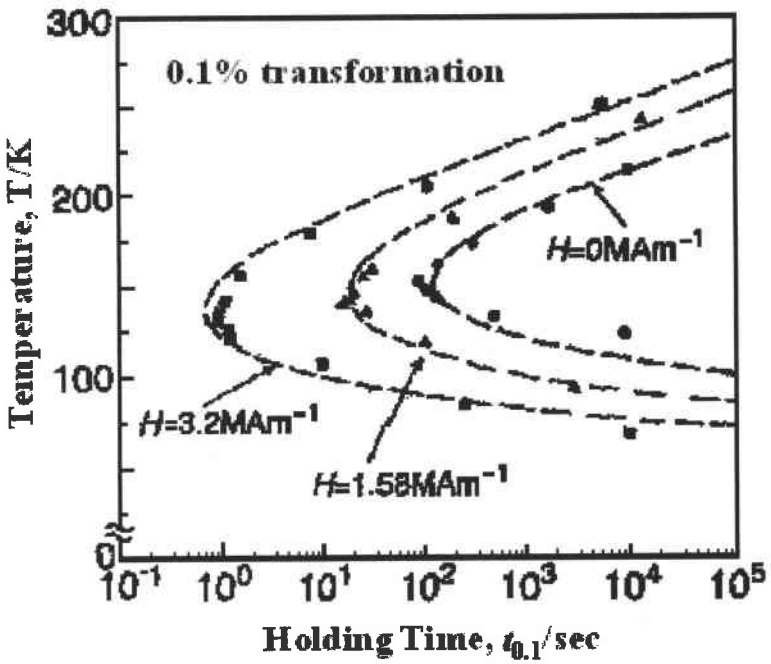

Figure 1-3 TTT diagrams of the isothermal martensitic transformation in an Fe-24.9Ni-3.9Mn (mass%) alloy under static magnetic fields [21].

2.2.3 The amount and morphology of the magnetic field-induced martensite

As magnetic field can greatly increase Gibbs free energy difference between austenite and martensite, the amount of transformation can also be affected since in most conventional treatment cases the transformation is not complete. However, the amount of magnetic field-

induced martensite with the strength of the magnetic field is different for thermoelastic and non-thermoelastic martensite. In the case of the former, the amount of magnetic field-induced martensite increased linearly with increasing strength of the magnetic field for any given $\Delta Ms\,(=Ms'-Ms)$ [11-14, 16, 24, 27]. The increase was due either to the growth of previously formed martensite [13] or to the formation of new martensite or to the both [17]. However, in the case of the latter, the amount was almost constant and did not increase, even if any magnetic field higher than the critical field was applied from the beginning [14, 16]. Kohno et al. [27] also observed no obvious change of the amount of martensite in an SUS3040L austenitic stainless steel after reheated even when a magnetic field of 26 T was applied and Shimozono et al. [28] found the amount of α' martensite reached saturation at a value lower than 10% by the application of magnetic field up to 26 T in an Fe-25.5%Ni-3-5%Cr austenitic stainless steel. Kurita et al. [29] conducted the investigation of the effects of magnetic field on the martensitic transformation amount in Fe-37.4wt.%Ni alloy, 304L and 316L stainless steels together with the effects of applied elastic stress and plastic deformation. However, in different materials the effects of the magnetic field showed different characters. They found that the amount of the deformation-induced martensite in 304L and 316L was obviously enhanced by the application of the magnetic field, while in Fe-37.4wt.%Ni alloy the increase was quite limited.

One positive application of the effect of field was to introduce high magnetic field into the transformation from paramagnetic γ-Fe_4N to ferromagnetic α'-$Fe_{16}N_2$ [30]. In that case magnetic field can greatly reduce the residual γ phase and make it possible to obtain balk α' phase, as the magnetization of iron-nitrides with bct structure has been debated for over 30 years due to difficulty of obtaining bulk single phase of either α' phase.

Besides, the influence of magnetic field on the morphology of martensite has been investigated in a variety of ferroalloys. Many studies showed that the morphology including the internal structures of the magnetic field-induced martensite was almost the same as that of the thermally induced one despite of the different formation temperatures and magnetic field strengths [12-25,30,31]. As the formation temperatures of magnetic field-induced martensite are different from those of thermally formed one, the fact is quite in contradiction to the viewpoint that the martensite morphology is determined by the formation temperature. Kekeshita et al. [16] also found that when the martensite was induced by magnetic field in single crystal Fe-Ni alloy, some matensite plates grew nearly parallel to the direction of magnetic field and ran through from one end to the other of the crystals. The reason for the

formation of directionally grown martensite was not clear and they thought it might be related to the shape magnetic anisotropy energy.

Thus with the new phenomena appearing during martensitic transformation under magnetic field, traditional martensitic transformation theory is facing new challenges and the study of martensitic transformation under magnetic field is surely helpful of clarifying vagueness in the old theory and drive it to a further development.

2. 3 Diffusion-controlled phase transformations in magnetic field

As magnetic field acts as a thermodynamic variable, it surely exerts considerable influence on high temperature phase transformations from FCC to BCC structure in Fe-base alloys. This is also due to the large difference in magnetization between the parent and the product phase. Magnetic field offers a unique opportunity to study the thermodynamics, kinetics and nucleation and growth behaviors of those transformations.

2.3.1 Phase equilibrium

The influence of magnetic field on phase equilibrium is expressed as the changing of transformation temperature. Initially, Ghosh et at. [32] studied the effect of thermomagnetic treatment on transformations in steels in relation to their TTT diagram. They proposed a thermodynamic equation to describe transformation temperature increase from austenite γ to ferrite α:

$$\frac{dT_0}{dH} = \frac{I^{\alpha} T_0}{q} \tag{1-3}$$

where H is the strength of magnetic field, q latent heat of the transformation, T_0 the equilibrium transformation temperature and I^{α} magnetization of α phase. The equation is approximate and applicable only in low field situation as it neglects the magnetization of γ phase considering that when weak field is applied, the magnetization of γ phase is very small. But in the case of application of high field, the situation would be quite different. In addition, a more systemic study on the effect of field with changing composition is also necessary.

In late 1990s and early 2000s, researchers from Korea and Japan started to study the effects of high magnetic field on phase equilibrium in Fe-C system [33, 34] and further in Fe-C-X(alloy) systems [33] in a more detailed way, since the calculations associated with the

change of phase diagram by field are very important in instructing the practical heat treatment processes from the viewpoint of thermodynamics as well as kinetics.

Magnetic field is considered to affect the Gibbs free energy of a material depending on its magnetization behaviors. The Gibbs free energy, associated with field can be expressed in terms of the magnetization M and the magnetic field strength H :

$$G_M(T,H) = \int H dM \tag{1-4}$$

or

$$G_M(T,H) = -\frac{1}{2}\chi H^2 \tag{1-5}$$

where χ is magnetic susceptibility. Eq. (1-4) is for ferromagnetic state and Eq. (1-5) for paramagnetic one. The key parameters in the above equations are M and χ. In the case of Fe-C system, the parent austenitic phase is always paramagnetic in temperature range concerned, χ was simply determined by fitting the susceptibility data to the Curie-Weiss law in [33]. However, for ferritic product phase, since it undergoes a magnetic transition from ferromagnetic state to paramagnetic state, the determination of its M or χ is quite difficult because so far no models can offer reasonable mathematical equations to calculate temperature variation of M or χ around Curie temperature. To obtain accurate values of M is the difficulty of this issue. Considering that the magnetic moment of ferrite is not linear and the magnetic susceptibilities from the Curie-Weiss equation disagree with experimental data near the Curie point, Joo and Kim et al. [33] used the magnetization determined by the Weiss theory rather than the susceptibility to calculate the Gibbs free energy of ferrite. They carried out the integration of Eq. (1-4) from $M-H$ curves at each temperature to yield the magnetic Gibbs free energy of ferrite as a function of applied magnetic field and then fitted the magnetic Gibbs free energy again as functions of temperature at some given strengths of field. This treatment by pure mathematical fitting is, to some extent, accurate but it failed to elucidate the physical relationships among M, H and temperature. Moreover, at each value of field strength, there is one set of coefficients for equations above and below the Curie temperature. The prediction of the magnetic Gibbs free energy at any field strength is not obtainable; therefore the application of this study is much more restricted. It is, nevertheless,

the first attempt to simulate the phase diagram under magnetic field. They obtained useful information of the influence of applied field on phase equilibrium in Fe-C system. Results showed that Ac_3 line moves to the higher temperature or higher carbon content side but Ac_m temperature remains unaltered. In this way, both the eutectic temperature and composition are increased, as shown in Fig. 1-4.

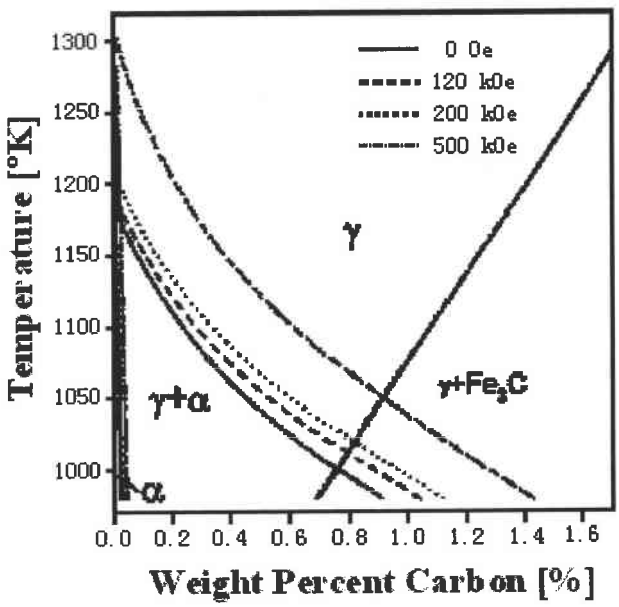

Figure 1-4 Fe-C phase diagram associated with the γ/α and γ/Fe_3C transformation under magnetic field [33]

From these results one can predict that as imposing magnetic field changes the equilibrium temperature and composition of the transformation, it can be applied to control microstructure. In addition, the possibility of improving mechanical properties may be realized from the eutectoid composition shift. Usually, the way to strengthen Fe-C materials is to increase their carbon content but it may also increase the amount of hypereutectoid cementite and create brittleness. Since external magnetic field enables to increase carbon content without hypereutectoid transformation, it may improve mechanical properties.

Guo and Enomoto [34] also conducted the study of effect of high magnetic field on the free energy and equilibrium of ferrite and austenite in Fe-C system and further enlarged it to Fe-C-Si and Fe-C-Mn systems. The magnetic partial molar free energy was calculated from Weiss molecular field theory and that of an alloying element was also evaluated in the framework of the Weiss theory by taking into account the influence of the alloying element on

the Curie temperature and the magnetic moment of iron solid solution. Their results showed that the ferrite to austenite transformation temperature is raised 1-3°C per Tesla depending on the alloy composition and the intensity of applied field, whereas the austenite to δ phase transformation temperature is lowered about 0.4°C per Tesla. They predicted that at about 100 Teslas α-Fe would directly transform to δ-Fe without going through γ-Fe stable range.

The study of [34] under discussion is based on Weiss molecular field model at all the temperatures considered and it is known that Weiss model obviously underestimates the magnetization at temperatures above the Curie point. The results are approximate to a large extent. Also the acceptance of materials to field, i.e., saturation of magnetization should be considered. Equilibrium behaviors at extreme high intensity of field, say, 100 Teslas, needs to be studied carefully.

2.3.2 New microstructure characteristics in magnetic field

Experimental studies have revealed that transformations between austenite and ferrite in steels have shown many new microstructure characteristics. In late 1970s, Pustovoit and Yu [35] applied a field of 1.2 T during the austenite decomposition in high carbon steels and found that the amount of ferrite was increased. Palmai [35] found that a magnetic field of 0.45 T retarded the inverse transformation in a 0.6%C (wt%) steel. Peters and Miodownik [36] observed that the phase equilibrium boundary between the austenite and ferrite of Fe-Co alloy was shifted to a higher temperature. Ghosh et at. [32] found that magnetic field can obviously accelerate the isothermal transformations from austenite to pearlite and bainite in high carbon high chromium AISI D_3 steel. Recently, the influence of a strong magnetic field of 7.5 T on the kinetics of proeutectoid ferrite transformation in Fe-C base alloys was investigated [37], and it was clarified that a magnetic field accelerates the transformation below and also above the Curie temperature.

Another important microstructural feature occurring during transformations between austenite and ferrite in steels is alignment. The first observation of aligned microstructures was made on Fe-0.1%C and Fe-0.6%C alloys undergoing ferrite to austenite transformation in a magnetic field of 8 T [38-40]. The microstructures are chains or columns of the austenite developed along the magnetic field in the matrix of ferrite. The authors attributed the alignment to anisotropic dipolar interactions between pairs of the paramagnetic austenite grains which were regarded as magnetic holes. Shortly after that H. Ohtsuka et al. [41] found the alignment of ferrite grains along the direction of applied magnetic field in austenite to

ferrite transformation during slow cooling in Nb alloys under a magnetic field of 10 T. They found that each ferrite grain was elongated and these grains were distributed head to tail along the direction of magnetic field. Enlightened by the phenomenon, M. Shimotomai et al. [35] further designed an experimental setup to study the magnetic alignment. The concept is characterized by deforming steels prior to the austenite to ferrite transformation to introduce ample nucleation sites in addition to applying magnetic field up to 12 T. Aligned two-phase microstructures with elongated ferrite grains along the applied field direction was found. Further theoretical analysis showed that the shape of the aligned ferrite grains is determined by a balance of the magnetostatic and the interfacial energies.

Research on effect of magnetic field, especially high field, on high temperature phase equilibrium and phase transformation is a new area in this field. It is still in its initial stage. Reports on this aspect are quite limited. As the basic theory of magnetism fails to give accurate description of magnetic property changes with temperature, especially the unclearness magnetic behaviors of materials around the Curie point under high magnetic field, it brings in uncertainties to the quantitative explanation of the effect of magnetic field and makes the uncovering of its influential mechanisms difficult.

2. 4 Recovery and recrystallization in magnetic field

Efforts [42-47] were also made to investigate effects of the magnetic field on the recover and recrystallization behaviors in deformed ferromagnetic alloys, especially, on recrystallization texture and GBCD, because the magnetic annealing was expected to offer a useful means to obtain the predetermined texture being applicable to improve the mechanical properties. In such a case, there is no crystal structure change during the transformation, therefore the thermodynamic influence of magnetic field takes another form instead of introducing extra magnetic Gibbs energy difference between the initial and final states.

Martikainen and Lindroos [44] first conducted investigation of effects of magnetic field on the recrystallization behaviors in a cold deformed Armco iron and obtained much useful information. They found magnetic field can obviously retard the process of recrystallization. Under the same heat treatment condition, the field treated specimens were in their recovery stage; while the non-field treated specimens were already in their recrystallization stage with only restricted region of recovery. They assumed that a magnetically ordered state induced by magnetic field might affect the grain boundary migration and grain growth during magnetic field annealing since the diffusion of ferromagnetic materials depends on the degree of magnetic order. In addition, the domain walls themselves could act as barriers to grain

boundary migration. Therefore, the recrystallization may be retarded. Texture analyses revealed that the field also had strong influence on texture evolution in this material. In the as cold-rolled state, the texture components were: {112}<110>, {111}<110> and {111}<112>. When treated without the field, the {111} component became favored, whereas when treated with the field, {100} component was increased. The enhancement of <100> was related to magnetic anisotropy. As the changes of magnetic field free energy (ΔG) affecting grains with <100>, <110> and <111> directions parallel to the direction of the magnetic field is in following sequence:

$$| \Delta G_{<001>} | > | \Delta G_{<110>} | > | \Delta G_{<111>} |$$

therefore, the nuclei with the <100> direction parallel to the magnetic field direction had the largest driving force for recrystallization.

Watanabe et al. [45] further carried out the study on effect of high magnetic field on grain-boundary character distribution (GBCD) in cold-rolled Fe-9%Co alloy, aiming at obtaining basic knowledge and to develop a technique for producing high-performance materials by grain-boundary design. They found that magnetic field had great influence on Grain-boundary type and frequency. For ordinarily annealed specimens, the frequency of low-angle boundaries and of coincidence boundaries tends to be decreased systematically as recrystallization proceeds with increasing annealing time and temperature in the ferromagnetic region below the Curie temperature but the frequency of high-angle random boundaries tends to be increased as recrystallization proceeds. However, for magnetically annealed specimens, in the ferromagnetic region, the frequency of low-angle boundaries was increased up to 7.8% with the increase of the magnetic field strength, being 3-4 times larger than the prediction for a random polycrystal. They attributed the above results to the retardation of recrystallization by field. They agreed with the ideas put forward by Martikainen and Lindroos et al. But they also noticed that the specimen annealed magnetically at paramagnetic temperature had the highest frequency of occurrence of high-angle random boundaries among all the specimens used in their work, however the reason remained unclear.

Masahashi et al. [46] found the similar phenomena of enhanced <001> texture component and high frequency of occurrence of low angle and coincidence boundaries in a magnetic annealed Fe-3.25%Si. From microstructural observation, they found irregularly shaped large

grains appeared in the magnetic annealed specimen hence suggested that in the magnetic annealed specimens grain coalescence mechanism operate extensively, as the frequency of occurrence of low angle boundaries was high. In their study, some results indicated that the magnetostriction was responsible for the orientation selectivity to favor the recovery and recrystallization of <001> grains that had the highest magnetostriction in the direction of magnetization under the applied high magnetic field. Therefore, they suggested another explanation of the retardation effect of magnetic field on recovery and recrystallization, that was a magnetostriction dependent influential mechanism, as the highest strain occurs along the <001> axis in silicon iron. He et al. [47] also observed the similar influence of the magnetic field on the recrystallization progress and texture evolution phenomena in a cold – rolled IF steel.

Unfortunately, little has been known about the effects of magnetic order, domain wall and magnetostriction on grain nucleation, grain growth and grain-boundary migration. So far there has not yet been direct proof to show the above effects. Moreover, recrystallization itself shows versatile characteristics in different materials. Further studies on this topic are still needed.

On the other hand in other non-ferromagnetic materials with low crystal symmetry, the influence of magnetic field seems relatively easy to identify. Molodov and coworkers [48, 49] have successfully distinguished the role of magnetic field in texture evolution, grain boundary migration and reorientation in diamagnetic polycrystalline Zinc alloy and Zinc bicrystals. For polycrystalline Zinc alloy [48], they found depending on the orientation of specimen to the applied field, the texture components can be strengthened, disappear or retain the original in intensity. The intensity of the components related to the grain orientations with lowest magnetic susceptibility increase during magnetic annealing whereas components related to higher susceptibility completely disappear. They attributed the change to a result of selective grain growth induced by additional driving force created by the anisotropy of the magnetic susceptibility. Later, they chose Zn bicrystals [49] with different planar individual boundaries and heat treated with and without the high magnetic field. According to boundary displacement they obtained the quantitative information of the additional driving force for grain growth exerted by magnetic anisotropy of Zn.

2. 5 Dislocation behaviors and fatigue feature in magnetic field

Magnetic field can exert influence on internal stress levels and dislocation behaviors and hence finally change mechanical properties of materials. Research on this aspect is also an important issue related to solid metallic materials area.

Tang et al. [50] applied a pulsed magnetic field of 0.6 T to a tensed 30CrMnSi structural steel for 120 seconds and found that pulsed magnetic field process strongly decreased the residual internal stress of specimens in uniaxial tension. TEM observation showed that after magnetic field treatment, the dislocation density in the ferrite matrix near carbide particles was remarkably reduced, dislocation loops and dipole dislocations were formed, the dislocation tangles opened and the number of cell walls decreased. They assumed that dynamic magnetostriction and motion of domain walls occurring during the magnetic treatment could change the binding energy between dislocations and impurities and thus result in an increase in the dislocation mobility. The experimental results in this investigation demonstrated that the pulsed magnetic field process promoted the dislocation motion and improved dislocation distribution.

Ferreira et al. [51] conducted a theoretical study to determine the influence of a magnetic field on the motion of twin dislocations in Fe-Al-C, Fe-Ni-C, Fe-Pt and Fe-34%Ni shape memory alloys. Simulation showed that the application of a magnetic field in certain directions with respect to the twin magnetization vector and the relative orientation between the twin variants in BCC ferrous alloys containing twinned martensite plates can impose, at the twin dislocations, high values of stress. However, in the cases where strong dislocation pinning occurs, or where grain boundaries act as barriers to dislocation motion, the influence of the magnetic field on the shape memory effect can be substantially diminished.

As fatigue life of materials are strongly dependent on dislocation behaviors, magnetic field will surely alter the fatigue process of ferro-materials. Bhat et al. [52] applied a pulsed magnetic field to a cold-rolled mild steel and found that the fatigue life of the material went down with increasing strength of the magnetic field. Later they conducted a theoretical study on the phenomenon [52] and suggested that the interaction between domain wall and dislocations was responsible for the phenomenon. When domains are at random in absence of a magnetic field, their walls usually exert a repulsive force on dislocations. Rotation of the domains towards the direction of applied field minimizes their randomness. As a result, the interactions among their walls and their resistance to the flow of dislocations are also reduced. This effect is expected to enhance further with increasing field. This led to easier material deformation in magnetic field than in its absence. Prasad et al. [53] observed the similar effect of the field in a cold-rolled AISI 4340 steel. They found that the hardness of the material was

lowered when exposed to an alternating magnetic field of 942 Oe at room temperature and suggested that vibrational effect of the field increased the mobility of dislocations. Their rearrangement offered less resistance to deformation. However, Fahmy et al. [54] found differently that magnetic field treatment increased the subsequent fatigue life of low-carbon steel when it was tested in magnetic pulsed field with a cyclic loading at stress amplitudes of 0.63 UTS and 0.73 UTS. But they came to similar conclusion that the resistance of domain walls to dislocation motion was reduced due to domain rotation in field and as a consequence, the initiation of cracks was delayed. Similarly, Lu et al. [55] reported that magnetic field had a repairing effect to early fatigue damage due to the similar influence of magnetic field on dislocation activity.

However, the influence of magnetic field on dislocation is a quite complicated process. So far, research on this aspect can only yield limited deductions and real influential mechanisms still remain unclear.

3 Influence of magnetic field on other physical processes

Owing to recent remarkable progress of superconducting magnets, the study of magnetic field effects on dia- or para-magnetic substances and some processes that include such materials have received considerable attention because the influence of the magnetic field is enhanced to obviously observable level. This indicates that the application of magnetic field in researches has been extended from the conventional ferromagnetic materials to an even larger scope of new materials including water, air, other nonmetallic materials and even organic tissues. A lot of new and interesting phenomena have been observed, such as magnetic field gradient can control air flows next to a diffusion flame and then influence the shape of the diffusion flame and the combustion rate [56]; magnetic levitation of paramagnetic materials which makes contactless processing technique used for melting and solidification of metallic materials under conditions of extreme purity possible [57]; also the area of creating favorable orientation in biological tissues by magnetic field has received particular attention.

3. 1 Effects of magnetic field on convection

The flow of electroconducting fluid under an external magnetic field generates electric currents in the fluid, and the electric currents interact with the external magnetic field to generate Lorentz force. Since external magnetic field influence the flow of electroconducting fluids by slowing down the speed of the melt flow, which is also called electromagnetic brake

or EMBr [57] under certain direction of the magnetic field, they have been used in various industrial fields, such as, in continuous casting of steel for controlling the liquid metal flow in steel making industry and magnetic suppression of molten semiconductor materials.

As the casting speed has to be increased to achieve high productivity, flow turbulence is highly enhanced, which causes the trapping of impurities. The application of a stationary magnetic field is one of the most effective methods for controlling heat and mass transfer in electrically conducting melts. The situation can be effectively improved by introducing the electromagnetic brake or compression wave to reduce the amount of trapping of non-metallic inclusions by the metal flow near the meniscus. A new method of non-contact generation of intense compression waves has been proposed recently by Wang et al. [58], in which both static and alternating magnetic fields were simultaneously imposed on a molten metal. As an effective non-contact method, it successfully resolved the problem of dissolution of a transmitter and power limitation of a vibrator aroused from the conventional compression wave generating method by electrostrictive or magnetostrictive vibrators and made the utilization of compression waves into practical materials processing possible.

As the problems met in metallurgical field, the quality of semiconductor crystals is also strongly influenced by the concentration and distribution of dopants and defects, which are controlled by motion of melt due to temperature gradients and the rotations of crystal and crucible. Many attempts [59-64] have been made to apply stationary magnetic field into crystal growth of semiconductors from the melt in order to eliminate impurity striations by introducing compressive waves and reduce temperature fluctuation. New methods and theories have been developed.

Since the behaviors of molten flow under magnetic field is a much complicate issue, in which many physical parameters of temperature, velocity, electric and magnetic fields are coupled with one another dynamically, new breakthroughs in magnetohydrodymanic theory and experimental observation are necessary and impendent.

3. 2 Application of magnetization force

Like the situation in which magnetic field imposes magnetic force, *i.e.*, Lorentz force, on moving electroconducting fluids and exerts influence on its convection, magnetic field can also impose a kind of magnetic force on electrically nonconducting fluids, such as inorganic oxide melts, pure water and gases. The force is so-called magnetization force. As convection of electrically nonconducting fluids is involved in many physicochemical processes that serves as the basis for the organization of the real and more complex processes, investigation

of the influence of magnetic field on this issue has received ever-increasing attention. From the late 1990's more and more studies related to magnetic field have been addressing this aspect [65-70].

Superconducting magnets are built to produce homogeneous magnetic fields of strong intensity. However, in the large frontiers beside this homogeneous area, the magnetic field is inhomogeneous in both radial and axial directions and very interesting phenomena can appear. Generally, the magnetization force experienced by a unit volume of material in an inhomogeneous magnetic field is:

$$F_m = \frac{1}{2}\mu_0 \chi \nabla H^2 = \frac{1}{2}\mu_0 \rho \chi_g \nabla H^2 \tag{1-6}$$

where μ_0 is permeability of free space, χ is volume magnetic susceptibility, H is the magnitude of magnetic field strength, χ_g is mass magnetic susceptibility and ρ is density. J. Qi et al. [65] numerically simulated thermal convection in pure water and suggested that the convection could be greatly damped and the maximum velocity decreased. Results also showed that the contribution from magnetization force to suppress convection was larger than that from Lorenz force.

Sugiyama et al. [66] examined the dissolution process of copper sulfate into water under a heterogeneous magnetic field vertical to the interface from the viewpoint of the self-organization process of the nonequilibrium fluctuations. They observed a changing surface morphology of the dissolved copper sulfate crystal due to the changing susceptibility at the interface that was resulted from changing solute concentration.

Magnetization force was also found existing near the liquid and gas boundary due to non-uniformity of magnetic susceptibility of dissolution of gas into liquid or evaporation from liquid even under a homogeneous field. An investigation of a magnetic field on the gas dissolution process into degassed water conducted by N. Hirota et al. [67] showed that under the magnetic fields up to 10 T, the dissolution rate was significantly accelerated. They proposed that the mechanism be based on magnetically induced convection in water due to the inhomogeneity of magnetic susceptibility created by the dissolution of oxygen into water phase, as oxygen is paramagnetic. In contrast, the dissolution of diamagnetic carbon dioxide gas was not accelerated by the magnetic field. However, under the coexistence of oxygen gas, the dissolution rate of carbon dioxide became fast. The study was of great significance. As

biological processes in nature, such as metabolism of living creatures, depend upon the oxygen dissolution process into water, it is possible that certain biological processes that are subjected to magnetic fields in the range of a few to several teslas may be affected via a change in the dissolution kinetics of oxygen into water. Moreover, since the convection of liquid plays an important role in some chemical and metallurgical processes, processes that include oxygen dissolution or degassing should be affected by magnetic fields due to the magnetically induced convection.

Another interesting phenomenon of magnetization force induced by magnetic field is the Magneto-Archimedes levitation. By making use of the magnetization of surrounding medium, such as pressurized oxygen that is paramagnetic, to create buoyancy, diamagnetic substance can be levitated [56], especially, when a larger field gradient is needed for the diamagnetic matter. One of the applications of Magneto-Archimedes levitation is the separation of a dry mixed powder [56]. Substances with different magnetic susceptibilities and densities can be levitated at different heights from an initially mixed powder. This indicates that a mixed powder can be separated by the magneto-Archimedes levitation in a dry state without any chemical treatments [56].

Another important application of magnetic force is to control crystal orientation in vapor-deposition and melt processing [68-70]. High magnetic field was utilized to rotate evaporated molecules agglomerate during their flying from the target to the substrate and then realize the alignment of crystals in a favorable direction on the substrate to improve the physical properties of surface coatings. Nonmagnetic elements of bismuth [68] and zinc [69] are ideal because they both have hexagonal crystal structures, which show a magnetic anisotropy depending on each direction of their unit crystals. The magnetic force was also utilized to create useful texture in high-T_c superconductors during their solidification in the melting process and thus improve their superconductivity [70].

There have been several different types of phenomena observed in which the magnetic field effects are significant on the processes of 'non-magnetic' substances. Although the appearances are different from one phenomenon to another, the mechanisms behind them are all based on the magnetization force due either to the inhomogenous distribution of the magnetic field or to the slight difference in the magnetic susceptibility of the component in non-magnetic substances or the inhomogeneity created in the steady state process in the liquid or gas phase. As the effect of magnetic field is proportional to field strength square, H^2, and most of the phenomena become observable only under strong magnetic fields above tesla range, the usage of which has become practically possible due to the recent development of

the cryogen-free superconducting magnet. Consequently, the development of further stronger magnetic fields in the future will see more varieties of the field effects.

4 Significance and contents of the present work

Although the application of magnetic field, especially high magnetic field, to materials science and engineering research area is facing a full development, as a young technique, research on this issue is still in its initial stage. Most of them are basic and remaining in phenomena revealing level. Sometimes the results are even discrepant and lack of regularity. In solid-state phase transformation area, the research also shows the same characters and the development is uneven. Most researches have been focused on the effect of magnetic field on martensitic transformations due to experimental convenience and have obtained fruitful achievements. However, for diffusion-controlled phase transformation, as the transformation show more rich microscopic processes and most of them happen at high temperature, the application of magnetic field, especially high field generated by superconducting magnets, has faced more difficulty in technique. Therefore, the research on this topic started much later around the turn of this century. Reports on this aspect are quite limited. So to develop the existing research to a wider and deeper scale is certainly necessary and imperative.

Based on this background, the present work has been orientated to the investigation of ***the influence of high magnetic field on diffusion-controlled phase transformations in steels***. The main content of the work can be summed up as follows:

1) By making use of magnetism theory and thermodynamic theory of phase transformation to conduct theoretical simulation on thermodynamic regulation of high temperature phase transformation in magnetic field.
2) Experimentally examine the thermodynamic and kinetic influence of magnetic field on transformation from austenite to ferrite in a medium carbon low alloyed steel and work out new transformation thermodynamic and kinetic regulations. Meanwhile, probe possible application of magnetic field to conventional annealing process. Investigate new microstructure features appearing during the above transformation under magnetic field and work out its formation mechanism.
3) Experimentally examine precipitation and recovery behaviors occurring during high temperature tempering in high magnetic field in the same steel and investigate (1) new phase interface behavior under magnetic field and its influence on precipitation behaviors; (2) the new recovery features in the magnetic field. Experimentally examine the

precipitation character happening during low temperature tempering in high magnetic field and establish the influential mechanism of the field.

The purpose of the present work is to find new phenomena and regulations during diffusion-controlled phase transformations in high magnetic field; through theoretical analyses to work out its affecting mechanisms; enrich and enlarge existing phase transformation theory.

References

[1] Brooks J S, Crow J E and Moulton W G., Science opportunities at high magnetic fields[J], *J. Phys. Chem Solids* 1998, 59(4):569-590

[2] Watanabe K, Awaji S, Motokawa M, Mikami Y, Sakuraba J and Watazawa K, 15 T cryocooler Nb_3Sn superconducting magnet with a 52 mm room temperature bore[J], *Jpn. J. Appl. Phys.* 1998, 37-38:L1148-L1150

[3] Watanabe K, Awaji S, Sakuraba J, Watazawa K, Hasebe T, Jikihara K Yamada Y and Ishihara M, 11 T Liquid helium-free superconducting magnet[J], *Cryogenics*, 1996, 36(12):1019-1025

[4] Sadovskii V D, Rodigin N M, Smirnov L V, Filonchik G M and Fakidov I G, The question of the influence of magnetic field on martensitic transformation in steel[J], *Fiz. Metal. Metalloved.*, 1961, 12(2):131-133

[5] Krivoglaz M A and Sadovskiy V D, Effect of strong magnetic fields on phase transformations[J], *Fiz. Metal. Metalloved.*, 1964, 18(4):23-27

[6]. Fokina Ye A, Smirnov L V, Sadovskiy V D and Peikul A F, Effect of a permanent magnetic field on the martensitic transformation in steel[J], *Fiz. Metal. Metalloved.*, 1965, 19(6):121-122

[7] Malinen P A and Sadovskiy V D, Effect of a magnetic field on the $\alpha \rightarrow \gamma$ transformation in iron-nickel alloys[J], *Fiz. Metal. Metalloved.*, 1966, 21(5):139-140

[8] Bernshteyn M L, Granik G I and Dolzhanskiy P R, Effect of magnetic field on the phase transformations in nickel steels[J], *Fiz. Metal. Metalloved.*, 1965, 19(6):77-83

[9] Estrin E I, Effect of a magnetic field on the martensitic transformation[J], *Fiz. Metal. Metalloved.*, 1965, 19(6):117-120

[10] Voronchikhin L V and Fakidov I G, Determining the latent heat of the martensitic transformation induced by a magnetic field in steel[J], *Fiz. Metal. Metalloved.*, 1966, 21(3):119-124

[11] Satyanarayan K R, Eliasz W and Miodownik A P, The effect of a magnetic field on the martensite transformation in steels[J], *Acta Metall.*, 1968, 16:877-887

[12] Kakeshita T, Shimizu K, Funada S and Date M, Magnetic field-induced martensitic transformations in disordered and ordered Fe-Pt Alloys[J], *Trans. JIM,* 1984, 25(12):837-844

[13] Kakeshita T, Shimizu K, Maki T, Tamura I, Kijima S and Date M, Magnetoelastic martensitic transformation in an ausaged Fe-Ni-Co-Ti alloy[J], *Scripta Metall.,* 1985, 19(8):pp973-976

[14] Kakeshita T, Shimizu K, Funada S and Date M, Composition dependence of magnetic field-induced martensitic transformations in Fe-Ni alloys[J], *Acta metall.,* 1985, 33(8):1381-1389

[15] Kakeshita T, Shimizu K, Kijima S, Yu Z H and Date M, Magnetic field-induced martensitic transformations in Fe-Ni-C invar and non-invar alloys[J], *Trans. JIM,* 1985, 26(9):630-637

[16] Kakeshita T, Furikado S, Shimizu K, Kijima S and Date M, Magnetic field-induced martensitic transformation in single crystals of Fe-31.6 at% Ni alloy [J] , *Trans. JIM,* 1986, 27(7):477-483

[17] Kakeshita T, Shirai H, Shimizu K, Sugiyama K, Hazumi K and Date M, Magnetic field-induced transformation from paramagnetic austenite to ferromagnetic martensite in an Fe-3.9Mn-5.0C (at%) alloy[J], *Trans. JIM,* 1987, 28(11):891-897

[18] Kakeshita T, Shimizu K, Ono M and Date M, Magnetic field-induced martensitic transformations in a few ferrous alloys[J], *J, Magn. & Magn. Mat.,* 1990, 90&91:34-36

[19] Kakeshita T, Shirai H, Shimizu K, Sugiyama K, Hazumi K and Date M, Effect of magnetic fields on martensitic transformations in alloys with a paramagnetic to antiferromagnetic transition in the austenitic state[J], *Trans. JIM,* 1988, 29(7):553-560

[20] Kakeshita T, Kuroiwa K, Shimizu K, Ikeda T, Yamagishi A and Date M, Effect of magnetic fields on athermal and isothermal martensitic transformations in Fe-Ni-Mn alloys[J], *Mat. Trans. JIM,* 1993, 34(5):415-422

[21] Kakeshita T, Yamamoto T, Shimizu K, Sugiyama K, and Endo S, Effects of static magnetic field and hydrostatic pressure on the isothermal martensitic transformation in an Fe-Ni-Mn alloys[J], *Mat. Trans. JIM,* 1995, 36(8):1018-1022

[22] Kakeshita T, Saburi T, Kindo K and Endo S, Effect of magnetic field and hydrostatic pressure on martensitic transformation and its kinetics[J], *Jpn. J. Appl. Phys.* 1997, 36(12A):7083-7094

[23] Kakeshita T, Fukuda T, Saburi T, Kindo K and Endo S, Effect of Magnetic Field and Hydrostatic Pressure on Martensitic Transformation Process in Some ferrous Alloys[J], *Phys. B* 1997, 237-238(12A):603-604

[24] Kakeshita T, and Fukuda T, Martensitic transformation in some ferrous and non-ferrous alloys under high magnetic field[C], *Proc. The 3th International Symposium on Electromagnetic Processing of Materials,* Nagoya: ISIJ, 2000, 584-589

[25] Kakeshita T, Takeuchi T, Fukuda T, Saburi T, Oshima R, Muto S and Kishio K, Magnetic field-induced martensitic transformation and giant magnetostriction in Fe-Ni-Co-Ti and ordered Fe_3Pt shape memory alloys[J], *Mat. Trans. JIM,* 2000, 41(8):882-887

[26] Kakeshita T, Saburi T and Shimizu K, Effects of hydrostatic pressure and magnetic field on martensitic transformations[J], *Materials Science and Engineering* 1999, A273-275:21-29

[27] Kohno Y, Konishi H, Shibata K, Watanabe K and Awaji S, Effect of reheating after solution treatment and magnetic fields on α' martensite formation in SUS324L steel during isothermal holding at cryogenic temperature[J], *Materials Science and Engineering*, 1999, A273-275:333-336

[28] Shimozono T, Kohno Y, Konishi H, Shibata K, Ohtsuka H and Wada H, Effect of pre-strain, heat treatments and magnetic fields on α' martensite formation in Fe-25.5%Ni-3-5%Cr alloys[J], *Materials Science and Engineering*, 1999, A273-275:337-341

[29] Kurita Y, Emura S, Fujita K, Nagai K, Ishikawa K and Shibata K, Effects of magnetic fields on martenistic transformation and serration of austenitic Fe-Ni and Fe-Cr-Ni steels at 4 K[J], *Fusion Engineering and Design*, 1993, 20(1):445-450

[30] Koyano T, Ikeda H, Yoshizaki R, Uehara K, Tasaki A, Ohtsuka H, Takamasu T, Wada H, Kido G and Ohba T, Effect of magnetic field on γ→α' martensitic transformation and magnetization of α' and α'' iron-nitrides[J], *Mat. Trans. JIM,* 2000, 41 (8):923-927

[31] Shibata K, Shimozono T, Kohno Y and Ohtsuka H, Effects of heat treatment, pre-strain and magnetic field on the formation of α' martensite in Fe-25.5Ni-4Cr and 304L steels[J], *Mat. Trans. JIM,* 2000, 41 (8):893-901

[32] Ghosh A K and Roy M N, Phase transformation of steel in magnetic field[J], *Transactions of the Indian Institute of Metals*, 1987, 40 (4):329-333

[33] Joo H D, Kim S U, Shin N S and Koo Y M, An effect of high magnetic field on phase transformation in Fe-C system, Materials Letters[J], 2000, 43(5-6):225-229

[34] Guo H and Enomoto M, Influence of magnetic fields on α/γ equilibrium in Fe-C(-X) alloys[J], *Mat. Trans. JIM,* 2000, 41 (8):911-916

[35] Shimotomai M, Maruta K, Mine K and Matsui M, Formation of aligned two-phase microstructure by applying a magnetic field during the austenite to ferrite transformation in steels[J], *Acta Mater.*, 2003, 51:2921-2932

[36] Peters C T and Miodownik A P, The effect of magnetic fields on phase equilibria in the iron-cobalt system[J], *Scripta Metall.*, 1973, 7(9):955-958

[37] Enomoto M Guo H, Tazuke Y, Abe Y R and Shimotomai M, Influence of magnetic field on the kinetics of proeutectoid ferrite transformation in iron alloys[J], *Metall. Mater. Trans.*, 2001, 32A:445-453

[38] Maruta K and Shimotomai M, Alignment of two-phase structures in Fe-C alloys by application of magnetic field[J], *Mat. Trans. JIM,* 2000, 41 (8):902-906

[39] Shimotomai M and Maruta K, Aligned two-phase structures in Fe-C alloys[J], *Scripta Mater.* 2000, 42(5):499-503

[40] Maruta K and Shimotomai M, Magnetic field-induced alignment of steel microstructures[J], *Journal of Crystal Growth*, 2002, 237-239:802-1805

[41] Ohtsuka H, Xu Yand Wada H, Alignment of ferrite grains during austenite to ferrite transformation in a high magnetic field[J], *Mat. Trans. JIM,* 2000, 41(8):907-910

[42] Smoluchowski R and Turner R W, Influence of magnetic field on recrystallization[J], *J. Appl. Phys.*, 1949,20:745-749

[43] Bhandary V S and Cullity B D, The texture and mechanical properties of iron wire recrystallized in a magnetic field[J], *Trans. Met. Soc. AIME,* 1962, 224:1194-1196

[44] Martikainen H O and Lindroos V K, Observations on the effect of magnetic field on the recrystallization in Ferrite[J], *Scand. J. Metall.*, 1981, 10:3-8

[45] Watanabe T, Suzuki Y, Tanii S and Oikawa H, The effects of magnetic field annealing on recrystallization and grain-boundary character distribution (GBCD) in iron-cobalt alloy polycrystals[J], *Philosophical Magazine Letters*, 1990, 62(1):9-17

[46] Masahashi N, Matsuo M and Watanabe K, Development of preferred orientation in annealing of Fe-3.25%Si in a high magnetic field[J], *J. Mater. Res.*, 1998, 13(2):457-461

[47]. He C S, Zhang Y D, Zhao X, Zuo L, He J C, Watanabe K, Zhang T, Nishijima G and Esling C, Effect of a high magnetic field on microstructure and texture evolution in a cold-rolled interstitial-free (IF) steel sheet during annealing[J], *Advanced Engineering Materials*,

2003, 5(8):579-583

[48] Sheikh-Ali A D, Molodov D A, and Garmestani H, Magnetically induced texture development in zinc alloy sheet[J], *Scripta Mater.*, 2002, 46(12), pp857-862

[49] Sheikh-Ali A D, Molodov D A, and Garmestani H, Migration and reorientation of grain boundaries in Zn bicrystals during annealing in a high magnetic field[J], *Scripta Mater.*, 2003,48(5)483-488

[50] Tang G, Lu A, Chen X, Zhou H and Tang F, Effect of a pulsed magnetic treatment on the dislocation substructure of a commercial high strength steel[C], *Proc. The 3rd International Symposium on Electromagnetic Processing of Materials, ISIJ*, Nagoya, 2000, 9:606-611

[51] Ferreira P J and Vander Sande J B, Magnetic field effects on twin dislocations[J], *Scripta Mater.*, 1999, 41(2)117-123

[52] Bhat I K, Ghosh A and Muju M K, Effect of magnetic field on fatigue[J], *J. Eng. Des.*, 1984, 2:582-593

[52] Bhat I K, Muju M K and Mazumdar P K, Possible effects of magnetic fields in fatigue[J], *Int. J. Fatigue*, 1993, 15(3):193-197

[53] Prasad S N, Singh P N and Singh V, Influence of pulsating magnetic field on softening behaviour of cold rolled AISI 4340 steel at room temperature[J], *Scripta Mater.* 1996, 34 (12):1857-1860

[54] Fahmy Y, Hare T, Tooke R and Conrad H, Effect of a pulsed magnetic treatment on the fatigue of low carbon steels[J], *Scripta Mater.* 1998, 38(9):1355-1358

[55] Lu B T, Qiao S R and Sun X Y, Exploration on repairing fatigue damage of steel specimens with magnetic treatment[J], *Scripta Mater.*, 1999, 40(7):767-771

[56] Kitazawa K, Ikezoe Y, Uetake H and Hirota N, Magnetic field effects on water, air and powders[J], *Phys. B*, 2001, 295-295:709-714

[57] Gillon P, Uses of intense d.c. magnetic fields in materials processing[J], *Materials Science and Engineering*, 2000, A287(2):146-152

[58] Wang Q, Momiyama T, Iwai K and Asai S, Non-contact generation of intense compression waves in a molten metal by using a high magnetic field[J], *Mat. Trans. JIM*, 2000, 41(8):1034-1039

[59] Inatomi Y, Kato A, Horiuchi K, Takada A and Kuribayashi K, Scaling analysis of semiconductor crystal growth from the liquid phase in an axis static magnetic field[J], *Mat. Trans. JIM*, 2000, 41(8):1026-1033

[60] Watanabe M, Yi K W, Hibiya T and Kakimoto K, Direct observation and numerical simulation of molten silicon flow during crystal growth under magnetic fields by X-ray

radiography and large-scale computation[J], *Porg. Crystal Growth and Charact.*, 1999, 38:215-238

[61] Hirata H and Hoshikawa K, Silicon crystal growth in a cusp magnetic field[J], *J. Crystal Growth*, 1989, 96(4):747-755

[62] Hirata H and Hoshikawa K, Homogeneous increase in oxygen concentration in Czochralski silicon crystals by a cusp magnetic field[J], *J. Crystal Growth*, 1989, 98(4):777-781

[63] Sabhapathy P and Salcudean M E, Numerical study of Czochralski growth of silicon in an axisymmetric magnetic field[J], *J. Crystal Growth*, 1991, 113(1-2):164-180

[64] Kakimoto K, Yi K W and Eguchi M, Oxygen transfer during single silicon crystal growth in Czochralski system with vertical magnetic fields[J], *J. Crystal Growth*, 1996, 163(3):238-242

[65] Qi J W and Wakayama N I, Suppression of natural convection in nonconducting and lowconducting fluids by the application of a static magnetic field[J], *Mat. Trans., JIM*, 2000, 41(8):970-975

[66] Sugiyama A, Morisaki S and Aogaki R, Dissolution process of copper sulfate into water in a heterogeneous vertical magnetic field[J], *Mat. Trans., JIM*, 2000, 41(8):1019-1025

[67] Hirota N, Ikezoe Y, Uetake H, Nakagawa J and Kitazawa K, Magnetic field effect on the kinetics of oxygen dissolution into water[J], *Mat. Trans., JIM*, 2000, 41(8):976-980

[68] Tahashi M, Sassa K, Hirabayshi I and Asai S, Control of crystal orientation by imposition of a high magnetic field in a vapor-deposition process[J], *Mat. Trans., JIM*, 2000, 41(8):985-990

[69] Taniguchi T, Sassa K, Yamada T and Asai S, Control of crystal orientation in zinc electrodeposits by imposition of a high magnetic field[J], *Mat. Trans., JIM*, 2000, 41(8):981-984

[70] Chen W P, Maeda H, Watanabe K, Motokawa M, Kitaguchi K and Kumakura H, Microstructures and properties of Bi2212/Ag tapes grown in high magnetic fields[J], *Physica C*, 1999, 324 (3-4):172-176

Chapter 1 Influence of Magnetic Field on Phase Equilibrium in Fe-C Binary System

Introduction

As magnetic field is one of the important thermodynamic parameters like temperature or pressure that changes the internal energies of different phases, phase equilibrium can be changed. In the case of magnetic field, the Gibbs free energy level of a given phase is lowered by the amount according to the magnetization or magnetic susceptibility. Therefore, the higher the magnetization or susceptibility is, the lower the Gibbs free energy becomes. For austenite, it is paramagnetic and its magnetization is lower than that of either paramagnetic or ferromagnetic ferrite at any temperature in the Fe-C binary system, so the amount of Gibbs free energy lowered by the magnetic field in ferrite is higher than that in austenite. Therefore the energy difference between these two phases will be increased by the application of the magnetic field. As a consequence, the phase equilibrium lines in the Fe-C diagram will be shifted to higher carbon concentration or higher temperatures.

In this chapter, the electronic band model is used to calculate the temperature variation of susceptibility of *fcc* Fe and based on this, the magnetization and further the magnetic Gibbs free energy of austenite are calculated. As for *bcc* Fe, it transits from ferromagnetic to paramagnetic state through the Curie temperature, *Tc* (1043K), within the temperature range concerned and up to now, none of the existing models (Weiss model or band model) are satisfactory in conducting the calculation of magnetization at the temperatures around *Tc*. The relatively simpler Weiss molecular field model is selected. Below *Tc*, the model is applied directly, as it is accurate. Above *Tc*, the model underestimates magnetization due to the neglect of short-range ordering existing in the matter, therefore in the present work, a correction is carried out. The model is corrected with a short range ordering coefficient above *Tc* by making use of the measured susceptibilities and extrapolated to temperatures below *Tc* to have a smooth connection to the calculation from Weiss model. The Magnetic Gibbs free energy difference between austenite and ferrite calculated based on the above methods is introduced as an extra driving force and the new phase equilibrium boundaries under magnetic field in Fe-C binary system are simulated. The shift of Ae_3 temperatures is also calculated and the change of eutectoid temperature and composition are predicted.

Influence of a Magnetic Field on Phase Equilibrium in Fe-C Binary System

Yudong Zhang[a,b], Changshu He[a], Xiang Zhao[a], Yandong Wang[a], Liang Zuo[a], and Claude Esling[b*]
[a] Key Laboratory (Northeasten University), Ministry of Education, Shenyang 110004, P. R. of China
[b] LETAM, CNRS-UMR 7078, University of Metz, Ile du Saulcy, 57045 Metz, France

Abstract: The Weiss model is extended by substituting the molecular field coefficient λ with a short-range-ordering coefficient γ valid around and above *Tc*. The temperature variations of susceptibility of fcc Fe are calculated with a band model. Based on these, the phase equilibrium diagram of Fe-C binary system under a magnetic field is calculated.

1. Introduction

The effects of magnetic field on phase transformation in ferrous alloys have received great attentions [1-3] due to some potential applications of the magnetic-field applied treatments in metallurgical industry. The phase diagrams at elevated temperatures in a high magnetic field are considered to provide the fundamental knowledge that is essential for controlling the microstructures of various product phases. In this respect, an accurate and simple model to capture the high-field magnetic susceptibility data is one of the key issues for the successful calculation of phase diagram.

So far, the Weiss molecular field theory [4] - based on the localized model - and band model [5] have intrinsic shortcomings for calculating the necessary magnetic parameters. Revisions on the models with the experimental data are required when a magnetic field is applied, as to obtain relatively accurate results for subsequent calculations on phase equilibrium. In this study, we extend the Weiss model by substituting a short-range ordering interaction for the long-distance ordering interaction field to calculate the magnetization of bcc phase around and above T_C. The temperature variations of susceptibility of fcc Fe are also derived with a band model. The temperature-dependent susceptibilities of both bcc and fcc phases calculated by those models show good agreement with the available experimental values. The influence of the magnetic field on the austenite/ferrite and ferrite/austenite phase equilibrium in the Fe-C binary system is calculated, which provides some essential parameters required for simulating microstructure evolution in steels treated in high magnetic field.

2. Brief Description of the Weiss Molecular Field Theory

The Weiss molecular field theory [4] has been most commonly used to calculate the temperature-dependent magnetization. It is suggested that in a ferromagnetic material the atomic magnetic moments are permanent and parallel to each other within magnetic domains. The interaction field causing moment ordering within domains is assumed proportional to magnetization, the proportionality factor λ being called as the molecular field coefficient. If N is the number of atoms per unit volume, the corresponding magnetization M under an applied magnetic field is

$$M = M_0 B_J(\alpha_J) \tag{1}$$

where M_0 is the saturation magnetization. The Brillouin function $B_J(\alpha_J)$ is defined as

$$B_J(\alpha_J) = \frac{2J+1}{2J} cth(\frac{2J+1}{2J})\alpha_J - \frac{1}{2J} cth\frac{\alpha_J}{2J} \tag{2}$$

with

$$\alpha_J = \frac{gJ\mu_B(B_0 + \lambda M)}{kT} \tag{3}$$

where g is the Landé factor, J the total angular momentum of an atom, μ_B the Bohr magneton, B_0 the magnetic induction of the applied magnetic field, k the Boltzmann constant and T the absolute temperature. The molecular field coefficient λ can be calculated from the experimental value of the Curie temperature *Tc* using the following equation

$$Tc = \frac{J(J+1)g^2\mu_B^2 N\lambda}{3k} \tag{4}$$

For the present study, J takes on the value *1/2* [6]. The temperature variations of spontaneous magnetization and induced magnetization of bcc Fe calculated at $B_0 = 10$ Teslas are shown in Fig. 1. It can be seen that the spontaneous magnetization and that induced by the magnetic field decrease markedly with increasing temperature. While the spontaneous

magnetization quickly drops to zero around T_C; the induced magnetization drops too, but maintains a small value well above *Tc*. The susceptibilities above T_C are calculated from the induced magnetization and compared with the experimental ones, as shown in Fig. 2. Obviously, the calculation underestimates the susceptibilities of bcc Fe at all temperatures above *Tc*.

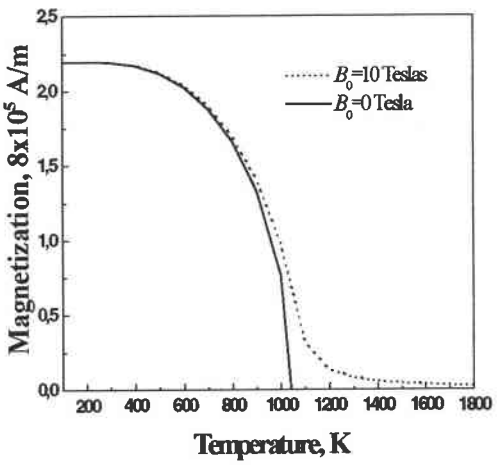

Figure 1 Variations of magnetization with temperature calculated at B_0=10 and B_0=0 Teslas

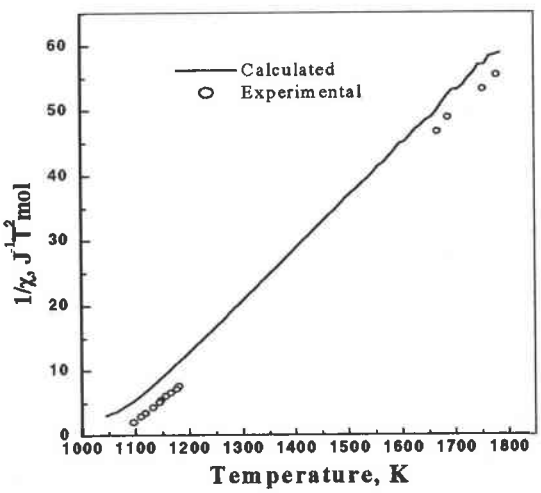

Figure 2 Susceptibilities calculated for bcc Fe above the Curie temperature, as compared with the experimental values

The difficulties encountered in calculating the variations of magnetization with the temperature in bcc Fe using the Weiss model around and above *Tc* have been discussed in detail in the work of Gao and Enomoto [7]. As it is based on the localized theory, the Weiss model is well adapted for a description of the magnetization of metals whose magnetism is determined by the close bound 4f electrons. However, the magnetic properties of iron are determined mainly by the 3d electrons that are relatively free to move - i.e. itinerant - through the solid. Although the Weiss model is not optimal, it allows basic calculations for ferromagnetism, which could not be obtained so easily with the other models. In fact, the Weiss model, when applied below *Tc*, yields relatively accurate predictions for the temperature variation of magnetization in bcc Fe. It can thus be considered as an adequate choice. However, some problems still exist, causing large errors on the subsequent calculation of phase equilibrium, especially when the applied field is high.

3. A Revised Model to Calculate the Magnetic Parameters

In the present study, the Weiss model around and above *Tc* is complemented to obtain relatively accurate results. The above mentioned problem caused by using the traditional Weiss model arises from the neglect of the short-range magnetic ordering that exists - according to the neutron diffraction results - above T_C, even without applying a magnetic field to materials. Therefore, taking the short-range ordering into account is necessary for successfully describing the experimental observations of susceptibilities. Here, the short-range interaction is described – in analogy to the long-range interaction – by the field γM where γ is the short-range magnetic ordering coefficient. As the transition from long- to short-range ordering stems from thermal agitation, it is thermodynamic in nature and γ can be written in an Arrhenius-type relation analogous to the diffusion coefficient, i.e.

$$\gamma = Ae^{-\frac{G}{RT}} \tag{5}$$

where A is a constant, R the gas constant and G an energy parameter reflecting atomic interaction. Since the short-range ordering is the residue of the long-distance ordering at high temperature and there may exist a smooth transition between the two ordering states, A is simply assigned the value of the molecular-field coefficient λ. The susceptibilities measured by W. Sucksmith and Pearce [8] are used to calculate the values of G at various temperatures. The results have shown that G is in a close linear relationship with temperature. The

following expression is obtained, without *a priori* hypothesis, by the least-square method

$$G = H - S \cdot T \tag{6}$$

where H and S are, at first, defined only as field-dependent parameters. Obviously, G in Eq. (6) takes the form of the free energy, whereas H corresponds to the enthalpy and S to the entropy.

The following relations of H and S with B_0: $H = 192.99955 - 1.92695(B_0)^{5/2}$ and $S = 0.46227 - 0.00116(B_0)^{5/2}$ are established by the numerical analysis. These results are consistent with the thermodynamic theory; the enthalpy represents here a large bonding energy of ordering and the small entropy shows a tendency to being disordered in atomic arrangement. Such a compromise between two opposing factors is in agreement with the situation of thermal agitation in opposition to magnetic ordering. A detailed analysis shows that the magnetization calculated with γ at temperatures ranging from Tc to about 100K below are higher than the one provided by the original Weiss model; however, they join up smoothly at some temperatures. Actually, the underestimation of magnetization by the Weiss model starts from about 200K below Tc, as it appears from the comparison with the spontaneous magnetization measured [6]. The connecting temperatures are well within this temperature range and change with B_0. The higher B_0, the lower the temperature is for the connection. The lowest one is just about 200K below Tc. The corrected model works well within the range from 2 to 18 Teslas. The calculations show that, above Tc, when B_0 exceeds 20 Teslas, the magnetization deviates from its linear relationship with the field as it approaches saturation. The temperature variations of susceptibility calculated with the short-range ordering coefficient are shown in Fig. 3 and appear to be in good agreement with the experimental values. It proves that the present revised Weiss model - taking into account a short-range ordering - is reasonable and practical.

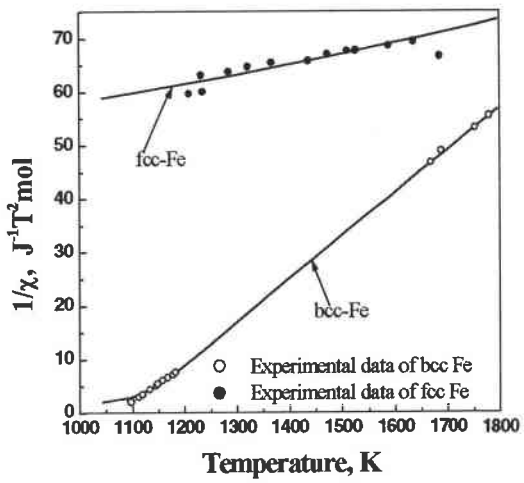

Figure 3 Calculated susceptibilities of both bcc Fe with the complement short-range magnetic ordering coefficient and fcc Fe with band model compared with measured results

Fcc Fe is seen as being paramagnetic for all the temperatures considered. Even if it is weak in magnetization, it can be magnetized to some extent under high magnetic field and should also be taken into account. Since the Weiss model failed to give a satisfactory description for the temperature variations of its susceptibility, the itinerant electron model based on the band theory is used as an alternative one. In the band model, all magnetic electrons are itinerant. They move within the average field of the other electrons and ions. The energy levels of electrons are distributed in the bands according to Fermi's statistics. The electron-electron interactions result in the exchange splitting of the bands and the redistribution of the electrons in the exchange split bands causes spontaneous magnetization. Following this, the paramagnetic susceptibility can be described as [5]

$$\chi = \frac{\chi^0(T)}{1-\alpha\chi^0(T)} \tag{7}$$

where α is also called molecular field coefficient. The unenhanced Pauli spin susceptibility $\chi^0(T)$ reads

$$\chi^0(T) = \frac{1}{2}(g\mu_B)^2 \int_{-\infty}^{\infty} d\varepsilon N(\varepsilon)\partial f(\varepsilon-\xi_p)/\partial\xi_p \tag{8}$$

where $N(\varepsilon)$ denotes the density of states, $f(\varepsilon-\xi_p)$ the Fermi distribution function and ξ_p Fermi energy. By means of the expansion formula for the Fermi integrals, $\chi^0(T)$ at low temperature is written as

$$\chi^0(T)=\frac{1}{2}(g\mu_B)^2\{1+\frac{1}{6}(\pi kT)^2[(N_2/N_0)-(N_1/N_0)^2]+...\} \tag{9}$$

with

$$N_i=[\partial^i N(\varepsilon)/\partial\varepsilon^i]_{\varepsilon=\xi_0} \tag{10}$$

where ξ_0 is Fermi energy at 0°K, $N_0=N(\xi_0)$ and N_i the i-th derivative with respect to ε.

By use of the reasonable density curves of states already calculated by Dalton [9], and the molecular field coefficient α and correcting the model with the orbital susceptibility χ_{orb} [10], the temperature variations of χ for fcc Fe can be calculated, as shown in Fig.3. This is in good agreement with the experimental values for all the temperatures.

4. Influence of the Magnetic Field on Fe-C Phase Equilibrium

As both ferrite and austenite can be magnetized, their magnetization could create an internal field that may change the Gibbs energy levels of the both phases. So, the influence of a magnetic field on phase equilibrium can be introduced via magnetic energy. Magnetism is a complicating issue and there exist several forms of magnetic energy, of different origins. Different references give various expressions, but in most of those dealing with the phase transformations under magnetic field, the free energies from field are simply expressed as MH or $\int_0^H MdH$ and there is no detailed definition, nor a description of its origin. It is surely helpful for subsequent calculations to provide a detailed definition of the various magnetic energies, based on the clear presentation in the reference [11]. The authors distinguish three types of energy for a magnetized material set in an applied field. The *demagnetization energy* is defined as the work required to overcome the repulsion between magnetic domains when the material is magnetized to align these domains parallel to the direction of the magnetic

field applied. The density of its volume energy is $\frac{1}{2}\vec{M}\cdot\vec{B}_d$ (B_d is the induction of demagnetization field). The *Zeeman energy* is the work required - the sample being already magnetized to a constant magnetization M - to raise the field from zero to H_0. The density of its volume energy is $\vec{B}_0\cdot\vec{M}$. The sum of the demagnetization energy and the Zeeman energy is called the *magnetostatic energy*. Finally, the *intrinsic magnetization energy* is the work provided to the material by raising the level of its magnetization to M with a field B_0. Its corresponding density of volume energy is $\int_0^M \vec{B}_0\cdot d\vec{M}$. Only the intrinsic magnetization energy is the energy provided to change the internal energy of the material. Therefore only this latter energy is concerned to determine the influence of the magnetic field applied on the transformation from one phase to another. Thus, the difference in energy between ferrite and austenite resulting from the field applied can be expressed as

$$\Delta G^M = -(\int_0^{M^\alpha} \vec{B}_0\cdot d\vec{M}^\alpha - \int_0^{M^\gamma} \vec{B}_0\cdot d\vec{M}^\gamma) \tag{11}$$

where the superscripts α and γ denote ferrite and austenite, respectively, and M magnetization.

The KRC's proeutectoid transformation driving force model summarized in Chang's work [12] is used for the thermodynamic calculation. The driving force for the transformation from austenite to ferrite is

$$\Delta G^{\gamma\to\alpha+\gamma'} = RT[x_\gamma \ln\frac{(1-\Phi)(1-z_\gamma x_\gamma)}{(z_\gamma-1)x_\gamma\Phi} + \frac{1-x_\gamma}{z_\gamma-1}\ln\frac{(1-x_\gamma)\Phi}{1-z_\gamma x_\gamma}] \tag{12}$$

where $z_\gamma = 1-\exp(-w_\gamma/RT)$, $w_\gamma = 5878J/mol$, $\Phi = \exp(z_\gamma-1)\Delta G_{Fe}^{\gamma\to\alpha}/RT$, x_γ is the molar volume fraction of the content of carbon in austenite and $\Delta G_{Fe}^{\gamma\to\alpha}$ the difference in Gibbs free energy between α-Fe and γ-Fe. The latter can be obtained from the data published by M. Hillert [13]. After being expressed in the form of proper units, ΔG_M is introduced as an extra driving force for phase transformation, assuming that the Gibbs chemical free energy in each phase is not affected by the magnetic field. The equilibrium configuration is reached

when the driving force on the phase boundary disappears. Following this, the content of carbon at the austenite/ferrite phase boundary (Ae_3 line) under magnetic field is calculated. With the equations published by Chang *et al* [12, 14], the carbon content at the ferrite/austenite and austenite/cementite phase boundaries are also calculated. Results are shown in Fig. 4. The shift of the Ae_3 temperature for pure iron and those of steels (C%>0.0218%wt) for the values of the different magnetic fields applied are shown in Table 1.

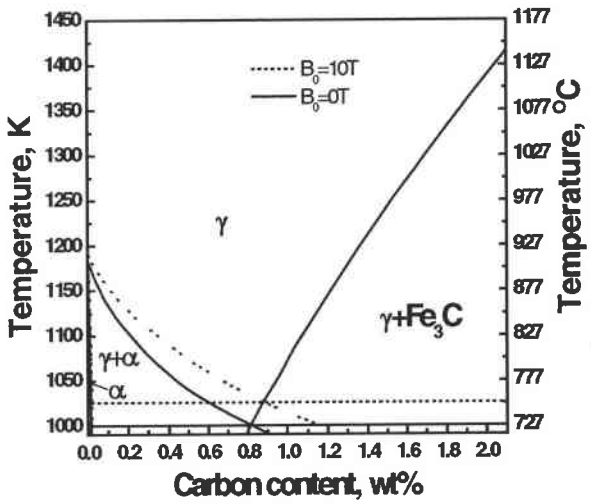

Figure 4 Influence of magnetic field on ferrite/austenite and austenite/ferrite phase equilibrium

Table 1 Increase of Ae_3 under magnetic field

Carbon content (wt%)		Ae_3 (°C)	Increase of Ae_3 under magnetic field (°C)		
			B_0=2 Teslas	B_0=4 Teslas	B_0=10 Teslas
Pure iron		910	0.317	1.566	7.636
Steel	0.05	886.24	3.356	6.401	14.162
	0.1	865.15	5.123	9.903	22.665
	0.2	830.77	8.351	15.289	32.432
	0.4	784.54	13.389	20.055	36.611
	0.6	753.30	14.123	20.542	35.821
	0.8	729.29	14.062	20.267	34.585

It can be seen from Fig. 4 that the magnetic field has an obvious influence on the austenite/ferrite and ferrite/austenite phase equilibrium, especially in the former case where there is a shift toward the higher carbon content or higher temperature side. In terms of thermodynamics, the Gibbs free energy corresponding to the phase specified as being stable under a particular condition is minimum. The applied magnetic field contributes to the Gibbs free energy of phases, which is a function of magnetization. The main effect of the magnetic field is changing the stability of phases in relation to their magnetic properties. Therefore, it influences the equilibrium conditions, i.e. modifies the phase equilibrium diagram. As the magnetization of the bcc phase in Fe-based alloys is higher than that of the paramagnetic fcc phase, its total Gibbs free energy under the applied magnetic field is considerably lowered, and its stability is correspondingly reinforced. Although the austenitic phase could be magnetized to some extent under a high magnetic field, the magnetization of the ferritic phase is much higher. Thus, in the phase diagram, the ferritic phase area extends at the expense of the austenitic one. Therefore, Ae_3 temperatures are increased and both the carbon content and the temperature of the eutectoid point are increased, as shown in Fig. 4. It can be seen in Tab. 1 that the increase of Ae_3 is a function of the carbon content. With pure iron, the Ae_3 is raised by about 7 C under a magnetic field of 10 Teslas and this observation is in fair agreement with the measurements performed by H. Ohtsuka *et al* [15].

5. Summary

In the present work, the Weiss molecular field model is extended by replacing the molecular field coefficient λ with the short-range ordering coefficient γ around and above T_C. The latter can be written in an Arrhenius-type relation analogous to the diffusion coefficient. The susceptibilities calculated according to the revised model are in good agreement with the ones measured at temperatures above T_C. The itinerate electron model corrected by Sakoh and Shimizu.[10] - which in fair agreement with the results of the measurements made - is adopted for calculating the susceptibilities of fcc Fe. It appears in the phase diagram that the magnetic field enlarges the ferritic phase area and shrinks the austenitic one. With pure iron, the Ae_3 is raised by about 7°C under a magnetic field of 10 Teslas, which is in fair agreement with the measured values [15].

Acknowledgments

The authors gratefully acknowledge the support of the National High Technology Research and Development Program of China (Grant No. 2002AA336010), the key project of National Natural Science Foundation of China (Grant No. 50234020) and the TRAPOYT of MOE of China. The authors are grateful to the support of the AFCRST in the framework of the Franco-Chinese Cooperative Research Project (PRA MX00-03).

References

[1] M. A. Krivoglaz , V. D. Sadovskiy, *Fiz. Metal. Metall.*. **1964**, *18*, 23.

[2] T. Kakeshita, K. Shimizu, S. Funada, M, Date, *Acta Metall.* **1985**, *33*, 1381.

[3] T. Kakeshita, T. Saburi, K. Kindo, S. Endo, *Jpn. J. Appl. Phy.* **1997**, *36*, 7083.

[4] D. Jile, in *Introduction to magnetism and magnetic materials* St Edmundsbury Press Ltd.; **1991**, 259.

[5] M. Shimizu, *Rep. Prog. Phys.* **1981**, *44*, 330.

[6] D. H. Martin, in *Magnetism in Solids* Iliffe books LTD.; London; **1967**, 224.

[7] H. Gao, M. Enomoto, *Mat. Trans., JIM* **2000**, *41*, 911.

[8] W. Sucksmith, R. R. Pearce, *Proc. Roy. Soc.* **1938**, *A167*, 189.

[9] J. W. Dalton, *J. Phys. C: Solid St. Phys.* **1970**, *3*, 1912.

[10] M. Sakoh, M. Shimizu, *J. Phys. Soc. Jan.* **1974**, *37*, 565.

[11] M. Cyrot, *et al*, in *Magnétisme,I-Fondements*, Presses Universitatires de Grenoble, Grenoble, **1999**, 69.

[12] H. B. Chang, Z. G. Li, T. Y. Hsu (Z. Y. Xu), X. Y. Ruan, *Acta Metal. Sinica (English Letters)* **1998**, *11*, 207.

[13] M. Hillert, in *Alloy Diffusion and Thermodynamics* (Chinese translation by H. H. Lai, G. X. Liu) Metallurgy Press of China, Beijing, **1983**, 230.

[14] Z. G. Li., H. B. Chang, T. Y. Hsu (Z. Y. Xu), X. Y. Ruan, *Acta Metal. Sinica (English Letters)* **1998**, *11*, 215.

[15] H. Ohtsuka, Y. Xu, J. K. Choi, Y. Oishi, T. Murai, H. Wada, *Proc. The 3rd International Symposium on Electromagnetic Processing of Materials*, Nagoya, Japan, ISIJ, **2000**, 596.

Chapter 2 Characteristics of Phase Transformation from Austenite to Ferrite in Magnetic field

Introduction

Theoretical simulation results show that magnetic field can considerably shift the Ae_3 line in the Fe-C diagram to the high temperature or high carbon side. Since γ/Fe_3C line remains unaltered, the carbon content of eutectoid point is increased. As a result, the final amount of ferrite obtained from the transformation of austenite will be increased. On the other hand, magnetic field greatly enhances the Gibbs free energy difference between austenite and ferrite, therefore the driving force of the transformation is greatly increased and then the transformation will be accelerated. This means that at high cooling rate the product of the transformation still remains like that obtained at low cooling speed. This could offer an innovative improvement to the conventional annealing during which slow cooling is applied.

In this chapter, the hot-rolled medium carbon content low alloyed steel, 42CrMo, is selected. The transformation from austenite to ferrite at different cooling rates is conducted without and with applying the high magnetic field. The thermodynamic and kinetic influence of the magnetic field is examined both experimentally and theoretically. A rapid annealing method under high magnetic field is put forward after being practically investigated.

The original austenite grain structure of the material after hot rolling is examined to investigate the homogeneity degree of deformation occurring during the hot rolling. Then an experimental setup is designed to allow the transformation from austenite to ferrite to happen in the magnetic field at both slow and fast cooling rates with the magnetic field direction parallel to the hot-rolling direction of the specimens. The influence of the magnetic field together with that of the previous deformation from hot rolling on the formation features of the final microstructures is identified from the point view of nucleation characters and transformation kinetics.

Thermodynamic and Kinetic Characteristics of the Austenite to Ferrite Transformation under High Magnetic Field in a Medium Carbon Steel

Yudong Zhang[a,b], Changshu He[a], Xiang Zhao[a] , Liang Zuo[a], Claude Esling[b*] and Jicheng He[a]
[a] Key Laboratory (Northeasten University), Ministry of Education, Shenyang 110004, P. R. of China
[b] LETAM, CNRS-UMR 7078, University of Metz, Ile du Saulcy, 57045 Metz, France

Abstract: The thermodynamic and kinetic characteristics of austenite-to-ferrite phase transformation in medium carbon steel in the high magnetic fields were investigated. Results showed that the magnetic field could obviously change the $\gamma/\alpha+\gamma$ phase equilibrium - by increasing the amount of ferrite obtained during cooling - and greatly accelerate the transformation. Thus the microstructure obtained under fast cooling with high magnetic field was still ferritic and pearlitic, while that obtained without the magnetic field under the same cooling conditions was bainitic. Exploration in this area contributes both to enriching the new theory on Electromagnetic Processing of Materials (EPM) and to establishing new techniques for materials processing.

PACS: 81.30.-t; 64.70.Kb; 61.50Ks

Keywords: magnetic field, phase transformation, thermodynamics, kinetics, phase equilibrium

1. Introduction

The technique of applying an external physical field, e.g. magnetic field, to the heat treatment of conventional materials to tap their property potential or to improve the existing processing method was initiated in the middle of the past century [1-3]. As the intensity of the magnetic field was much lower than in the present case, the effect was limited. With the current development of superconducting materials and the progress of the cryocooling technique, more than 10-Tesla magnetic field generators are now available. Therefore, performing heat treatment in a high magnetic field is possible. Under the influence of a high magnetic field, new phenomena have emerged in the phase transformation of ferroalloys. Previous work [4-6] has focused on the influence of a magnetic field on the martensitic phase transformation in some materials with lower martensitic transformation start temperatures. Recently, investigation has been launched on the effect of a high magnetic field on high-temperature phase transformations. Special attention has been paid to the transformations between austenite-to-ferrite. Ohtuska and coworkers [7-9] have conducted investigations on the effects of a high magnetic field on the austenite-to-ferrite isothermal transformations in

steels. They found the transformation has been accelerated mainly because of the increase in the nucleation rate of ferrite [7, 8]. They also found that the transformed microstructure appears to align along the magnetic field direction [9]. Many interesting phenomena were revealed.

Quite recently, the present authors have studied the kinetic influence of the high magnetic field on the formation of aligned microstructure in medium carbon steel during the austenite-to-ferrite continuous cooling transformation (the cooling rates were relatively faster). It was found that the magnetic field could obviously lower the nucleation barrier of ferrite and therefore change its nucleation sites [10]. As a continuation of the previous work, the thermodynamic and kinetic effects of the high magnetic field on the austenite-to-ferrite transformation in the same material at different cooling rates are studied in the present work. The possible ways to improve conventional heat treatment are also investigated.

2. Experimental

The material used in this study was 42CrMo, medium carbon low alloyed steel. Its chemical composition is given in Table 1. Specimens of dimensions 20mm×10mm×2mm were cut from a hot rolled rod with their length parallel to the rolling direction. Heat treatments were carried out in the furnace set in a 15-T cryocooled superconducting magnet 52mm in bore size at the High Magnetic Field Laboratory for Superconducting Materials, Institute for Materials Research, Tohoku University [11]. Specimens were kept in the central (zero magnetic force) region, with their longitudinal direction parallel to the axis of the magnet. The austenitization process was performed at 880°C for 33min. Specimens were sorted in two groups according to the cooling conditions, specifically 10°C/min and 46°C/min. An external magnetic field of respectively 6, 10 and 14 Tesla was applied for those cooled down at a rate of 10°C/min, but only 14 Tesla was applied to those cooled down at 46°C/min. Comparative heat treatments without the magnetic field were also carried out under the same heating and the two cooling conditions. The transformed microstructures were etched and observed with an image analyzer. The hardness of specimens cooled at 46°C/min under a 14-Tesla field was also tested.

Table 1 Chemical composition of 42CrMo steel (wt.%)

C	Si	Mn	Cr	Mo	others
0.38~ 0.45	0.20 ~ 0.40	0.50 ~ 0.80	0.90 ~ 1.20	0.15 ~ 0.25	P≤0.04 S≤0.04 Cu≤0.30

3. Results and discussion

3.1 Thermodynamic characteristics

The variation of the area percentage of ferrite in specimens cooled in a magnetic field at the rate of 10°C/min are shown in Fig. 1. It can be seen that the amount of ferrite increases with the magnetic field applied.

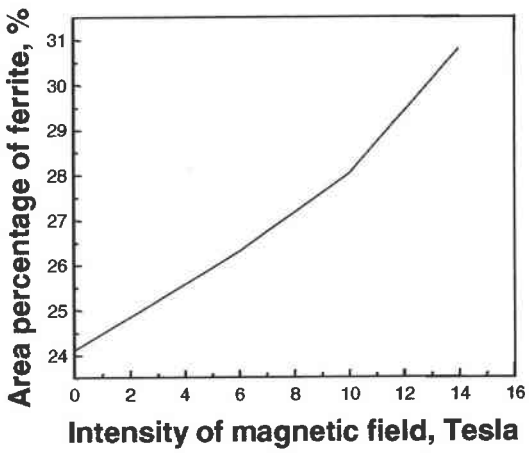

Figure 1 Influence of magnetic field on the amount of ferrite

It is known that both parent austenite and product ferrite can be magnetized to some extent in a high magnetic field. The corresponding Gibbs free energy is lowered by the application of the field. The energy difference resulted from the magnetic field can be expressed as follows:

$$\Delta G^M = -(\int_0^{M^\alpha} \vec{B}_0 \cdot d\vec{M}^\alpha - \int_0^{M^\gamma} \vec{B}_0 \cdot d\vec{M}^\gamma) \qquad (1)$$

where the superscripts α and γ denote ferrite and austenite, M magnetization and B_0 the induction of the applied magnetic field. As the magnetization of ferrite is much higher than that of austenite, a negative ΔG^M - with the same sign as the Gibbs chemical free energy difference- resulted. As a consequence, the equilibrium between the two phases was changed. Previous simulation work [12] has shown that the $\alpha/\alpha+\gamma$ and the $\gamma/\alpha+\gamma$ boundaries in the Fe-C phase diagram shift under a magnetic field towards the high carbon content or high temperatures, as shown in Fig. 2. However, the influence on the latter boundary is more pronounced. According to the 'Metallurgical Lever Law', the amount of ferrite at a given temperature is proportional to the difference between the carbon solubility in austenite and the

carbon content of the steel and inversely proportional to carbon solubility difference between austenite and ferrite at the same temperature, i.e. $\frac{ab(b')}{cb(b')}$, as schematically illustrated in Fig. 2. Therefore, the influence of a magnetic field on the phase equilibrium leads to a larger amount of ferrite, as evidenced by microstructure observation.

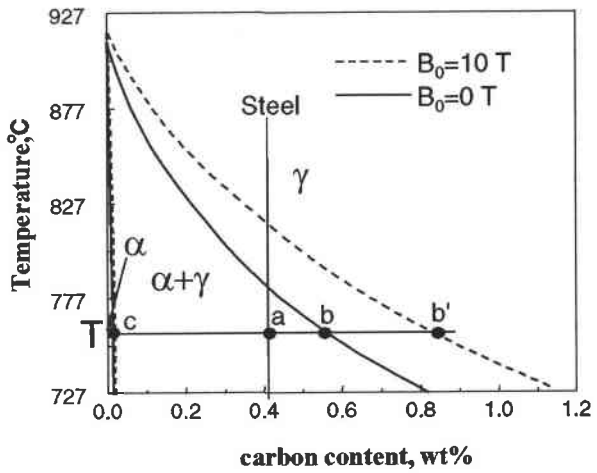

Figure 2 Influence of the magnetic field on the α/γ+α and γ+α/α equilibrium

3.2 Kinetic characteristics

The microstructures obtained under a cooling rate of 46°C/min without and with a 14-Tesla magnetic field are shown in Fig. 3. It can be seen that the microstructure obtained without a magnetic field (Fig. 3 (a)) is mainly composed of bainite, with a slight amount of ferrite (bright areas), whereas the one obtained with a 14-Tesla field (Fig. 3(b)) is still ferritic (bright areas) and pearlitic (dark areas). Ferrite grains and pearlite groups are fine and randomly distributed. Image analyses showed that the area percentage of ferrite obtained at the cooling rate of 46°C/min without the magnetic field is about 2%, whereas it is about 23.1% with the magnetic field. The hardness of these specimens heat-treated under a magnetic field ranges from HB192 to 210.

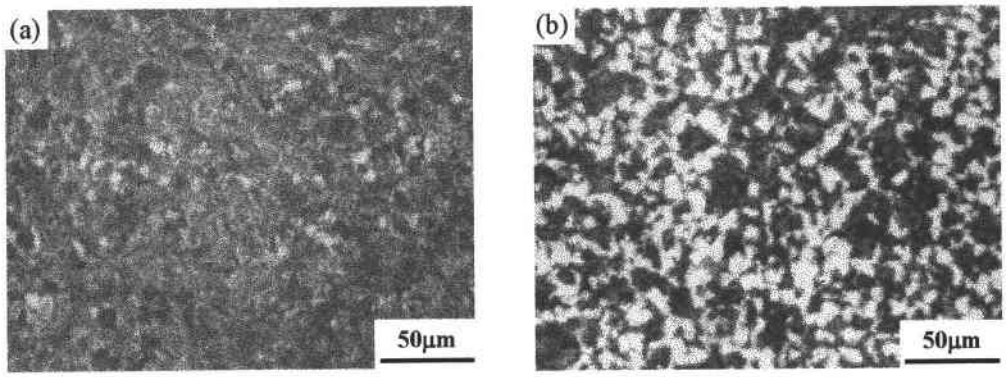

Figure 3 Microstructure of specimen heat treated at 880°C for 33min and cooled at 46°C/min without (a) and with (b) a 14T-magnetic field, Field direction is vertical in the picture

From the Johnson-Mehl equation, the amount of a new phase produced in solid-state phase transformation f is related to its nucleation rate $\dot{N}$, growth rate v and transformation time t:

$$f = 1 - \exp(-\frac{A}{4}\dot{N}v^3t^4) \tag{2}$$

By substituting the nucleation and growth rate equations [13] on the basis of the features of proeutectoid ferritic transformation into the above Johnson-Mehl equation, the kinetic equation of the proeutectoid ferritic transformation from austenite decomposition can be obtained as:

$$\ln t = A\ln(\ln\frac{1}{1-f}) + B\frac{Q}{RT} + C\frac{\sigma^3}{\Delta G_V^{\ 2}} - E\ln\frac{x^\gamma - x}{x^\gamma - x^\alpha} \tag{3}$$

where A, B, C and E are constants; t is the transformation time; Q, R and T are the activation energy for diffusion, the ideal gas constant and the absolute temperature; σ and ΔG_V are the interfacial energy and the Gibbs volume free energy difference between the product and the parent phases; x^γ and x^α are solubility of austenite and ferrite at temperature T, and x carbon content of the steel. The incubation time at different temperatures can thus be obtained by solving the above equation. However, when a magnetic field is introduced, the third and fourth item in Eq. 3 can be affected and change their forms into $C\frac{\sigma^3}{(\Delta G_V + \Delta G^M)^2}$ and $E\ln\frac{x_M^\gamma - x}{x_M^\gamma - x_M^\alpha}$, where the M stands for the magnetic field. By making use of the Weiss

molecular field model and itinerant electron model corrected with orbital susceptibility by Shimizu et al. [14], the magnetization of ferrite and the susceptibility of austenite and correspondingly ΔG^M can be calculated. By applying the KRC model [13], ΔG_V and the composition parameters in Eq. (3) can also be calculated. Final calculation showed that the fourth - or composition- item in Eq. (3) does not change greatly with the magnetic field. The major controlling factor is ΔG^M. The ratio of ΔG^M to $(\Delta G^M + \Delta G_V)$ - the total Gibbs energy difference between the two phases in the magnetic field - is shown in Fig. 4. It can be seen that, as compared with

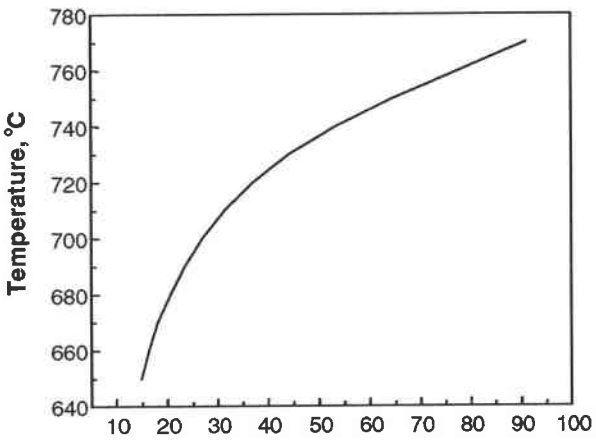

Figure 4 Temperature Variations of $\frac{\Delta G^M}{\Delta G_V + \Delta G^M} \times 100\%$ under 14T

$(\Delta G^M + \Delta G_V)$, ΔG^M is large enough within the whole range of transformation temperatures, especially at higher temperatures; it can greatly reduce the incubation time for austenite-to-ferrite transformation. Consequently, even at the higher cooling rate of 46°C/min, holding time at ferritic and pearlitic transformation temperature range is longer than the incubation time needed in the magnetic field to allow ferrite and pearlite to form and therefore, the high temperature equilibrium microstructure of ferrite and pearlite is obtained. However, in the case of a transformation without the magnetic field, holding time at high temperature is about the same or slightly longer than the incubation time for austenite to ferrite transformation. Thus, only a small amount of austenite transforms into ferrite. When the specimen is cooled down to lower temperatures, the retained austenite transforms completely into bainite. A final microstructure of bainite with only 2% of ferrite is then obtained, according to image analysis. Due to the additional thermodynamic influence exerted by the magnetic field, as above-

mentioned, the amount of ferrite obtained under 14 T at 46°C/min is almost the same as that obtained at the cooling rate of 10°C/min without the magnetic field. Therefore, the thermodynamic and kinetic influence of a high magnetic field result in an equilibrium microstructure produced under a fast cooling rate.

A ferritic and pearlitic microstructure in medium carbon steels or alloyed steels can be obtained through conventional full annealing. The aim of annealing is to adjust the hardness of the work pieces for subsequent machining and also to improve the microstructure for final quenching and tempering.

The optimal hardness for machining is within HB160~230. To obtain it, furnace cooling of about 1 °C/min is required. For 42CrMo, the cooling time from 880 to 550 °C might be 330 minutes or 5.5 hrs. Adding to this both heating and holding times, one furnace batch time is likely to be much longer, depending on the size of the work parts.

However, under the 14-Tesla magnetic field, the situation is greatly improved, both in processing and in the final microstructure. In addition, the hardness of HB192~210 obtained is just within the optimum range and meets the needs of the subsequent machining process. Therefore, fast annealing under high magnetic field offers two improvements. First, cooling time can be reduced to a large extent. In the case of this work and with the present specimen size, it is only 7.2 minutes, which is 45 times shorter than the conventional one. By applying a high magnetic field to full annealing, the furnace batch time can be greatly reduced and the productivity increased accordingly. Second, the microstructure obtained is much finer and the degree of randomness is more pronounced, which is surely beneficial for an improvement of the final properties of the material.

The above results open up a new avenue of investigation to reform the conventional processing methods.

4. Conclusions

The application of a high magnetic field can considerably enhance the total Gibbs free energy difference between the product ferrite and the parent austenite phase and, as a result, the amount of newly formed ferrite is increased and the austenite-to-ferrite phase transformation is accelerated. The two effects put together produce a randomly distributed ferritic and pearlitic microstructure, with an equilibrium amount of ferrite under a fast cooling rate. The application of a high magnetic field opens new avenues to improve the conventional heat treatment methods. Having a better insight into the effect of a high magnetic field is

likely to offer a theoretical base for its practical application.

Acknowledgments

This study was financially supported by the key project of National Natural Science Foundation of China (Grant No. 50234020) and the National High Technology Research and Development Program of China (Grant No. 2002AA336010) and the TRAPOYT in Higher Education Institutions of MOE, P.R.C.

The authors also gratefully acknowledge the support obtained in the frame of the Chinese-French Cooperative Research Project (PRA MX00-03). The authors would like to thank the High Magnetic Field Laboratory for Superconducting Materials, Institute for Materials Research, Tohoku University, for the access to the magnetic field experiments.

References

[1] M. A. Krivoglaz, V. D. Sadovskiy. Fiz. Metal. Metall. 18 (1964) 23.

[2] P. A. Malinen, V. D. Sadovskiy. Fiz. Metal. Metall. 21 (1966) 139.

[3] K. R. Satyanarayan, W. Eliasz, A. P. Miodownik. Acta Metall. 16 (1968) 877.

[4] T. Kakeshita, K. Shimizu, S. Funada, M. Date. Acta Metall. 33 (1985) 1381.

[5] T. Kakeshita, K. Kuroiwa, K. Shimizu, T. Ikeda, A. Yamagishi, M. Date. Mater. Trans. JIM 34 (1993) 415.

[6] T. Kakeshita, T. Saburi, K. Kindo, S. Endo. Jpn. J. Appl. Phys. 36 (1997) 7083.

[7] H. Ohtuska, Y. Xu, J. K. Choi, Y. Oishi, Y. Murai, H. Wada, Proc. of the International Conference on Solid-Solid Phase Transformations '99 (JIMIC-3), Kyoto Park Hotel, The Japan Institute of Metals, (1999) 393.

[8] Y. Xu, H. Ohtuska, H. Wada, Trans. Mater. Res. Soc. Jpn. 25 (2000) 505.

[9] J. K. Choi, H. Ohtuska, Y. Xu, W. Y. Choo, Scripta Mater. 43 (2000) 221-226.

[10] Y. D. Zhang, C. S. He, X. Zhao, L. Zuo, C. Esling, J. Mag. Mag. Mater. Accepted (2004).

[11] K. Watanabe, S. Awaji, M. Motokawa, Y. Mikami. Jpn. J. Appl. Phys. 37 (1998) L1148.

[12] Y. D. Zhang, C. S. He, X. Zhao, L. Zuo, Y. H. Sha, J. C. He, Workshop on New Generation Steel '2001 (2001) 222.

[13] H. B. Chang, Z. G. Li, T. Y. Hsu (Z. Y. Xu) and X. Y. Ruan, Acta Metall. Sinica (English Lett.) 11 (1998) 207.

[14] M. Sakoh, M. Shimizu. J. Phys. Soc. Jan. 37 (1974) 565.

Rapid Full Annealing under High Magnetic Field

Y. D. Zhang[1,2], C. S. He[1], X. Zhao[1], L. Zuo[1], C. Esling[2] and J. C. He[1]
[a]Key Laboratory (Northeasten University), Ministry of Education, Shenyang 110004, P. R. of China
[2]LETAM, CNRS-UMR 7078, Université de Metz, Ile du Saulcy, F-57045 Metz Cedex 01

G. Nishijima, T. Zhang and K. Watanabe
Institute for Materials Research, Tohoku University, Sendai 980-8577, Japan

Abstract

The kinetic effect of a magnetic field on high temperature phase transformation during cooling in 42CrMo steel is investigated. Results show that the magnetic field can considerably increase the driving force for the transformation from austenite to ferrite by enhancing the Gibbs free energy difference between the two phases. Even at the high cooling rate of 46°C/min, the decomposition of austenite in a 14-Tesla high magnetic field is still ferritic and pearlitic, instead of being bainitic as is usually observed. A microstructure of fine and randomly distributed ferrite grains and pearlite colonies is obtained. In addition, this rapid magnetic annealing process can also effectively prevent the formation of the banded structure that occurs commonly during the conventional full annealing due to previous hot working. Image analyses and hardness tests show that the amount of ferrite obtained in this way is almost the same as that obtained by the conventional annealing and the hardness is still within the optimum range for the subsequent machining. Magnetic annealing has thus the merits of improving the microstructure by avoiding banded structure and also optimizing the process by greatly shortening the cooling time. Therefore, it is a promising approach for the innovation of conventional processes. Probing into this issue is of both theoretical significance and technical interest.

Keywords: Structural steel; Magnetic field; Annealing; Microstructure; Phase transformation

Introduction

The study of the influence of a magnetic field on heat treatment and the phase transformations of ferro-alloys was initiated in the middle of the past century. [1, 2] However, most of the literatures [1-6] have focused on martensitic transformation in a limited range of materials with low martensitic start temperatures from the physical, metallographical and crystallographical point of view. Quite recently, with the development of superconducting materials and the progress of cryocooling technique, thermal treatment at higher temperatures in a magnetic field higher than 10 Teslas has been possible and research [7, 8] on the effect of high magnetic field on high-temperature phase transformation has been developed. As the

research is still in its initial stage, it is still basically of the fundamental sort. However, just like most scientific researches, their ultimate goal is to develop practical applications in production and achieve progress in technology. Attempts in applying high magnetic field to practical heat treatment processes are necessary and have technical importance.

In the present work, a medium carbon-content alloyed steel was annealed conventionally without a magnetic field, and annealed rapidly with a 14-T magnetic field. The aim was to investigate the kinetic influence of the magnetic field on the austenite-ferrite transformation from a technological point of view. Moreover, the possible improvement to the conventional annealing process is also analyzed.

Experimental

The material used in this study was 42CrMo, a Chinese structural steel with chemical composition (wt%) of 0.38-0.45%C, 0.90-1.20%Cr, 0.15-0.25%Mo, 0.20-0.40%Si, 0.50-0.80%Mn, ≤0.04%P, ≤0.04%S and ≤0.30%Cu. Specimens of dimensions 20mm×10mm×2mm were cut from a hot-rolled rod* with their longitudinal direction parallel to the rolling direction. Magnetic field heat treatment was carried out in the furnace set in a 15-T cryocooled superconducting magnet of 52mm in bore size at the High Magnetic Field Laboratory for Superconducting Materials, Institute for Materials Research, Tohoku University [9]. Specimens were kept in the central - zero magnetic force - region, with their hot-rolling direction parallel to the axis of the magnet. Magnetic field annealing was performed at 880°C for austenization for 33min. Its cooling was conducted at the rate of 46°C/min within a 14-T magnetic field. Conventional full annealing was carried out in an ordinary chamber furnace. Specimens were heated up to 860°C and isothermal held for 30 min and cooled naturally inside the furnace at a cooling rate of about 1°C/min. The transformed microstructures were etched and analyzed with an image analyzer. Their original austenite grain structure was also obtained and observed. Vicker's hardness was tested with a 5-kg load.

Results

The microstructure obtained by conventional annealing is shown in Fig. 1. It can be seen that it consists of typical ferrite (bright areas) and pearlite (dark areas). Ferrite grains and pearlite colonies aligned alternately along the direction of the previous rolling (horizontal in

* For the composition distribution of the alloyed elements in the material, please consult the Appendix

the picture). The original austenite grain structure was also obtained and shown in Fig. 2. It is found that along the same rolling direction (horizontal in the picture) fine- and coarse-grained zones are alternately distributed; this can be attributed to the inhomogeneous deformation occurring in the hot-rolling stage. The microstructure of the specimens rapidly annealed in the 14-T high magnetic field is shown in Fig 3. It still consists of a typical mixture of ferrite and pearlite, but they are distributed randomly with obviously smaller average sizes. Image analyses show that the area percentage of ferrite is about 24.4% in conventionally fully annealed specimens and about 23.1% in the magnetically rapidly annealed specimens. The two values are very close to each other. Hardness values - expressed as Brinell Hardness - of the specimens rapidly annealed are in the range of HB192~210, which is just within the optimum hardness range of HB160~230 for machining.

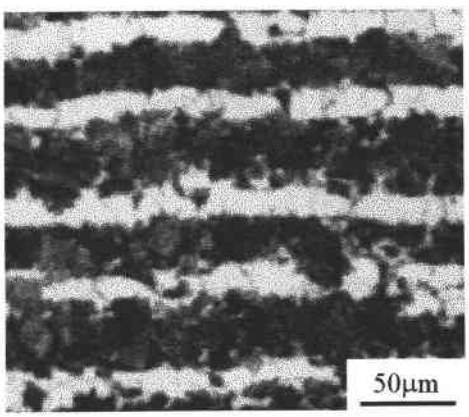

Figure 1 Banded microstructure in 42CrMo obtained by conventional annealing. Specimens were heated up to 860°C for 30 minutes and cooled inside the furnace at a cooling rate of about 1°C/min (the rolling direction is horizontal in the picture)

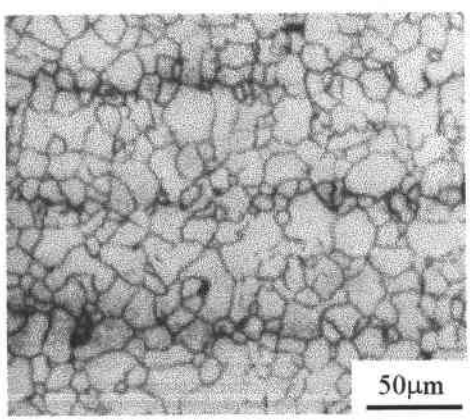

Figure 2 Original austenite grain structure of 42CrMo after rolling (the rolling direction is horizontal in the picture)

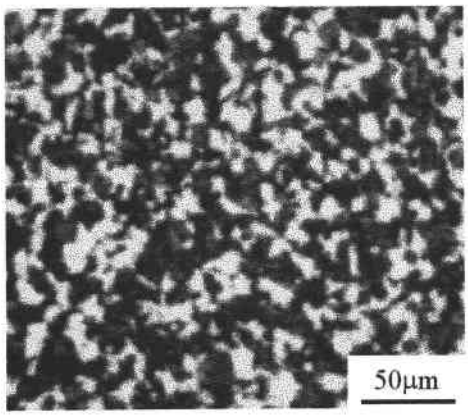

Figure 3 Microstructure in 42CrMo obtained by rapid annealing under a high 14-Tesla magnetic field. Specimens were heated up to 880°C for 33 minutes and cooled at a rate of 46°C /min (the rolling direction is horizontal in the picture)

Discussion

The microstructure in Fig. 1 obtained through conventional full annealing displays the typical banded structure. Its formation can obviously be associated with the previous hot-working stage. As seen in Fig. 2, the original austenite grain sizes are not homogeneous. Fine and coarse grain are distributed alternately along the same rolling direction, which indicates that the previous deformation was not homogeneous. The fine-grained zones used to be the heavily deformed areas, while the coarse-grained zones the weak deformation areas. Evidently, this inhomogeneous austenite grain structure will exert considerable influence on the subsequent phase transformation during annealing. With fully austenitized 42CrMo, austenite transforms first to ferrite between Ar_3 and Ar_1 temperatures and then to pearlite below Ar_1 during the following slow cooling. As furnace cooling in the conventional full annealing is very slow - about 1°C/min, the nucleation of proeutectoid ferrite occurs at higher temperatures with relatively lower undercooling degrees, and thus with a smaller driving force. In such a case, nucleation of ferrite mainly happens on austenite grain boundaries. Considering that grain boundaries are distributed densely within the fine-grained zones, the amount of nucleation in those areas is much higher than that in the coarse-grained ones. With the formation of ferrite, the excessive carbon atoms diffuse out. Then the coarse-grained zones receive more carbon atoms due to the high nucleation rate in the fine-grained zones and become rich in carbon. Consequently, the probability for ferrite nucleation in these areas tends to decrease. Therefore the final banded microstructure of alternately distributed ferrite and pearlite was obtained.

Structural steels with medium carbon content are commonly used to manufacture key structure components under heavy loads such as gearboxes, crankshafts, connecting rods, fastening pieces and the like. Most of them are forged for blanks. Therefore, banded structures

occur easily in subsequent cooling or full annealing whose aim is to modify the microstructure and improve machinability. This kind of microstructure is detrimental to materials as it creates anisotropy in performance; it should therefore be avoided. To eliminate it, normalizing is usually applied. But it always yields a bainitic or martensitic microstructure that is high in hardness and unfavorable to machining, high temperature tempering is indispensable. As the method is not economical in furnace batches and is complicated in operation, it is not satisfactory.

However, rapid annealing in high magnetic field could offer a potential alternative. As seen in Fig. 3, when rapidly cooled at 46°C/min in 14-T after having been fully austenitized at 880°C, the microstructure is still composed of ferrite and pearlite, but they distribute randomly and the grain sizes are smaller than those obtained by conventional annealing. Usually, at such a high cooling rate, the specimens of 42CrMo are composed mostly of bainite [10], but when a 14-T magnetic field is applied, as was done in this work, the microstructure still remains as ferritic and pearlitic. Obviously, the magnetic field has a strong effect to accelerate the transformation from austenite to ferrite.

According to the Johnson-Mehl equation, the amount of a new phase produced during solid state phase transformation f is related to its nucleation rate $\dot{N}$, growth rate v and transformation time t:

$$f = 1 - \exp(-\frac{A}{4}\dot{N}v^3t^4) \tag{1}$$

By substituting the nucleation and the growth rate equations [11] on the basis of the features of proeutectoid ferritic transformation, the kinetic equation of proeutectoid ferritic transformation from austenite can be obtained as follows:

$$\ln t = A\ln(\ln\frac{1}{1-f}) + B\frac{Q}{RT} + C\frac{\sigma^3}{\Delta G_V^2} - E\ln\frac{x^\gamma - x}{x^\gamma - x^\alpha} \tag{2}$$

where A, B, C R and E are constants; Q and T are the activation energy for diffusion and the absolute temperature; σ and ΔG_V are the interfacial energy and the driving force or Gibbs volume free energy difference between ferrite and austenite; x^γ and x^α are the solubility values of austenite and ferrite at temperature T, and x the carbon content of the material. As magnetic properties, such as magnetization or susceptibilities, of the product ferrite and the parent

austenite are different, the applied magnetic field inevitably has an influence on the decomposition of austenite by modifying the stability of both phases. As both austenite and ferrite can be magnetized to some extents in a high magnetic field, their Gibbs free energies will then be lowered. The extra energy difference induced by the magnetic field between these two phases can be expressed as follows:

$$\Delta G^M = W_\alpha - W_\gamma \tag{3}$$

where W_α and W_γ are the energies lowered by magnetic field for ferrite and austenite, respectively. In the case of a transformation in a magnetic field, the third item in Eq. (2) should be complemented by a magnetic term as:

$$C\frac{\sigma^3}{(\Delta G_V + \Delta G^M)^2} \tag{4}$$

Since the degree of magnetization of ferrite is higher than that of austenite, the decrease in the amount of energy is larger for ferrite than for austenite. Thus, ΔG^M is negative i.e. and has the same sign as ΔG_V. As a result, the transformation time from austenite to ferrite in the magnetic field is sufficiently reduced or, in other words, the transformation is greatly accelerated. Therefore, even at a high cooling rate of 46°C/min, the staying time at ferritic transformation temperature range is still sufficient for austenite to transform into ferrite and thus the final microstructure of ferrite and pearlite is obtained. Due to the introduction of ΔG^M, the overall driving force for the transformation into ferrite under the magnetic field is greatly increased and thus the nucleation barrier considerably reduced. As a consequence, ferrite is nucleated at a high nucleation rate. More sites inside austenite grains other than those along their boundaries are available for nucleation. Therefore, the final microstructure of randomly distributed ferrite grains and pearlite colonies with smaller sizes is obtained, as shown in Fig. 3.

In addition, image analysis shows that the area percentage of ferrite obtained by rapid annealing in the 14-T magnetic field is 23.1% and very close to the figure 24.4% obtained by conventional annealing. Besides, the hardness of the specimens rapidly annealed in the 14-T field ranges from HB192 to 210, which lies just within the optimum hardness range of HB160-230 for machining. So the microstructure and hardness of specimens rapidly annealed in the magnetic field fully meet the technical requirements.

It can thus be seen that rapid annealing in a high magnetic field can effectively avoid the formation of the banded microstructure occurring after hot working. Moreover, it improves the microstructure by refining grains and providing a more uniform distribution. Finally, it also greatly enhances the productivity by greatly reducing the cooling time required by conventional annealing. For the specimen size used in the present work, the cooling time from 860°C down to the furnace discharging temperature of 550°C is 300 minutes (5 hours) for conventional annealing, whereas it is only 7.2 minutes for rapid magnetic field annealing, i.e. about 45 times shorter. The above results lead to a promising approach for a reforming of the conventional processing methods.

Conclusions

1. The banded structure in 42CrMo in this work obtained during conventional full annealing is related to the inhomogeneous deformation occurring in the previous hot-rolling process. During the slow cooling of the conventional annealing, the nucleation of ferrite starts at higher temperature with lower undercooling degree. Consequently, the austenite grain boundaries are the main sites for ferrite nucleation. The fine-grained zones resulted from the previous heavy deformation offer more nucleation sites than the coarse-grained zones and finally lead to the formation of the banded microstructure.

2. The magnetic field can obviously increase the driving force for the transformation from austenite to ferrite by increasing the Gibbs free energy difference between the two phases and therefore accelerate the transformation. Even at the high cooling rate of 46°C/min, the decomposition of austenite in the high magnetic field of 14 T is still ferritic and pearlitic, instead of bainitic as usual, with a fine and randomly distributed grain structure. The amounts of ferrite obtained without and with the magnetic field are almost the same and the hardness of the specimens rapidly annealed in the 14-T field is also favorable to the subsequent machining.

3. With the combined merits of an improved microstructure and enhanced process by shortening the cooling time for annealing, thus leaving out additional heat treatments to eliminate the banded structure in one, the rapid annealing in a high magnetic field is a promising approach for an updating of conventional processes. Gaining new insights into the kinetic effect of a high magnetic field on phase transformation is of both theoretical and technical significance.

Acknowledgments

This study was financially supported by the key project of National Natural Science Foundation of China (Grant No. 50234020) and the National High Technology Research and Development Program of China (Grant No. 2002AA336010) and the TRAPOYT in Higher Education Institutions of MOE, P.R.C.

The authors also gratefully acknowledge the support obtained in the frame of the Chinese-French Cooperative Research Project (PRA MX00-03)

References

[1] M. A. Krivoglaz, V. D. Sadovskiy, Fiz. Metal. Metall. 1964, 18, 23-27.

[2] P. A. Malinen, V. D. Sadovskiy, Fiz. Metal. Metall. 1966, 21, 787-788.

[3] T. Kakeshita, K. Shimizu, S. Funada, M. Date, Acta Metall. 1985, 33, 1381-1389.

[4] T. Kakeshita, K. Kuroiwa, K. Shimizu, T. Ikeda, A. Yamagishi, M. Date, Mat. Trans. JIM 1993; 34; 415-422.

[5] T. Kakeshita, T. Yamamoto, K. Shimizu, K. Sugiyama, S. Endo, Mat. Trans. JIM 995, 36, 1018-1022.

[6] T. Kakeshita, T. Saburi, K. Kindo, S. Endo. Jpn. J. Appl. Phys. 1997, 36, 7083-7049.

[7] K. I. Maruta, M. Shimotomai, Mat. Trans. JIM 2000, 41, 902-906.

[8] H. Ohtsuka, Y. Xu, H. Wada, Mat. Trans. JIM 2000, 41, 907-910.

[9] K. Watanabe, S. Awaji, M. Motokawa, Y. Mikami, Jpn. J. Appl. Phys. 1998, 37, L1148-1150.

[10] Y. D. Zhang, Ph. D dissertation, 2003, p. 45.

[11] H. B. Chang, Z. G. Li, T. Y. Hsu (Z. Y. Xu), X. Y. Ruan, Acta Metal. Sinic (English Letters) 1998, 11, 207-214.

New microstructural features occurring during transformation from austenite to ferrite under the kinetic influence of magnetic field in a medium carbon steel

Yudong Zhang[a,b], Changshu He[a], Xiang Zhao[a] , Liang Zuo[a], Claude Esling[b*], Jicheng He[c]

[a] Liaoning Key Laboratory of NMT, Northeastern University, Shenyang 110004, China

[b] LETAM, CNRS-UMR 7078, University of Metz, Ile du Saulcy, 57045 Metz, France

[c] Key Laboratory (Northeasten University), Ministry of Education, Shenyang 110004, P. R. China

Abstract:

The effects of magnetic field on nucleation barrier of the phase transformation from austenite to ferrite at different cooling rates in 42CrMo steel have been investigated. The aligned microstructures of ferrite and pearlite along the magnetic field direction (parallel to the hot-rolling direction) are obtained at a cooling rate of 10 °C/min, which are resulted from the kinetic effects of the applied magnetic field during cooling and the microstructural influences of an inhomogeneous deformation occurring during the previous hot rolling. In this case, the formation of ferrite grains at higher temperatures is attributed mainly to the preferential nucleation at austenite boundaries. However, a fairly uniform microstructure of randomly distributed ferrite and pearlite is formed at a high cooling rate of 46 °C/min in the magnetic field of 14 T, as a result of both intergranular and intragranular nucleations at relatively low temperatures. Probing into this issue is helpful to gain a better understanding of kinetic influences of magnetic field on the phase transformation from austenite to ferrite.

PACS: 81.30.-t; 64.70.Kb; 61.50Ks

***Keywords*:** Steel, Magnetic field; Phase transformation; Microstructure; Orientation.

1. Introduction

The magnetic properties of various phases in ferro-alloys are known to be quite different, due to their differences in structure. The application of an external magnetic field may thus have considerable influences on their phase transformations during heating and cooling. With the development of superconducting materials and the progress of cryocooling techniques, more than 10 Teslas magnetic field generators have been available, which make heat treatments in a high magnetic field possible. So far, a number of investigations have been

* *Claude Esling. Tel.: +33 3 87315390; Fax: +33 3 87315377
E-mail address: esling@letam.sciences.univ-metz.fr

devoted to the possible effects of magnetic fields on lower temperature martensitic transformation [1-6]. Recently, the high temperature diffusion-controlled phase transformations of steels in magnetic field have attracted wide attention and been investigated from the thermodynamic [7, 8], kinetic [9, 10] and metallographical [11-13] points of view. The strong effect of high magnetic field on the ferrite nucleation rate has been quantitatively evidenced by Xu et al. [14]. However, the high temperature diffusion-controlled phase transformation is a complicated thermodynamic and kinetic process concerning nucleation and growth of product phases, the clear and thorough understanding of the acting mechanism of magnetic field is still not reached. Further research on the kinetic influences of magnetic field on the nucleation of product phases is of fundamental interest.

In this study, the magnetic heat treatments were performed on a hot-rolled 42CrMo steel rod. The possible influences of magnetic field and cooling rate on the nucleation of ferrite during the phase transformation from austenite were investigated from the view point of microstructural features.

2. Experimental

The chemical composition of 42CrMo steel is given in Table 1. Specimens of dimensions 20 mm × 10 mm × 2 mm were cut from a hot-rolled rod with their longitudinal direction parallel to the hot-rolling direction. The magnetic heat treatments were carried out with the furnace installed in a 15 T cryocooled superconducting magnet with a bore size of 52 mm in diameter [15]. The specimens were kept in the central - zero magnetic force - region, with their longitudinal (hot-rolling) direction parallel to the axis of the magnet (magnetic field direction). The austenitization process was performed at 880 °C for 33 min (Ac_3 = 780 °C). While the specimens were cooled down with a slow cooling rate of 10 °C/min, the external magnetic fields of respective 6, 10 and 14 T were applied. For comparison, the non-magnetic heat treatment was also carried out under the same heating and cooling conditions. Moreover, a high cooling rate of 46 °C/min in the magnetic field of 14 T after the austenization was also selected, as to investigate some possible influences of cooling rate on the phase transformation in a high magnetic field

The microstructures of the specimens after heat treatments, as well as their original austenite grain structure, were examined by optical microscopy. For the specimen cooled at the rate of 10 °C/min in the magnetic field of 14 T, the crystallographic orientations of manually selected 209 ferrite grains were determined by means of the EBSD technique and

presented in the form of inverse pole figures.

3. Results

The original austenite grain structure of 42CrMo after hot rolling is shown in Fig. 1. It is seen that fine- and coarse-grained zones are distributed alternatively along the hot-rolling direction (vertical in the picture), which correspond to relative heavy and weak deformation areas arising from an inhomogeneous deformation in the hot rolling stage. The microstructures of the specimens fully austenitized and cooled at 10 °C/min without and with a magnetic field are shown in Fig. 2 and Fig. 3, respectively. In the both cases, they are composed of ferrite grains (bright areas) and pearlite colonies (dark areas) that are nearly equiaxed with basically uniform sizes. For the non-magnetic heat treatment, only a few of ferrite grains and pearlite colonies align along the hot-rolling direction but most of them are distributed randomly (Fig. 2). However, they tend to align themselves to the direction of the applied magnetic field, and such a tendency becomes stronger with the increasing magnetic field (Fig. 3(a), 3(b) and 3(c)). Fig. 4 shows the inverse pole figures of the aligned ferrite grains in the specimen after cooling at 10 °C/min with a magnetic field of 14 T, where the longitudinal direction of the specimen is parallel to the applied magnetic field direction. As the polar densities of the longitudinal and normal directions of the specimen are quite uniform within the crystallographic triangles in Fig. 4, there exist no preferred grain orientations in those ferrite chains although the easy magnetization directions of ferrite are <100>. This may suggest non-preferential nucleation and growth of ferrite grains in the applied magnetic field. When increasing the cooling rate to 46 °C/min in the magnetic field of 14 T, the obtained microstructure is still characteristic of ferrite and pearlite but no alignment appears and the average sizes of ferrite grains and pearlite colonies become smaller, as shown in Fig. 5.

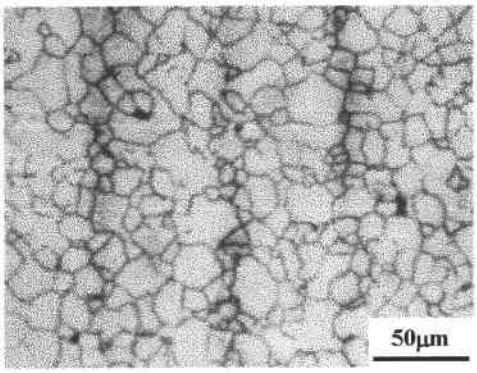

Figure 1 The original austenite grain structure after hot rolling. (The rolling direction is vertical in the picture)

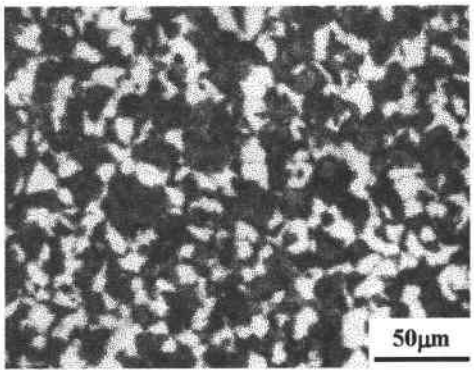

Figure 2 Microstructure of specimen heated at 880°C for 33min and cooled at 10°C/min without a magnetic field. (the rolling direction is vertical in the picture)

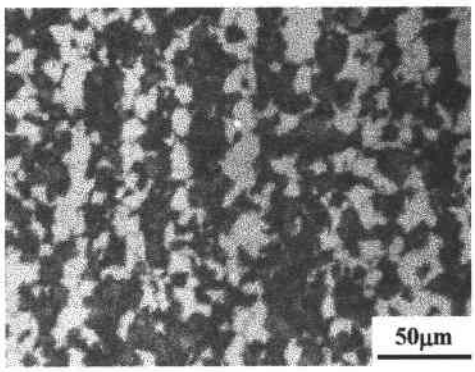

(a) 6 Tesla

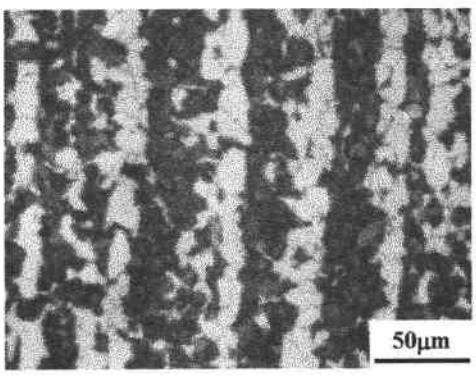

(b) 10 Tesla

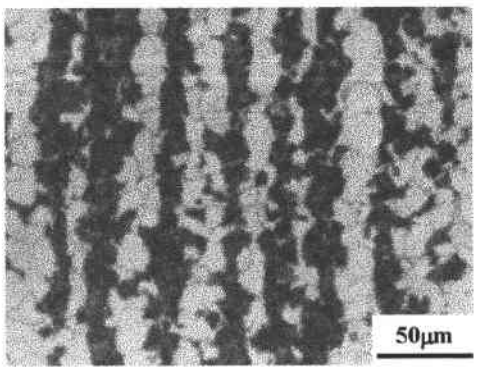

(c) 14 Tesla

Figure 3 Microstructures of specimens heated at 880°C for 33min and cooled at 10°C/min with magnetic field. (The magnetic field direction and hot-rolling direction are vertical in the pictures)

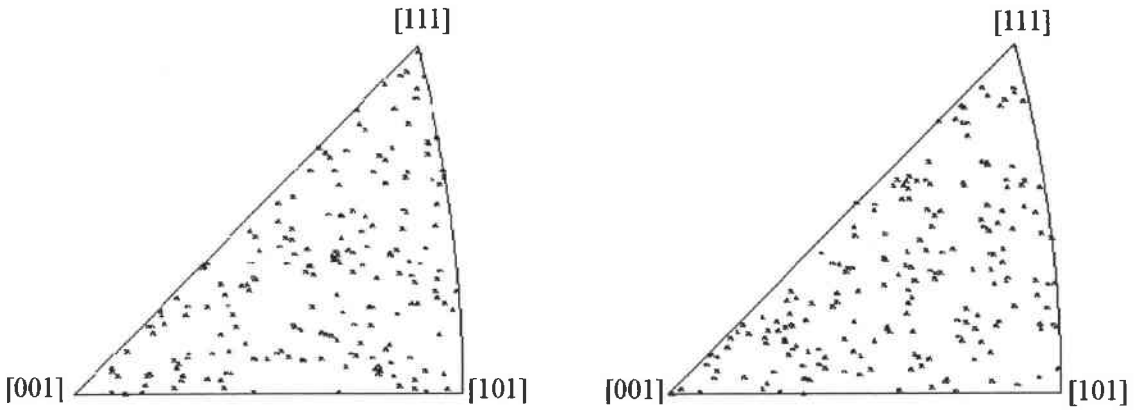

(a) Longitudinal direction (b) Normal direction

Figure 4 EBSD inverse pole figures of aligned ferrite grains formed in 14T at a cooling rate of 10□/min.

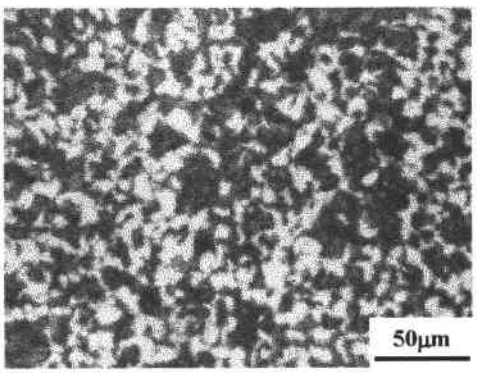

Figure 5 Microstructure of specimen heated at 880°C for 33min and cooled at 46°C/min with a magnetic field of 14T. (The magnetic field direction and hot-rolling direction are vertical in the picture)

4. Discussion

For fully austenitized 42CrMo, austenite transforms first to ferrite between Ar_3 and Ar_1 temperatures and then to pearlite below Ar_1 during subsequent slow cooling. Since the magnetization of the product ferrite is different from that of the parent austenite, the nucleation and growth of ferrite grains might be affected by the applied magnetic field. However, as the shapes of the ferrite grains obtained without and with a magnetic field do not change much and, in addition, there appear no preferential crystallographic orientations along the magnetic field direction, the influence of the magnetic field would be mainly on the nucleation stage.

According to [16], the nucleation rate of a new phase in solid phase transformation can be expressed as

$$\dot{N} = N_0 \exp(-\frac{Q}{RT}) \exp(-\frac{\Delta G^*}{RT}) \tag{1}$$

Where N_0 is a constant, Q the diffusion activation energy, R gas constant and T the absolute temperature. The nucleation barrier ΔG^* reads

$$\Delta G^* = C \frac{\sigma^3}{\Delta G_v^2} \tag{2}$$

where C is a constant, σ the interfacial energy between the newly formed phase and the parent phase and ΔG_v the Gibbs volume free energy difference between the two phases or the driving force of the transformation. σ does not change much with temperature, while ΔG_v strongly depends on temperature and increases greatly with decreasing temperature or increasing undercooling degree. For the nucleation at a given temperature, it is governed by the two exponential terms (or the diffusion and nucleation barrier terms) in Eq. (1). But they are always in a conflicting state. The diffusion term favors to high temperature nucleation owing to the easiness in atom diffusion but then the nucleation barrier is high as ΔG_v is small and cannot counterbalance the increase of σ. On the other hand, the nucleation barrier term favors to low temperature nucleation due to relative low nucleation barrier but then atom diffusion becomes difficult. Therefore, there may reach a compromise through changing the nucleation sites. When nucleation happens at high temperature, as it is the case for slow cooling, the interfaces of parent phase, especially triple boundaries, are the main nucleation sites for the new phase formation. The increased energy due to the creation of new interfaces between the product and the parent phases can be lowered by consumption of the existing grain boundary energy. Oppositely, when nucleation happens at relatively low temperature, as the case for fast cooling, the nucleation barrier is small owing to the large ΔG_v, and nucleation happens not only along parent phase boundaries but also at energetically favored sites inside parent grains.

In the present work, as parent austenite grains are not uniform in size and grain boundaries are more curved and densely distributed within the fine-grained zones than those in the coarse-grained zones (Fig. 1), the grain boundary energy in the fine-grained areas is generally higher than that in the coarse-grained ones. If ferrite nucleates mainly on austenite boundaries, the nucleation rate would be higher in the fine grain zones, along which there may

form ferrite grain chains or bands, as previously observed at a very low cooling rate of about 1 °C/min [10]. However, there appears no obvious ferrite alignment when cooling at 10 °C/min without a magnetic field (Fig. 2). It means that the cooling is fast enough so that the cumulated time at higher temperatures is not long enough to allow ferrite to nucleate. Therefore, ferrite is formed at relatively low temperatures with high undercooling degrees (or driving force) and thus the ferrite nucleation occurs not only along parent austenite boundaries but also at energetically undulating sites at grain interiors. Consequently, the final microstructure consists of randomly distributed ferrite and pearlite.

When a high magnetic field is applied at the cooling rate of 10 °C/min, ferrite grains and pearlite colonies align themselves alternately along the hot-rolling direction (the magnetic field direction), as shown in Fig. 3. It is known that the magnetization of ferrite is higher than that of austenite. The Gibbs free energy of ferrite can be lowered more than that of austenite by the applied magnetic field. For the transformation from austenite to ferrite, the total Gibbs free energy difference (or driving force) ΔG_v in Eq. (2) is then replaced by $\Delta G_v + \Delta G^M$, where ΔG^M is the magnetic-field induced energy change and has the same sign as that of ΔG_v [10]. ΔG^M is also temperature dependent and increases with the increasing undercooling degree. Therefore, on one hand, the nucleation barrier ΔG^* of ferrite is reduced and the ferrite nucleation could happen at higher temperatures. On the other hand, as the driving force for the transformation is increased by the magnetic field, the transformation is accelerated and the transformation time can be reduced as analyzed elsewhere [10]. In consequence, the cumulated time at higher temperatures is long enough for ferrite to nucleate at the cooling rate of 10 °C/min, and austenite grain boundaries and triple junctions are the dominant nucleation sites. It should be emphasized that the fine-grained zones in Fig. 1 have advantage in the nucleation rate of ferrite over those coarse-grained zones.

Furthermore, the magnetization of ferrite nuclei leads to their one end along the magnetic field direction N pole and the other end in the opposite direction S pole. When the magnetic field is applied along the hot-rolling direction, the alignment of ferrite nuclei along the applied magnetic field direction would make one nucleus's S pole just on the top of its neighboring nucleus's N pole, as schematically shown in Fig. 6. The interaction between the N and S poles could lower the total energy of the whole system and further drive the subsequent formation of ferrite nuclei in the area to create ferrite chains. The attraction between ferrite grains along the magnetic field direction is increased with the increasing magnetic field, and the tendency of the ferrite alignment would become stronger. With the progress of the transformation,

excess carbon atoms diffuse out from newly formed ferrite nuclei. The preferential nucleation of ferrite along the magnetic field direction makes the diffusion happen in its transverse direction. The coarse-grained austenite zones thus receive more carbon atoms from the fine-grained zones and become rich in carbon. Then the formation of ferrite within these carbon-rich zones becomes difficult. When temperature goes below Ar_1, these areas transform into pearlite. Finally, there results in a microstructure consisting of alternately aligned ferrite grains and pearlite colonies along the magnetic field (hot rolling direction).

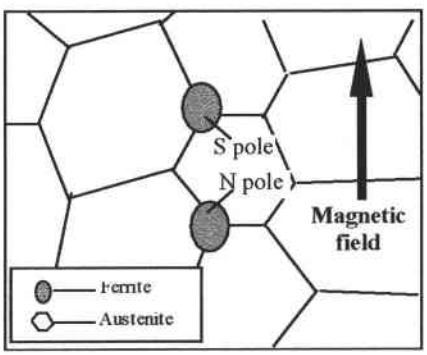

Figure 6 The schematic illustration of nucleation of ferrite at austenite grain boundary triple junctions along magnetic field direction.

When cooling at a high rate of 46 °C/min in the magnetic field of 14 T, the transformed microstructure does not show an alignment feature and the average sizes of ferrite grains and pearlite colonies become rather small (Fig. 5). In this case, the holding time at higher temperature is greatly reduced and the nucleation is postponed to lower temperatures owing to the insufficient time for atom diffusion. It leads to higher undercooling degrees and greatly increased undercooling dependent items ΔG_v and ΔG^M. Thus, the nucleation barrier ΔG^* is considerably reduced. More sites in addition to those favored to ferrite chains are available for nucleation. Therefore, the final microstructure is obtained of randomly distributed ferrite grains and pearlite colonies with smaller sizes.

5. Conclusions

1. The imposition of a magnetic field during the phase transformation from austenite to ferrite increases the value of Gibbs free energy change by introducing an extra magnetic energy difference between parent austenite and product ferrite. As a consequence, the

nucleation barrier of ferrite is lowered and the transformation is accelerated.

2. When cooling at a rate of 10 °C/min, the contribution of an applied magnetic field in lowering the nucleation barrier and accelerating the transformation makes the nucleation of ferrite at higher temperatures. The nucleation occurs preferentially along austenite grain boundaries, especially triple junctions. Due to the inhomogeneous deformation of the previous hot rolling and the dipolar attraction between ferrite nuclei in the magnetic field, the final microstructure of alternately distributed ferrite grains and pearlite colonies along the magnetic field direction is obtained.
3. When the cooling rate reaches 46 °C/min, the nucleation at higher temperatures is greatly inhibited due to insufficient time for atom diffusion. At lower temperatures, more sites inside austenite grains in addition to those on grain boundaries are available for the ferrite nucleation. The final microstructure is characteristic of randomly distributed ferrite grains and pearlite colonies with smaller sizes.

Acknowledgments

This work was supported by the National Science Fund for Distinguished Young Scholars (Grant No. 50325102), the National Natural Science Foundation of China (Grant No. 50234020) and the National High Technology Research and Development Program of China (Grant No. 2002AA336010). We also gratefully acknowledge the support in the frame of the Key International Science and Technology Cooperation Program.

The authors would like to thank the High Magnetic Field Laboratory for Superconducting Materials - Tohoku University, Japan, for the access to the magnetic field facilities.

References

[1] M. A. Krivoglaz, V. D. Sadovskiy. Fiz. Metal. Metall. 18 (1964) 23.

[2] P. A. Malinen, V. D. Sadovskiy. Fiz. Metal. Metall. 21 (1966) 139.

[3] K. R. Satyanarayan, W. Eliasz, A. P. Miodownik. Acta Metall. 16 (1968) 877.

[4] T. Kakeshita, K. Shimizu, S. Funada, M. Date. Acta Metall. 33 (1985) 1381.

[5] T. Kakeshita, K. Kuroiwa, K. Shimizu, T. Ikeda, A. Yamagishi, M. Date. Mater. Trans. JIM 34 (1993) 415.

[6] T. Kakeshita, T. Saburi, K. Kindo, S. Endo. Jpn. J. Appl. Phys. 36 (1997) 7083.

[7] H. D. Joo, S. U. Kim, N. S. Shin, Y. M. Koo, Mater. Lett. 43 (2000) 225.

[8] H. Guo, M. Enomoto. Mater. Trans. JIM 41 (2000) 911.

[9] M. Enomoto, H. Guo, Y. Tazuke, Y. R. Abe, M. Shimotomai. Metall. Mater. Trans. 32A

(2001) 445

[10] Y. D. Zhang, C. S. He, X. Zhao, C. Esling, L. Zuo, Adv. Eng. Mater. (2004), accepted.

[11] K. I. Maruta, M. Shimotomai. Mater. Trans. JIM 41 (2000) 902.

[12] H. Ohtsuka, Y. Xu, H. Wada, Mater. Trans. JIM 41 (2000) 907.

[13] M. Shimotomai, K. Maruta, K. Mine, M. Matsui. Acta Mater. 51 (2003) 2921.

[14] Y. Xu, H. Ohtsuka, H. Wada, J. K. Choi. Trans. Mater. Res. 25 (2000) 505.

[15] K. Watanabe, S. Awaji, M. Motokawa, Y. Mikami. Jpn. J. Appl. Phys. 37 (1998) L1148.

[16] T. Y. Hsu, Theory of Phase Transformation, Science Press of China, Beijing, 1988.

Chapter 3 Tempering Behaviors in High Magnetic Field

Introduction

Tempering is an important procedure in materials heat treatment processes, as it directly affects the final performances of materials. The most important structural change is the precipitation of various carbides since the supersaturation of the as-quenched martensite is relieved and equilibrium mixtures of phases are approached with increasing temperature. The process offers versatility as at different stages carbides have different crystal structures and different carbon contents. Another structural phenomenon is the recovery and recrystallization of the matrix at temperatures above 500°C. Unlike the research areas concerning martensitic, ferritic and pearlitic transformations, the influence of magnetic field on carbide precipitation behaviors and matrix recovery behaviors, up to now, has received little attention and has yet not much been studied and exploited. As there still exists the magnetization difference between the parent and product phases, the introduction of magnetic field may introduce influence. Moreover, tempering processes (after quenching) directly determine the final properties of materials; therefore study on this aspect will eventually bring about new microstructure modification and property control methods. Research on this topic is important and of both theoretical and technical significance.

In this chapter, The transformation behaviors in the high magnetic field during high temperature tempering (600 and 650°C) are experimentally examined. The morphology difference of cementite due to the introduction of the magnetic field is analyzed from the point view of interfacial energy and magnetostrictive strain energy. The influence of the magnetic field on the progress of recovery of the matrix and on the texture characteristics of the recovered parts is also investigated experimentally.

The precipitation behavior under high magnetic field during low temperature tempering (200°C) and its subsequent influence on mechanical properties are also experimentally investigated. The effect of magnetic field on precipitation sequence of transition carbides is analyzed thermodynamically. The influential mechanism is clarified.

High temperature tempering behaviors in a structural steel under high magnetic field

Yudong Zhang[a,b], Nathalie Gey[b], Changshu He[a], Xiang Zhao[a] , Liang Zuo[a], Claude Esling[b*]
[a]Key Laboratory (Northeasten University), Ministry of Education, Shenyang 110004, P. R. China
[b] LETAM, CNRS-UMR 7078, University of Metz, Ile du Saulcy, 57045 Metz, France

Abstract

An as-quenched structural steel is tempered at 600 and 650 °C for 1 h without and with a 14-T magnetic field. The magnetic field can effectively prevent the directional growth of cementite along martensite plate boundaries and twin boundaries by increasing both the cementite/ferrite interfacial energy and the magnetostrictive strain energy. Finally, particle-like cementite is obtained. Moreover, the magnetic field can obviously retard the formation and growth of 'distortion-free' regions in the matrix, though without having any noticeable effect on the orientation distribution of the 'distortion-free' part. Investigating this subject contributes to the understanding of the way a magnetic field influences phase transformation in solid metallic materials.

Keywords: tempering; precipitation; magnetic field; recovery; orientation.

Introduction

The application of a magnetic field to solid phase transformation in steels has been a subject of much attention in materials science. If the parent and product phases have different saturation magnetization and are open to transformation under the magnetic field, the temperature and extent of transformation can be considerably affected as the Gibbs free energy of a phase can be lowered by an amount corresponding to its magnetization [1 and 2]. This effect was first investigated theoretically and experimentally using several ferro-alloys undergoing non-diffusional martensitic transformation [3, 4, 5, 6 and 7]. Quite recently, attention has shifted to high-temperature diffusion-controlled transformations. Research on this topic focuses on the following aspects: (1) theoretical simulation of the effect of the magnetic field on the ferrite/austenite and austenite/ferrite phase equilibrium [1]; (2) morphological features appearing during ferrite-to-austenite [8] and austenite-to-ferrite [9 and 10] transformation; (3) kinetic characteristics of proeutectoid ferrite transformation under a magnetic field [11]. Another important research topic in solid-state phase transformation under a magnetic field has been recrystallization and recrystallization texture development in deformed ferromagnetic materials [12, 13, 14 and 15]. Obvious retardation of recovery and

recrystallization and enhancement of <001> texture component along the direction of magnetic field appeared in most of the materials investigated during magnetic field annealing. As there are various types of diffusional phase transformation, research under a magnetic field is restricted to limited subjects. So far, the transformation resulting from oversaturation, i.e., precipitation in a magnetic field and the influence of the magnetic field on the recovery or recrystallization due to lattice distortion from oversaturation of solutes have seldom been reported. Studying these aspects is certainly necessary and helpful to extend magnetic field application in materials science. High-temperature tempering is an ideal object for this study.

The purpose of the present work is to investigate the growth behavior of cementite in a structural steel under a high magnetic field and evidence the influence of the magnetic field on recovery and orientation distribution characteristics of the matrix. Insight into these issues is of great theoretical significance.

Experimental

The material used in this study was 42CrMo structural steel with the following chemical composition (wt%): 0.38–0.45%C, 0.90–1.20%Cr, 0.15–0.25%Mo, 0.20–0.40%Si, 0.50–0.80%Mn, ≤0.04%P, ≤0.04%S and ≤0.30%Cu. Specimens of dimension 55 mm × 10 mm × 2 mm were cut from the hot-rolled rod with their longitudinal direction parallel to the hot-rolling direction. They were then heated up to 860 °C and held for 20 min followed by water quenching to obtain a martensitic microstructure for subsequent tempering. Both magnetic tempering and non-magnetic tempering were carried out at 600 and 650 °C for 60 min in the same furnace installed in a 15-T cryocooled superconducting magnet of 52 mm in bore size [16]. The specimens were placed in the central (zero magnetic force) region with their longitudinal direction parallel to the magnetic field direction (MFD). In the case of the magnetic tempering, a 14-T high magnetic field was applied during the whole heating, isothermal maintaining and cooling processes.

After the above thermal treatment, the specimens were cut out lengthwise for SEM and TEM observation, EBSD measurements and mechanical tests for strength and impact toughness. Non-standard tensile and Charpy impact specimens were used, as shown in Fig. 1. The morphology of the as-quenched martensite and its substructure were examined using a Philips CM 200 LaB_6 cathode TEM. Carbide precipitates were observed with a JEOL JSM-6500F SEM. The area percentage of carbide was analyzed with the Aphelion software. The

EBSD technique was used to analyze the recovery behavior of the matrix. The Orientation Imaging Microscopy (OIM) analysis was performed with the same FEG SEM equipped with the HKL's Channel 5. The 'beam controlled' mode was applied with a step size of 50 nm. The areas analyzed in each sample covered about 8–10 original austenite grains. Tensile tests were carried out on a Shimadzu AG-5000A unit with a load of 2500 kg, and Charpy impact tests were conducted on a JB-5 Charpy impact machine with a maximum measurement range of 29.4 J. The fractographs of the tensile and impact specimens were also observed with the SEM.

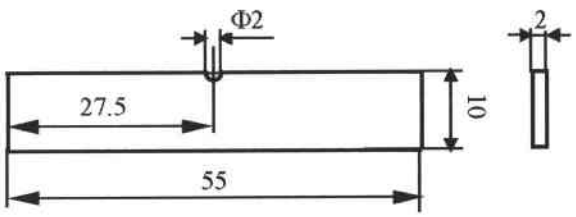

(a) Charpy impact specimen

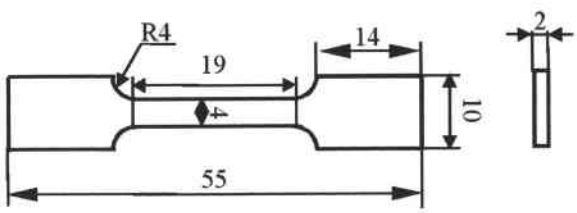

(b) Tensile specimen

Figure 1 Illustration of the tensile and the Charpy specimens

Results

The microstructure of the as-quenched specimen in Fig. 2 shows martensitic plates. Their substructure is composed mostly of micro-twins, as displayed in Fig. 3. When tempered at 600 and 650 °C for 1 h, without and with a 14-T magnetic field, carbides precipitate in the two cases, as shown in Fig. 4 and Fig. 5. The pronounced difference lies in their morphology. Without magnetic field, two different carbide morphologies are present: the one is strip-like and the other one is particle-like. Most of the strip-like carbides are in parallel arrays. With

the magnetic field, the morphology of the carbide is either of the short-bar (Fig. 4(b)) or particle-like (Fig. 5(b)) type, and the degree of spheroidization increases with increasing tempering temperature. No preferential distribution of carbides along the MFD is observed. The area percentages of carbides obtained without and with the magnetic field are shown in Table 1. It can be seen that – at the same temperature – the amounts of carbide formed without and with the field are almost equal.

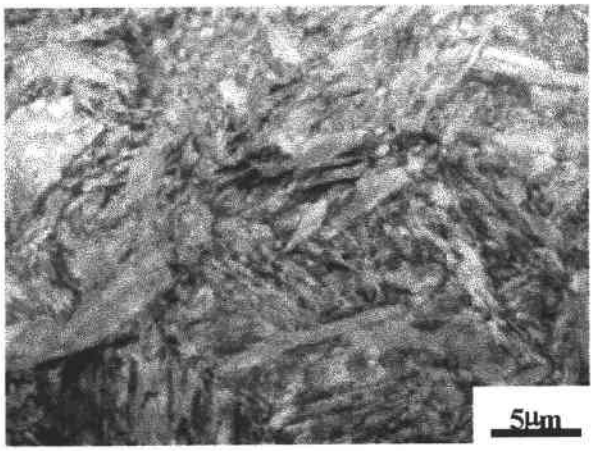

Figure 2 TEM bright field morphology of martensite obtained by water quenching from 860°C

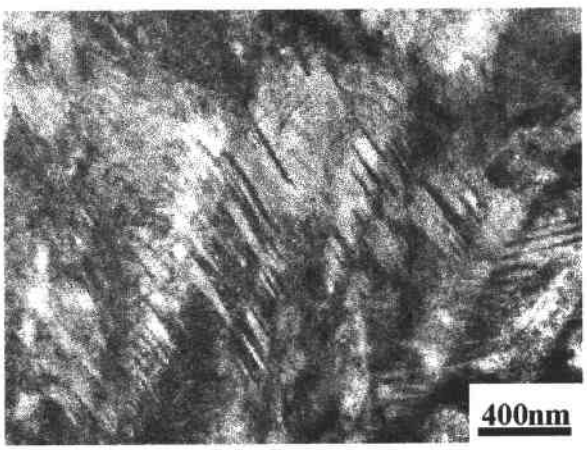

Figure 3 TEM bright field morphology of micro-twins inside martensite plates.

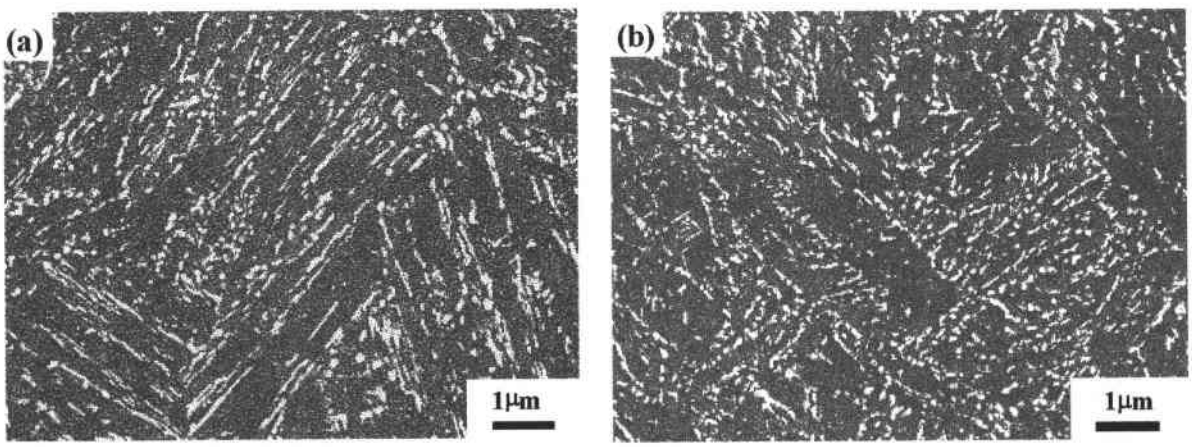

Figure 4 SEM micrographs of carbides obtained by tempering at 600°C for 1 h (a) without magnetic field; (b) with a magnetic field of 14 T. The field direction is vertical. SEM secondary electron images

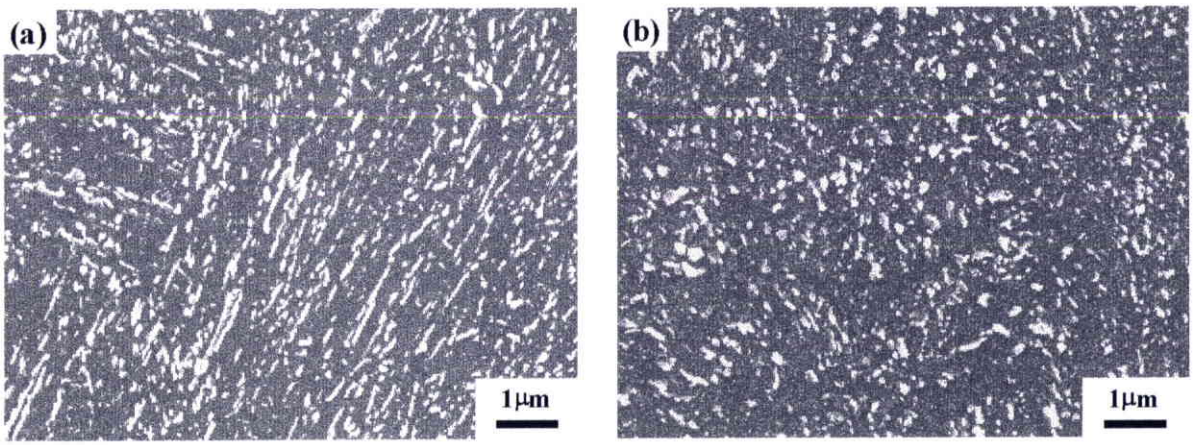

Figure. 5 SEM micrographs of carbides obtained by tempering at 650°C for 1 h (a) without magnetic field; (b) with a magnetic field of 14 T. The field direction is vertical. SEM secondary electron images

Table 1 Area percentage of the cementite

	0T	14 T
600°C for 60min	15.76%	15.30%
650°C for 60min	16.91%	16.74%

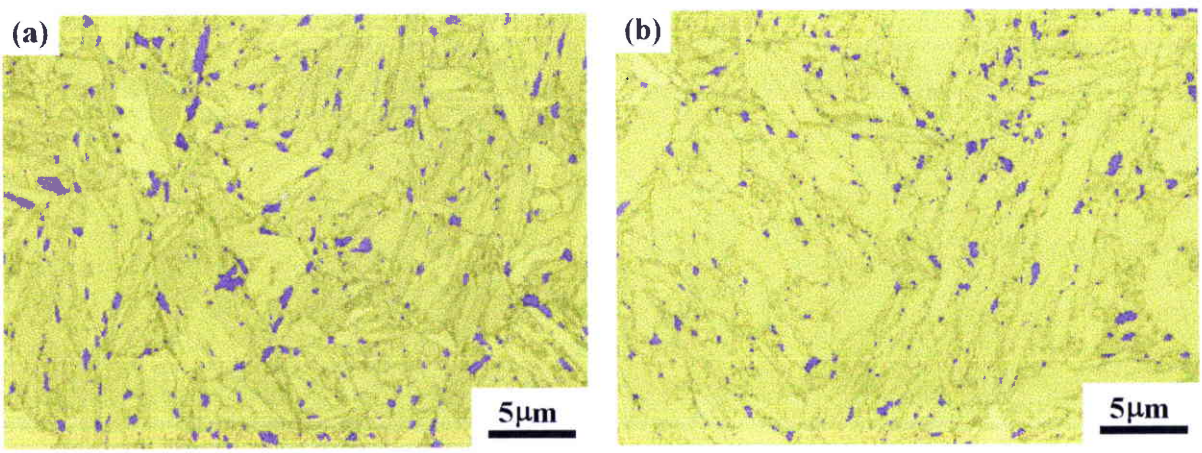

Figure 6 OIM maps of specimens tempered at 600 for 1 h (a) without field and (b) with a magnetic field of 14 T. The field direction is vertical.

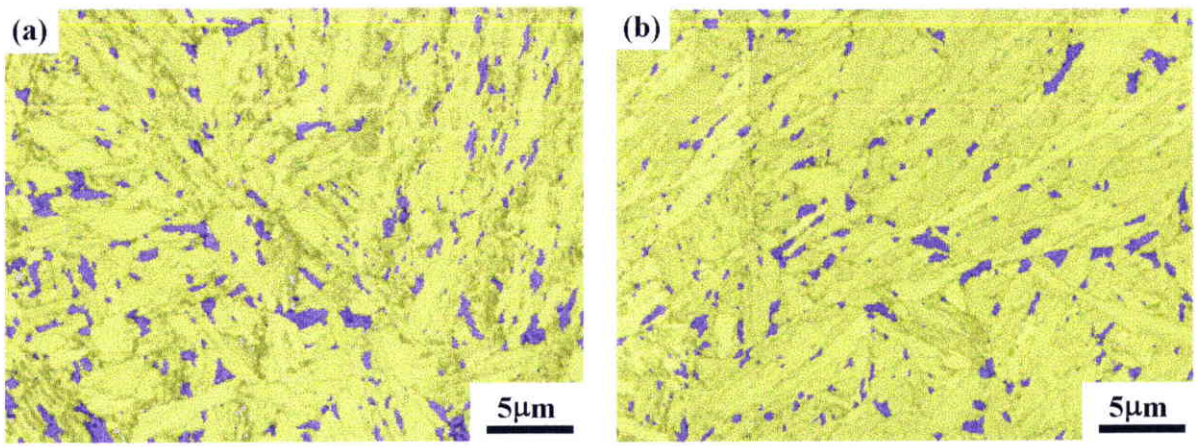

Figure 7 OIM maps of specimens tempered at 650 for 1 h (a) without field and (b) with a magnetic field of 14 T. The field direction is vertical.

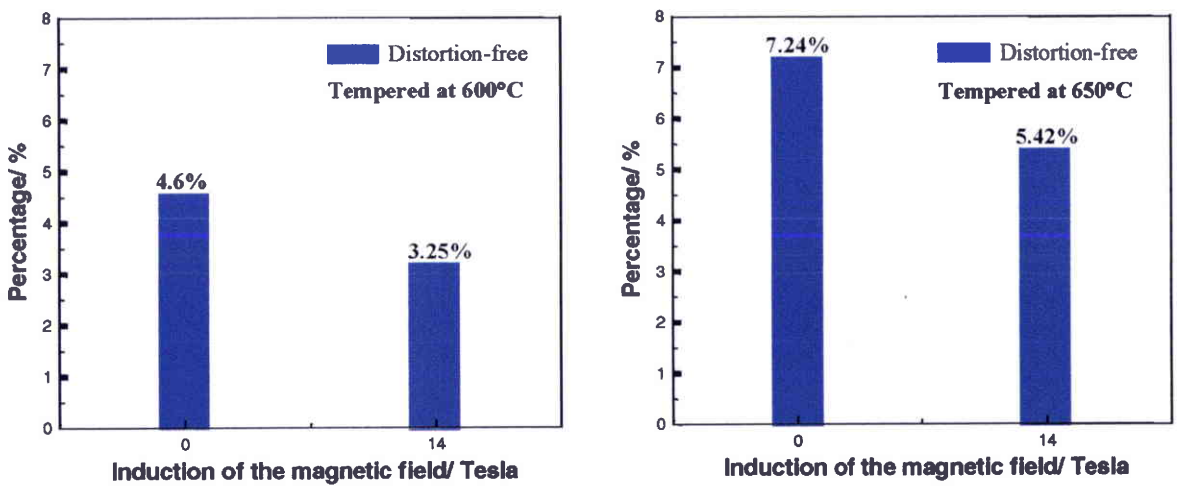

Figure 8 The area percentage of 'distortion-free' regions obtained at different tempering temperatures without and with the magnetic field of 14 T

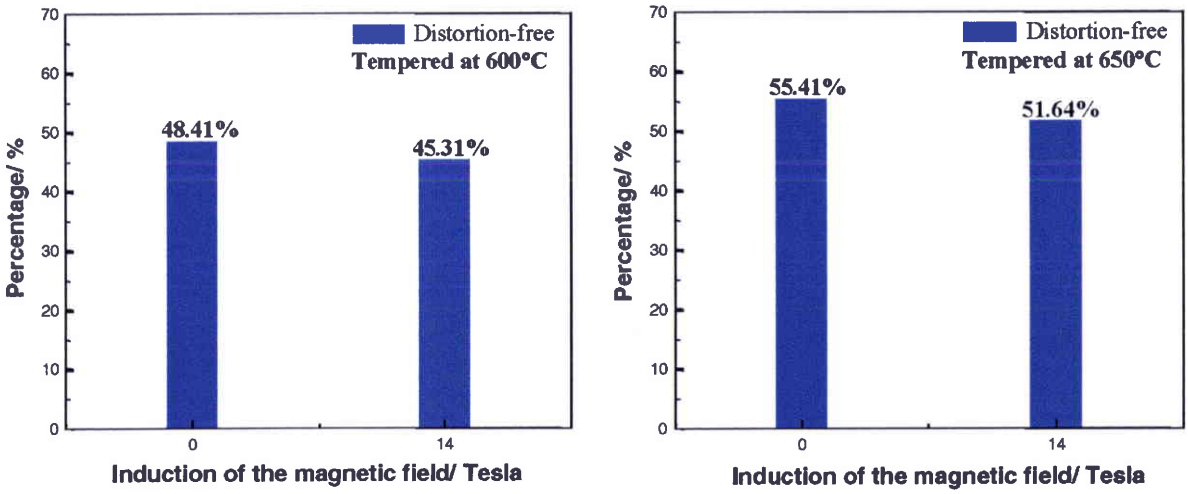

Figure 9 The number percentage of 'distortion-free' regions obtained at different tempering temperatures without and with the magnetic field of 14 T

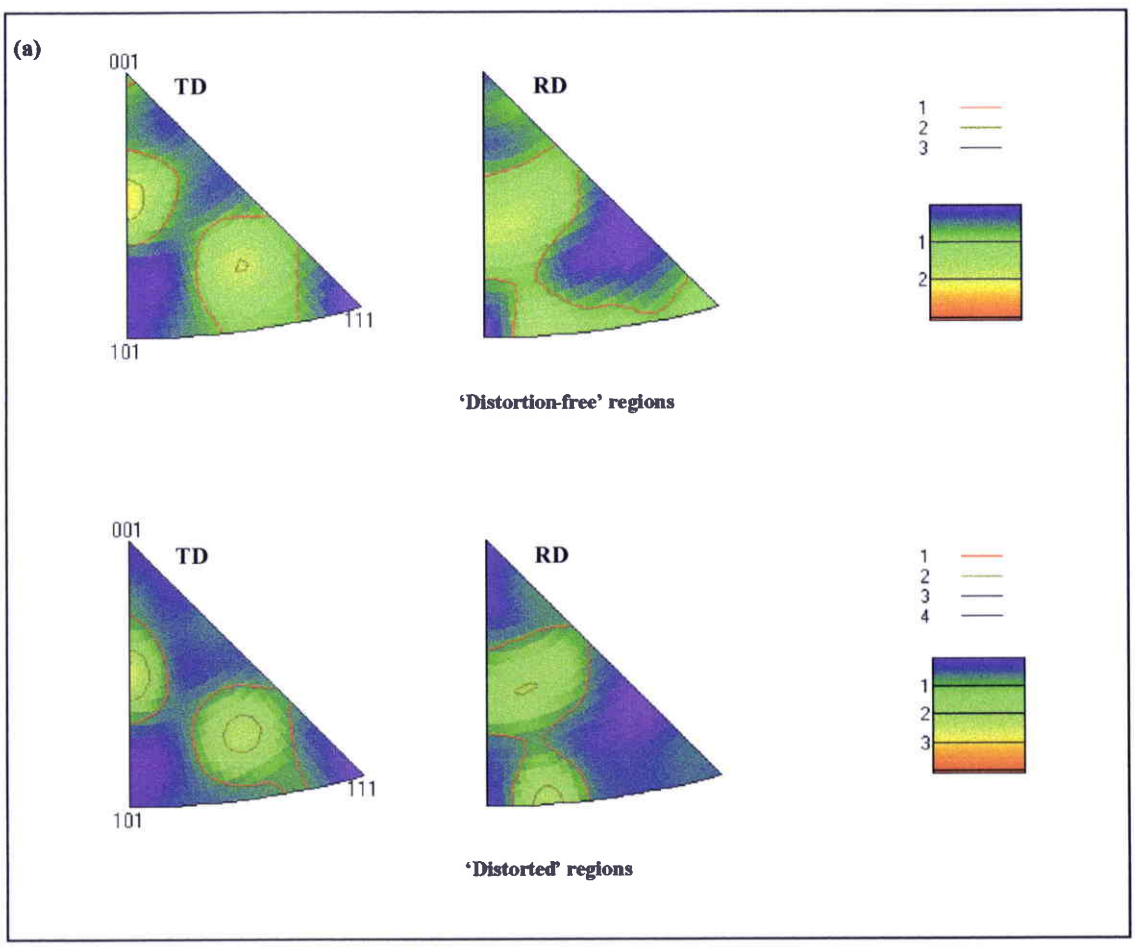

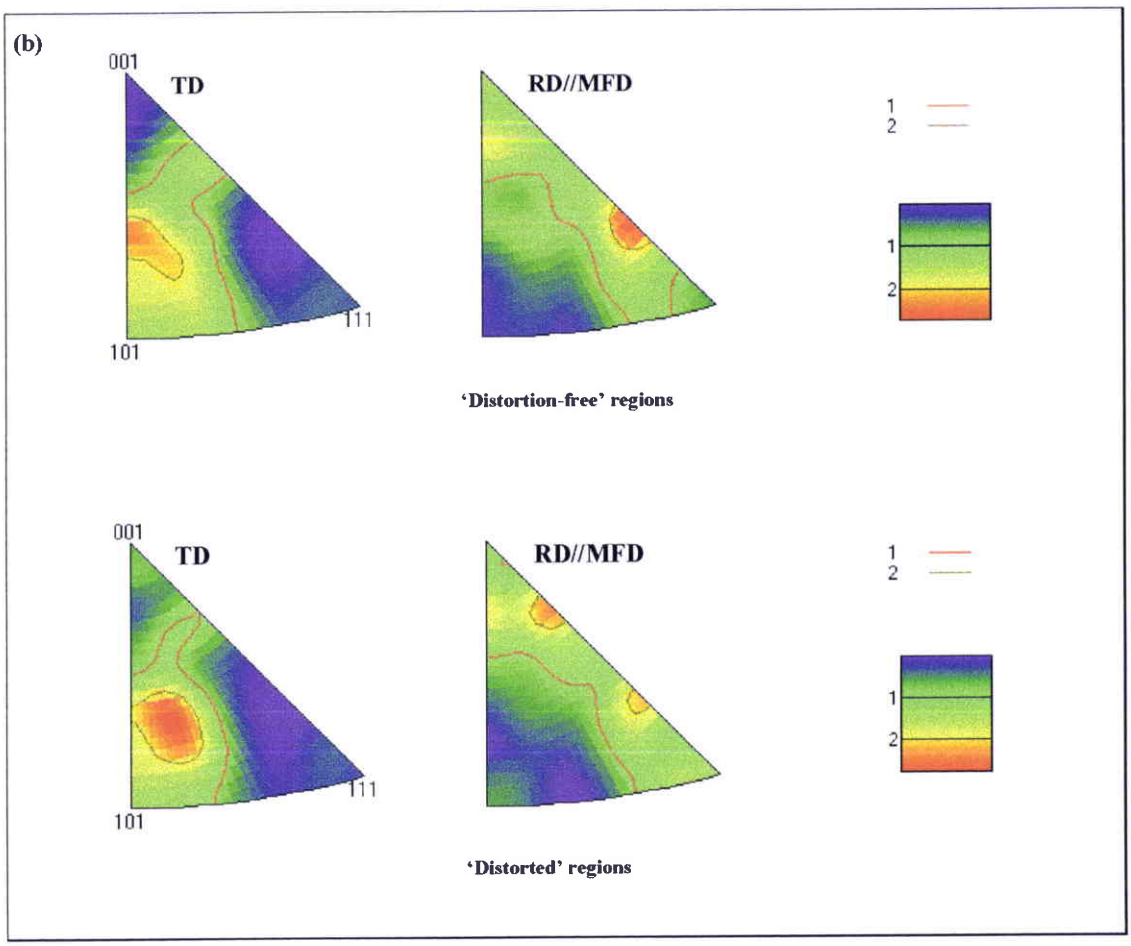

Figure 10 Transverse direction (TD) and rolling direction (RD//MFD) inverse pole figures of the 'distortion-free' and the 'distorted' regions obtained by tempering at 650°C for 1 h (a) without and (b) with the magnetic field of 14 T

The mechanical properties of specimens tempered at 600 °C are given in Table 2. It is seen that the tensile strength of the specimens tempered under magnetic field are slightly higher than those for the non-field ones whereas the impact toughness remains almost unchanged in the two cases. Fig. 11 shows fractures of the tensile specimens consisting mainly of dimples.

Table 2 Mechanical properties of the steel tempered at 600 °C for 1 hour without and with a field

Field induction	Yield strength (MPa)	Tensile strength (MPa)	Impact toughness (MJ/m^2)
0T	935.33	1033.73	0.974
14T	945.33	1040.17	0.968

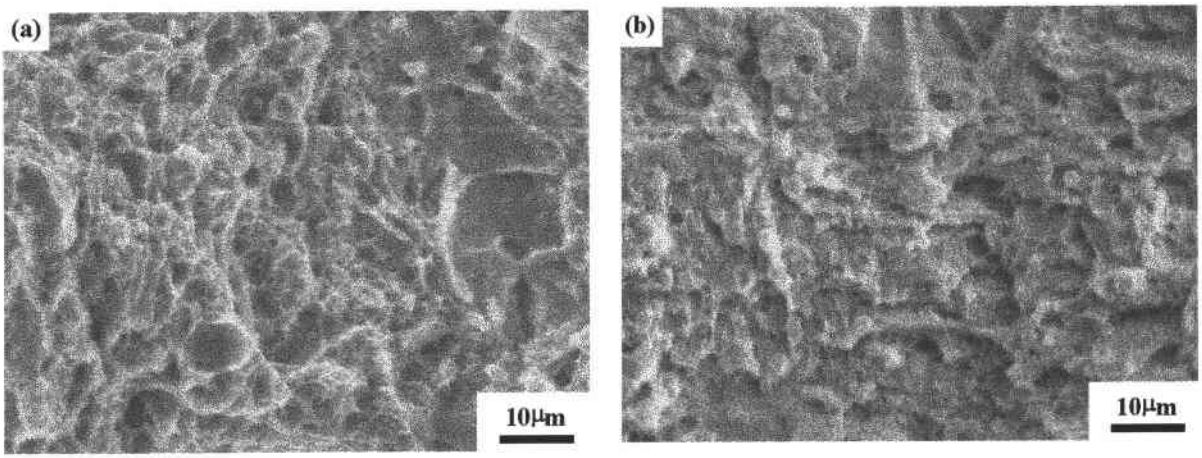

Figure 11 Tensile fractures of specimens tempered at 600°C for 1 h (a) without magnetic field and (b) with magnetic field of 14 T. SEM secondary electron images

Discussion

Martensite is highly unstable. When it is heated, the supersaturation of carbon atoms in the body-centered tetragonal crystal lattice of martensite supplies the driving force for carbide to precipitate. When temperature is higher than 350 °C, carbide takes the form of cementite, Fe_3C [17]. The high strain energy due to lattice distortion in the matrix also provides the driving force for recovery, and the high interfacial energy supplies the driving force for grain growth or coarsening of the ferrite matrix [17]. As the magnetic properties of the product and the parent structure are different, the magnetic field is assumed as exerting an influence on the precipitation of carbide and also the recovery of the ferrite matrix.

1. Influence of magnetic field on the formation of carbides

Similar to any solid phase transformation, the formation process of a new phase consists of two stages – nucleation and growth. The introduction of the magnetic field may have an influence on both. The morphologies of cementite in Fig. 4 and Fig. 5 obtained without the magnetic field are related to three kinds of nucleation sites. Concerning these cementite strips, the nucleation sites are on twin boundaries, considering that the parallelism and spacing between adjacent cementite strips correspond to that of micro-twins inside martensite plates, as displayed in Fig. 3. As for the cementite strips, running as a contour around the martensite plates, nucleation sites are located on the plate boundaries, whereas they are in the intra-plate areas in the case of particle-like cementites. These three types of nucleation sites are common

for cementite, as reported in [17]. When tempered at 600 °C with the 14-T magnetic field (Fig. 4(b)), cementites other than the intragranular ones still show the parallel character or run along the limits of martensite plates, although they precipitate in short bars instead of long strips. This suggests that the nucleation sites of cementite in the magnetic field are not different from those without the magnetic field. Consequently, the magnetic field has little effect on the nucleation sites of cementite and its formation is mainly driven by the supersaturation of carbon atoms in the matrix.

However, when cementite growth occurs, the situation changes. Without field, cementite on boundaries shows a strong tendency to directional growing along those boundaries and long strips are eventually formed. This growth is energetically favorable as it can make use of the existing interfacial energy to lower the additional energy required for the formation of new cementite/ferrite interfaces. But this tendency to grow is not favored by the magnetic field. At the two temperatures selected, i.e. 600 and 650 °C, the cementite morphology is still of the short-bar or particle-like type, as shown in Fig. 4 and Fig. 5. The magnetic field applied has thus an obvious effect on cementite growth. As ferrite is ferromagnetic and cementite is paramagnetic [18] at these two temperatures, the magnetic properties – such as magnetization of the two phases – are widely different. When cementite grows, the interfacial area becomes larger. If there is no magnetic field, the cementite/ferrite interfacial energy is only determined by the crystal structure and composition differences between the two phases; conversely, if there is the magnetic field, the interfacial energy resulting from the difference in magnetization between the two phases should also be taken into account. For a solid phase, when magnetized by the magnetic field applied, the Gibbs free energy can be decreased. The amount of energy per unit volume reduced by magnetization can be expressed as [19]:

$$\Delta G^M = \int_0^M \vec{B}_0 \cdot d\vec{M} \qquad (1)$$

where B_0 is the induction of the external field and M the magnetization of the phase. Therefore, the Gibbs free energy values for ferrite and cementite on both sides of the cementite/ferrite interface can be reduced by an amount corresponding to the degree of magnetization. Conversely, the energy level of the interface remains unchanged, as the magnetization of interface is very low due to the disorderly atom arrangement and the large number of crystal defects. This energy change caused by the introduction of the magnetic field can be represented schematically in Fig. 12. For the sake of simplicity, the energy transition in the marginal regions in both phases – the latter being noticeably affected by the

presence of the interface – has been neglected. Therefore, the relative interfacial energy increases in the magnetic field. If the vertical coordinate in Fig. 12 represents the volume energy, the shaded areas in the figure give the interfacial energy of the cementite/ferrite interface. In the figure, σ^0 represents the interfacial energy without the magnetic field and σ^M represents the new energy as increased by the magnetic field. By calculating the shaded area of σ^M in Fig. 12, the additional energy can be obtained as

$$\begin{aligned}\sigma^M &= \frac{\delta}{2}(\Delta G_f^M + \Delta G_c^M) \\ &= \frac{\delta}{2}(\int_0^{M^f} \vec{B}_0 \cdot d\vec{M}^f + \int_0^{M^c} \vec{B}_0 \cdot d\vec{M}^c)\end{aligned} \tag{2}$$

in which δ is the thickness of the interface; the superscripts and subscripts 'f' and 'c' represent ferrite and cementite, respectively. As the magnetic field can obviously raise the cementite/ferrite interfacial energy, the shape of cementite that has minimum interface area is advantageous to minimize the final total interfacial energy. Therefore, the sphere- or particle-like cementite is most favorable, whereas the directional growth that forms long cementite strips is not favored by the magnetic field as it increases the overall area of the cementite/ferrite interface.

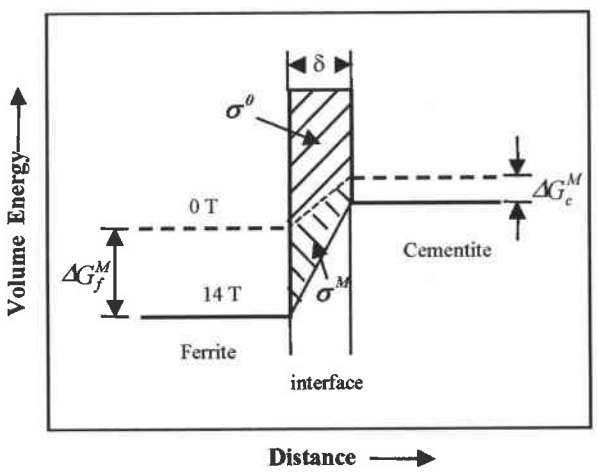

Figure 12 Schematic illustration of cementite/ferrite interfacial energy without and with the magnetic field

In addition, the magnetostriction of cementite is different from that of ferrite. The growth of cementite will result in a difference in volume and therefore an increase in strain energy. According to the phase transformation theory, the strain energy resulting from this difference in volume depends on the shape of precipitates. When the hardness of the precipitates is much higher than that of the matrix, spherical precipitates generate the lowest strain energy [20]. Thus, in the case of the hard cementite growing within the soft ferrite matrix, the directional growth of cementite will cause a noticeable increase in strain energy and it is thwarted.

Under the two effects of the magnetic field, the shape of particle-like cementite that has the minimum total interfacial area and minimum magnetostrictive strain energy is most favorable – in terms of energy – and consequently appears in the magnetic field. Therefore, the magnetic field has a positive effect by preventing directional growth of cememtite along plate and twin boundaries and, simultaneously, by promoting cementite spheroidization.

Conversely, the application of a magnetic field has little effect on the amount of cememtite formed, as shown in Table 1. Consequently, the precipitation of cementite is mainly driven by the carbon supersaturation in the matrix.

2. Influence of magnetic field on the recovery of the ferrite matrix

After the oversaturated carbon atoms have diffused out of the matrix to form precipitates, the matrix acquires the ability to recover lattice distortion. As illustrated in Fig. 8, the measurement of 'distortion-free' regions increases without and with the field as temperature rises. In fact, this results from both the rising number of 'distortion-free' regions (Fig. 9) and the growth of the existing ones (Fig. 6 and Fig. 7). The difference lies in the fact that the amount obtained without the field is higher than that with the field, for the two temperatures. The application of the magnetic field has a noticeable impact in retarding this process. The orientation distributions of the 'distortion-free' and 'distorted' regions in both non-field treated (650 °C) and field treated (650 °C) samples display obvious similarities, as shown in Fig. 10(a) and (b). The similarities were also observed in the 600 °C treated samples. This suggests that most of the 'distortion-free' regions might be enlarged directly from the distortion-free areas of the matrix and have the same orientation as the matrix, instead of newly formed nuclei. As the EBSD-analyzed areas of the samples are selected locally to identify the origin of 'distortion-free' regions formed, the orientation distributions are local and not statistically representative of the orientation distributions in the whole sample. For the

same reason, the orientation distributions obtained without (Fig. 10(a)) and with the magnetic field (Fig. 10(b)) are not comparable either. Nevertheless, the similarities in Fig. 10(b) suggest that the magnetic field has no obvious effect on the origin of nucleation in the 'distortion-free' regions. The influence it has is mainly to postpone the recovery of the lattice distortion of the matrix and delay the growth of existing 'distortion-free' regions.

The delaying effect caused by the magnetic field on the recovery and recrystallization processes has been observed in several cold-rolled steels [12, 13, 14 and 15]. In the present work, a similar effect, i.e. retardation of recovery in the magnetic field, also exists. Although the cold-rolling and quenching are different processing procedures, they both cause crystal lattice distortion and therefore generate strain energy in the microstructures obtained. This strain energy provides the driving force for the recovery. Consequently, the driving forces for recovery of the cold-rolled microstructure and the as-quenched martensite have similar origin. Concerning the retardation of the recovery and recrystallization processes occurring in the deformed matrix, Martikainen and Lindroos [12] suggested that the magnetic ordering induced may affect grain boundary mobility since the diffusion of ferromagnetic materials depends on the degree of magnetic order. In addition, the domain walls also act as barriers to grain boundary migration. As the magnetic field may lower the mobility of the grain boundaries by either atomic diffusion through magnetic ordering or the obstructive effect of domain walls, recovery and recrystallization can be delayed. Since the recovery of the lattice distortion in martensite also requires atom rearrangement and the growth of 'distortion-free' regions calls for boundary migration, the retardation effect caused by the magnetic field may be attributed to the same influential factors as those suggested by Martikainen and Lindroos [12].

Contrary to what was found in the literature on cold-rolled steels [12, 13, 14 and 15], no <001> texture component was detected along the MFD in the present work. The formation of the <001> component in those materials was attributed to magnetic anisotropy in the magnetic field. The direction of easy magnetization is <001> for the *bcc* ferromagnetic phase. The nuclei with <001> directions parallel to the MFD have the largest driving force for recrystallization [12] and the <001> component is thus enhanced. However, in the present work, as the 'distortion-free' regions in the material are enlarged directly from the matrix, the matrix orientation remains unchanged. No enhanced <001> component could be obtained. This result also shows that, at this stage of recovery, the 14-T field has no obvious impact on

the selection of 'distortion free' regions – whose easy magnetization direction is along the field direction – to nucleate or grow preferentially.

As illustrated in Fig. 11, the fractographs of both non-field and field-tempered tensile specimens show typical ductile rupture behavior; consequently, the intragranular properties of the matrix are dominant. The releasing of supersaturation and recovery progress of the ferrite matrix thus plays an important role in affecting the rupture behavior of the material. Both are softening processes to the material. As shown in Table 2, the slight increase in the strength of the field-tempered specimens could be related to the retardation of the progress of recovery for the matrix. This slight increase is also reflected in the morphology of the fractures. In Fig. 11, the dimples in (b) with a field are slightly shallower than those in (a) without a field, showing that the deformation capacity is slightly poorer – i.e. the strength slightly higher – with than without a field. However, as the progress of recovery is still in its early stage, the changes in strength are still modest.

Conclusions

1. A magnetic field can effectively prevent the cementite from growing directionally along the plate and twin boundaries. The application of a field indeed raises the cementite/ferrite interfacial energy since the magnetization-related Gibbs free energy decreases on both sides of the interface. In addition, the strain energy increase caused by the difference in magnetostriction between the two phases is also unfavorable to directional growth. Therefore, short-bar or particle-like cementite is obtained. The magnetic field applied has no obvious effect on the nucleation sites or on the total amount of cementite.
2. The magnetic field can obviously delay the progress of recovery for the ferrite matrix; this can be attributed to the influence of magnetic ordering and domain walls on the mobility of grain boundaries. No preferential orientations are detected for the 'distortion-free' regions in the magnetic field. The driving force for the formation and growth of the 'distortion-free' regions is still generated by the lattice distortions, due to the supersaturation by carbon atoms.

Acknowledgements

This work was financially supported by the National Natural Science Foundation of China (Grant No. 50234020), the National High Technology Research and Development

Program of China (Grant No. 2002AA336010) and the TRAPOYT in Higher Education Institutions of MOE, China. The authors also gratefully acknowledge the support offered in the framework of the Chinese-French Cooperative Research Project (PRA MX00-03). The authors would like to express gratitude to the High Magnetic Field Laboratory for Superconducting Materials, Institute for Materials Research, Tohoku University which offered access to the magnetic field facilities.

References:

[1] Joo HD, Kim SU, Shin NS, Koo YM. Materials Letters 2000;43:225

[2] Krivoglaz MA, Sacovskiy VD. Fiz Metal Metalloved 1964;18:23

[3] Sadovskii VD, Rodigin NM, Smirnov LV, Filonchik GM, Fakidov IG. Fiz Metal Metalloved 1961; 12:302

[4] Fokina YeA, Zavadskiy EA. Fiz Metal Metalloved 1963;12:311

[5] Satyanarayan KR, Eliasz W, Miodownik AP. Acta Metall 1968;16:877

[6] Kakeshita T, Shimizu K, Funada S, Date M. Acta Metall, 1985;33:1381

[7] Kakeshita T, Fukuda T, Saburi T, Kindo K, Endo S. Phys B 1997;237-238:603

[8] Shimotomai M, Maruta K. Scripta Mater 2000;42:499

[9] Ohtsuka H, Xu Y, Wada H. Mat Trans JIM Vol. 41, No. 8(2000), pp907-910

[10] Shimotomai M, Maruta K, Mine K, Matsui M. Acta Mater 2003;51:2921

[11] Enomoto M Guo H, Tazuke Y, Abe YR, Shimotomai M. Metall Mater Trans 2001;32A:445

[12] Martikainen HO, Lindroos VK. Scand J Metall 1981;10:3

[13] Watanabe T, Suzuki Y, Tanii S. Philosophical Magazine Letters 1990;62:9

[14] Masahashi N, Matsuo M, Watanabe K. J Mater Res Vol. 1998;13:457

[15] He CS, Zhang YD, Zhao X, Zuo L, He JC, Watanabe K, Zhang T, Nishijima G, Esling C. Advanced Engineering Material 2003;5:579

[16] Watanabe K, Awaji S, Motokawa M, Mikami Y. Jpn J Appl Phys 1998;37:L1148.

[17] Krauss G, Principles of Heat Treatment of Steel. Ohio: American Society for Metals; 1980. p. 200.

[18] Adachi K, Bonnenberg D, Franse JJM, Gersdorf R, Hempel KA, Kanematsu K, Misawa S. Shiga M, Stearns MB, Wijn HPJ. In: Wijn HPJ, editor. Landolt-Bornstein Numerical Data and Functional Relationships in Science and Technology, Magnetic Porperties of Metals, Vol. 19c. Berlin: Springer-Verlag; 1988. p. 24.

[19] Cyrot M, *et al*, Magnétisme. Grenoble: Presses Universitaires de Grenoble, 1999. p. 69.

[20] Hsu TY. Theory of Phase Transformation. Beijing: Science Press of China, 1988. p.35.

Precipitation in high magnetic field in a medium carbon steel

Y.D. Zhang[a, b], N. Bozzolo[b], C.S. He[a], X. Zhao[a], L. Zuo[a], Claude Esling[b*] and J.C. He[a]
[a] Key Laboratory (Northeasten University), Ministry of Education, Shenyang 110004, P. R. of China
[b] LETAM, CNRS-UMR 7078, University of Metz, Ile du Saulcy, 57045 Metz, France

Abstract

The effects of low temperature magnetic tempering on the carbide precipitation in medium carbon steel, 42CrMo, have been investigated. The as-quenched specimens are tempered at 200°C for 60 min without and with a 14-T magnetic field. Results show that, under field processing, relatively high-temperature monoclinic χ-Fe_5C_2 carbide forms with a denser distribution and smaller sizes, instead of the usual orthorhombic η-Fe_2C carbide obtained without field. The impact of the magnetic field is that it changes the precipitation sequence of the transition carbide by effectively lowering the Gibbs free energy of the high magnetization phase. The denser distribution and smaller size of χ-Fe_5C_2 precipitates are attributed to the increased nucleation rate and weaker diffusion capacity required for growth as the formation temperature is lower. This offers additional dispersion strengthening to compensate for the strength and hardness decrease due to the loss of supersaturation of carbon in the matrix and raises the toughness of the material.

Keywords: low temperature tempering; transition carbides; orientation; magnetic field

Introduction

As properties of materials are determined by their microstructures, performance optimization through microstructure modification and control - to meet the ever-increasing demands imposed by almost all branches of industry - has become one of the most challenging subjects in the field of materials science and engineering. Traditional processing methods have become less efficient in the face of these new requirements and gradually lost their dominant status. As a consequence, the introduction of new techniques to materials processing has become a major objective. Recently, Electromagnetic Processing of Materials-EPM has emerged as a key procedure and aroused wide attention among materials researchers, especially since high magnetic fields have been applied to conventional heat treatment processes.

So far, research on this topic has focused on the effect of a magnetic field on martensitic

transformation [1-4] and high-temperature diffusional phase transformations between austenite and ferrite [5-7]. A couple of reports deal with the precipitation behavior of transition carbides. As most transition carbides are ferromagnetic with various magnetization degrees, the introduction of magnetic field can effectively change their stability by altering their Gibbs free energy levels and thus affect their precipitating courses and behaviors, following which the final properties of the material will be changed and controlled. Insight into this aspect is also helpful to gain a better understanding of the complex precipitation processes and behavior of transition carbides and is of significance, from both theoretical and technical point of view.

In the present work, medium carbon steel was tempered at 200°C for 60 min without and with a magnetic field of 14 T, after having been quenched in the traditional way. The effect of the magnetic field on the course and behavior of carbide precipitation and its subsequent influence on the mechanical properties of the material has been investigated.

Experimental

The chemical composition of the medium carbon steel used in this study is given in Table 1. Specimens of dimensions 55 mm×10 mm×2 mm were cut from a hot-rolled rod* with their longitudinal direction parallel to the hot-rolling direction. They were then all heated to 860°C and held for 20 min followed by water quenching to obtain a martensite microstructure for subsequent tempering. Both the magnetic and non-magnetic tempering were carried out at 200°C and 150°C for 60 min in the same furnace installed in a 15-T cryocooled superconducting magnet of 52 mm in bore size. The specimens were placed in the central (zero magnetic force) region with their longitudinal direction parallel to the magnetic field direction. In the case of the magnetic tempering, a high magnetic field of 14 T was applied during the whole heating, isothermal holding and cooling processes.

Table 1 Chemical composition of 42CrMo steel (wt.%)

C	Cr	Mo	Si	Mn	others	Fe
0.38 - 0.45	0.90 - 1.20	0.15 - 0.25	0.20 - 0.40	0.50 - 0.80	P≤0.04 S≤0.04 Cu≤0.30	Bal.

* For the composition distribution of the alloyed elements in the material, please consult the Appendix

The specimens tempered were further cut out along their longitudinal direction for the SEM and TEM observations and the mechanical tests for hardness, strength and impact toughness. Non-standard tensile and Charpy impact specimens were used, as shown in Fig. 1. The morphologies of precipitates and the orientation relationships between precipitates and matrix were examined by using a JEOL JSM-6500F SEM and a Philips CM 200 LaB_6 cathode TEM, respectively. Vicker's hardness was measured with a load of 5 kg. Tensile tests were carried out on a Shimadzu AG-5000A unit with a load of 2500 kg, and Charpy impact tests on a JB-5 Charpy impact machine with a maximum measurement range of 29.4 J. The fracture morphologies of the tensile and impact specimens were also observed with SEM.

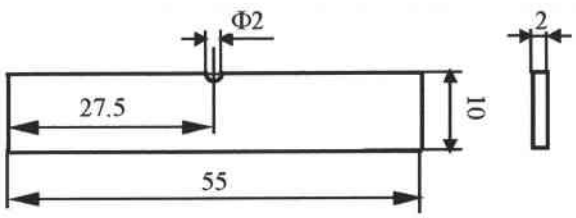

(a) Charpy impact specimen

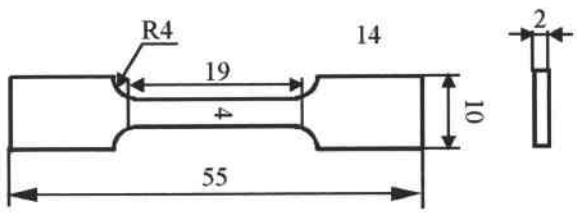

(b) tensile specimen

Figure 1 Illustration of tensile and Charpy specimens

Results

Fig. 2 shows the initial microstructure of an as-quenched specimen, which is characteristic of α' martensite plates. For the specimens tempered at 200°C for 60 min, without and with an applied high magnetic field of 14 T, the precipitation of carbides occurred within martensite plates (Fig. 3). In the both cases, the precipitates appeared in the

form of thin platelets, arranged in parallel to some directions within matrix. However, the imposition of a magnetic field to tempering has yielded more densely distributed platelets with a smaller average size in length, as compared with the non-magnetic tempering case. Moreover, no carbide precipitation was observed in the specimens tempered at 150°C for 60 min. using the SEM.

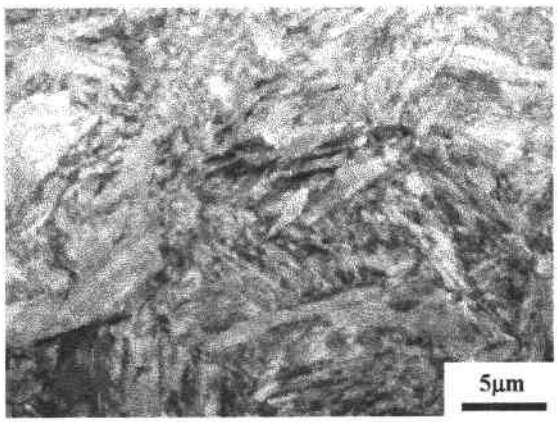

Figure 2 Bright-field TEM micrograph of initial martensite in as-quenched specimen

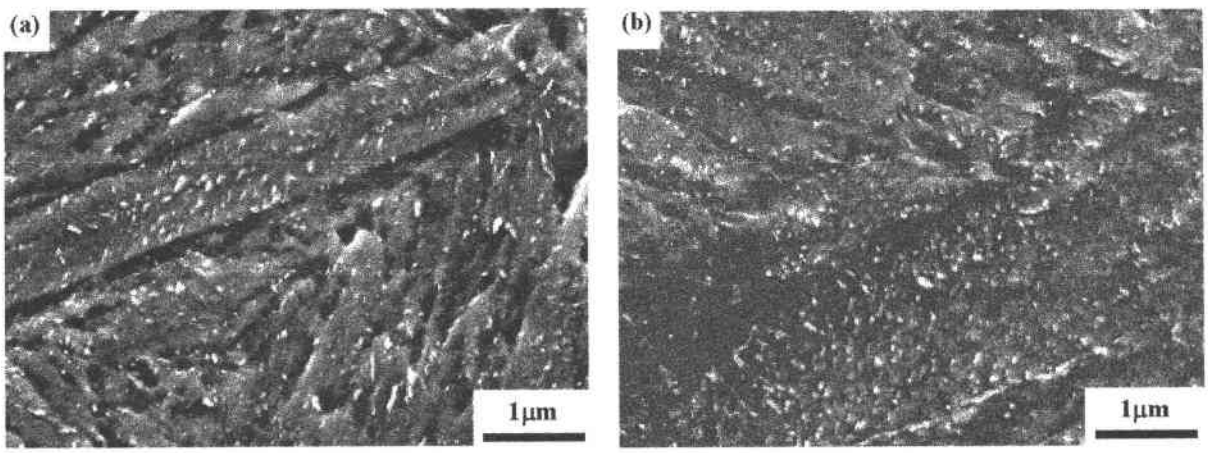

Figure 3 SEM secondary electron images of carbide precipitates (bright areas) within martensite in specimens tempered at 200°C for 60 min (a) without and (b) with a 14-T magnetic field (the magnetic field direction is vertical in the micrograph).

The crystal structure of precipitates and their orientation relationship with matrix has been identified by electron diffraction of TEM. The carbide formed during non-magnetic tempering is of typical orthorhombic η-Fe_2C type and is correlated to tempered martensite α''

by $(110)\alpha''//(200)\eta$ and $[1\bar{1}\bar{3}]\alpha''//[0\bar{2}0]\eta$ (Fig. 4(a)). However, the precipitated carbide in the magnetic field is referred to as the monoclinic χ-Fe_5C_2 type with the orientation correlation by $(01\bar{1})\alpha''//(021)\chi$ and $[1\bar{3}\bar{3}]\alpha''//[5\bar{3}6]\chi$ (Fig. 4(b)).

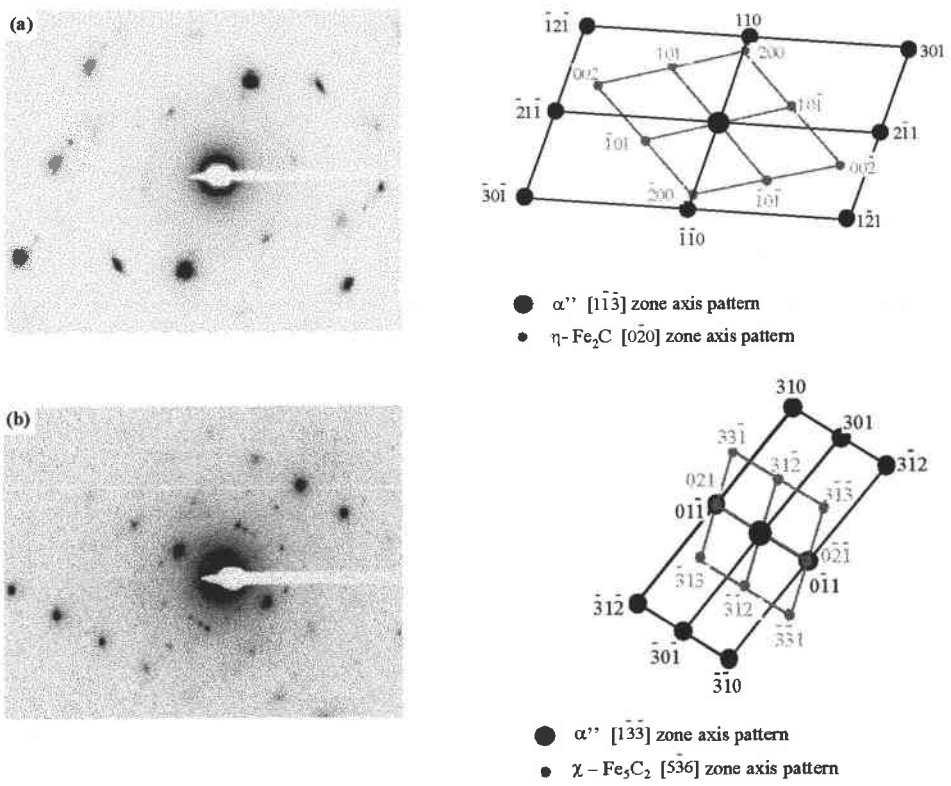

Figure 4 Diffraction patterns and their indexing of (a) η-Fe_2C formed during non-magnetic tempering at 200°C for 60 min and (b) χ-Fe_5C_2 formed during magnetic tempering at 200°C for 60 min.
Note: the two patterns are taken with different camera lengths, therefore the same reciprocal spots in the two patterns have different reciprocal vector lengths

The mechanical properties of the as-tempered specimens are given in Table 2. It is noted that, with the applied magnetic field, the impact toughness of the tested steel was enhanced by an amount of 9%, while its Vicker's hardness and yield strength were not changed significantly. The fractures of all the impact specimens were featured with a mixture of dimples and intragranular cleavages (Fig. 5). However, the magnetic tempering has resulted in a higher ratio of dimples with improved impact toughness than that of non-magnetic tempering. As there exists intragranular fracture to some extent in the both cases, crack propagation along certain planes of tempered martensite and the interfaces between carbide

and tempered martensite must have played an important role.

Table 2 Mechanical properties of specimens tempered at 200°C for 60 min without and with a 14-T magnetic field

Magnetic field (Tesla)	Vicker's hardness	Yield strength (MPa)	Tensile strength (MPa)	Elongation (%)	Impact toughness (MJ/m^2)
0	570.8	1583	1850	2.0	0.767
14	552.6	1557	1877	2.1	0.838
Change rate	-3%	-1%	1%	5%	9%

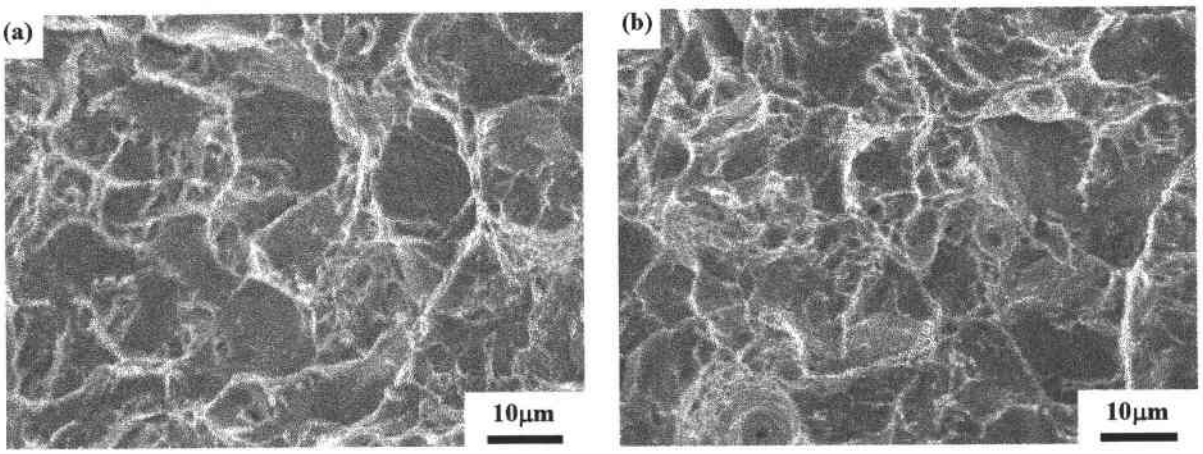

Figure 5 SEM secondary electron images of impact fractures in specimens tempered at 200°C for 60 min (a) without and (b) with a 14-T magnetic field. The fractographs show the mixture of dimples and intergranular cleavages.

Discussion

It has been well established that a quenched martensite microstructure is highly unstable due to (1) the supersaturation of carbon atoms in the body-centered tetragonal crystal lattice, (2) the strain energy associated with fine dislocation or twin substructure, (3) the interfacial energy associated with high density of lath or plate boundaries and (4) the retained austenite. When it undergoes a tempering, those factors causing instability provide various driving forces for microstructural evolutions and finally give rise to property modification. According to Cohen and coworkers [8-11], Hirotsu and Nagakura [12], transition carbide, either hexagonal ε-Fe_2C or orthorhombic η- Fe_2C, precipitates from martensite at low tempering

temperatures. The driving force for the carbide precipitation is provided by the supersaturation of carbon atoms in the matrix. When tempering temperature goes up, the metastable ε-Fe_2C or η- Fe_2C dissolves into the matrix and the monoclinic χ-Fe_5C_2 precipitates. As χ-Fe_5C_2 is also metastable, it transforms to Fe_3C at higher tempering temperatures.

In the present work, for the specimens tempered at 150°C for 60 min, the precipitation of transition carbides was not found. When tempered at 200°C for 60 min, without or with a 14-T magnetic field, carbide precipitated and took the respective type of η-Fe_2C and χ-Fe_5C_2. It is interesting to note that, in the case of magnetic tempering, χ-Fe_5C_2 precipitated directly from matrix martensite without an intermediate stage of the η- Fe_2C formation. This result may indicate that imposition of magnetic field has an effect to change the precipitation sequence of these transition carbides.

ε-Fe_2C, η-Fe_2C, χ-Fe_5C_2 and Fe_3C are all ferromagnetic at 200°C, and from the thermodynamic point of view, the application of an external magnetic field can lower their Gibbs free energies and thus their formation sequence. At the present stage, the magnetic property data for ε-Fe_2C and Fe_3C are well-documented [13], but those for η-Fe_2C and χ-Fe_5C_2 are quite limited. Actually, the overall magnetic moments of these iron carbides are determined by the magnetic moments of their iron atoms [13] and for each iron atom, its magnetic moment originates from the unsaturated spins of its extranuclear electrons. As the total magnetic moment of an assembly of atoms has an additive property and can be added up with individual ones [14], it can be deducted that the magnetic properties of metallic compounds are mainly determined by their constitution and crystal structure. Therefore, metallic compounds with similar constitutions and structures may be considered to have similar magnetic properties. Indeed, such a similarity in structure exists between η-Fe_2C and ε-Fe_2C [15] and between χ-Fe_5C_2 and Fe_3C [13].

Based on the above assumption, the temperature variations of magnetization of η-Fe_2C, χ-Fe_5C_2 as well as α-Fe were calculated by using the Weiss molecular field model [16], as shown in Fig. 6. Since the both carbides can be magnetized to some extents in a magnetic field, their Gibbs free energies would be lowered according to their magnetization. The corresponding energy drop amounts to $\int \vec{B}_0 \cdot d\vec{M}$ (B_0 is the induction of applied magnetic field and M the magnetization). It is seen from Fig. 6 that the magnetization of χ-Fe_5C_2 at 200°C is obviously higher than that of η- Fe_2C. Therefore, in a magnetic field of 14 T, the

Gibbs free energy of χ-Fe_5C_2 probably goes lower than that of η- Fe_2C, and χ-Fe_5C_2 becomes more stable at this temperature. Their stability changes with the magnetic field at this tempering temperature can be illustrated schematically with their Gibbs free energy versus carbon concentration curves given in Fig. 7. Therefore in the magnetic field, χ-Fe_5C_2 precipitates before η- Fe_2C.

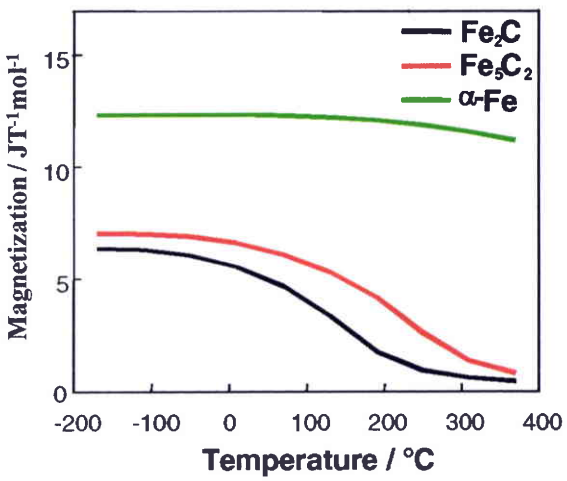

Figure 6 Temperature variations of magnetization of Fe_2C, Fe_5C_2 and α-Fe.

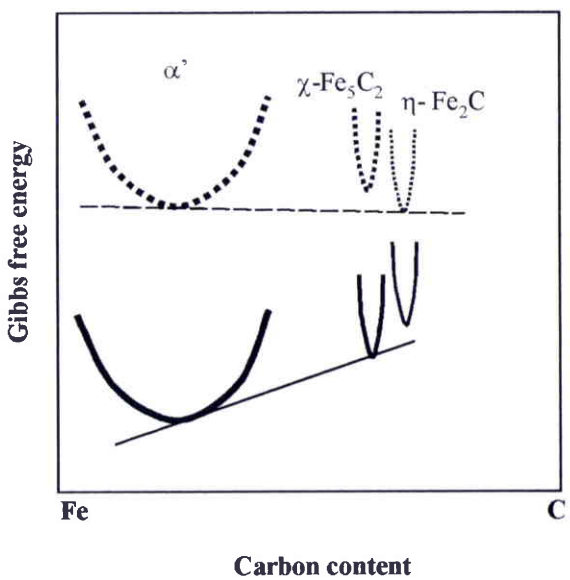

Figure 7 Schematic diagram of Gibbs free energy *vs.* carbon concentration for α' martensite, χ-Fe_5C_2 and η- Fe_2C at 200°C without (dash line) and with (solid line) a 14-T magnetic field.

As magnetic field lowers the formation temperature of χ-Fe_5C_2, it nucleates at lower temperature with higher undercooling degree and then its nucleation rate is increased. As a result, χ-Fe_5C_2 formed in the magnetic field of 14 T is distributed more densely. In addition, the growth of carbides needs the diffusion of both carbon and iron atoms but the low formation temperature inactivates their mobility and shortens their diffusion length. Consequently, the average sizes of χ-Fe_5C_2 are smaller than those of Fe_2C, compare Fig. 3 (a) with (b).

As the supersaturated carbon atoms in martensite diffuse out to form χ-Fe_5C_2 carbide, the mechanical properties of the material are changed. Usually, with increasing tempering temperature, the toughness and plasticity of materials rise and the strength and hardness drop. Although, in the present study, with the precipitation of χ-Fe_5C_2 in the magnetic field, the toughness and plasticity increase, the strengths of the material do not drop but remain almost the same, as can be seen from the change rate resulted from the magnetic field in Table 2. This may be attributed to the denser distribution and the smaller size in their length direction of the χ-Fe_5C_2 carbides. On one hand, the denser distribution results in additional dispersion strengthening and compensates for the decrease in strengths due to the loss of supersaturation of carbon atoms in the matrix. On the other hand, as the carbide/matrix interfaces are phase interfaces in the material and crack grows easily along these areas, the smaller sizes of the carbides may effectively decrease the easy propagation areas for the crack path. As a result, the toughness of material is improved.

Conclusions

When specimens of 42CrMo are tempered at 200°C for 60 min in a 14-T magnetic field, a high temperature monoclinic χ-Fe_5C_2 carbide is precipitated with an orientation relationship of $(01\bar{1})\alpha''//(021)\chi$ and $[1\bar{3}\bar{3}]\alpha''//[5\bar{3}6]\chi$. However, when tempered under the same thermal conditions but without the field, the precipitates are common orthorhombic η- Fe_2C having a orientation relationship of $(110)\alpha''//(200)\eta$ and $[1\bar{1}\bar{3}]\alpha''//[0\bar{2}0]\eta$.

As at 200°C the magnetization of χ-Fe_5C_2 is higher than that of η-Fe_2C, its Gibbs free energy goes lower than that of η- Fe_2C and then it precipitates before η-Fe_2C. So magnetic field has an effect to change the precipitation sequence of these carbides.

Since χ-Fe_5C_2 is precipitated at relatively lower temperature with higher undercooling degree, its nucleation rate is higher compared with that of η-Fe_2C. Then its denser distribution

offers an additional dispersion strengthening which compensates for the loss of strength due to the decrease of carbon supersaturation in the matrix. Meanwhile, the lower formation temperature reduces the mobility of atoms and hence restrains the growth of χ-Fe_5C_2. The final sizes of χ-Fe_5C_2 are smaller, which contributes to the improvement of the toughness of the material by reducing the areas of carbide/matrix interfaces for the propagation of the crack. The insight into these aspects provides better understanding of precipitation procedure of transition carbides under magnetic field and is of both theoretical and technical significance.

Acknowledgements

This work was financially supported by the National Natural Science Foundation of China (Grant No. 50234020), the National High Technology Research and Development Program of China (Grant No. 2002AA336010) and the TRAPOYT in Higher Education Institutions of MOE, China. The authors also gratefully acknowledge the support in the frame of the Chinese-French Cooperative Research Project (PRA MX00-03). The authors would like to express thanks to the High Magnetic Field Laboratory for Superconducting Materials, Institute for Materials Research, Tohoku University, for the access to the magnetic field experiments.

References

[1] Krivoglaz MA, Sacovskiy VD. Fiz Metal Metalloved 1964; 18:23.

[2] Bernshteyn ML, Granik GI, Dolzhanskiy PR. Fiz Metal Metalloved 1965;19:882.

[3] Kakeshita T, Shimizu K, Maki T, Tamura I, Kijima S, Date M. Scripta Metall 1985;19:973.

[4] Kakeshita T, Fukuda T, Saburi T, Kindo K, Endo S. Phys B 1997;237-238:603.

[5] Shimotomai M, Maruta K. Scripta Mater 2000;42:499.

[6] Enomoto M, Guo H, Tazuke Y, Abe YR, Shimotomai M. Metall Mater Trans

2001;32A:445.

[7] Shimotomai M, Maruta K, Mine K, Matsui M. Acta Mater 2003;51:2921.

[8] Roberts CS, Averbach BL, Cohen M. Trans ASM 1953;45:576.

[9] Lement BS, Averbach BL, Cohen M. Trans ASM 1954;46:851.

[10] Werner FE, Averbach BL, Cohen M. Trans ASM 1957;49:823.

[11] Lement BS, Averbach BL, Cohen M. Trans ASM 1955;47:291.

[12] Hirotsu Y, Nagakura S. Acta Met 1972;20:645.

[13] Adachi K, Bonnenberg D, Franse JJM, Gersdorf R, Hempel KA, Kanematsu K, Misawa S. Shiga M, Stearns MB, Wijn HPJ. Landolt-Bornstein Numerical Data and Functional Relationships in Science and Technology. In: Wijn HPJ, editor. Magnetic Properties of Metals. Vol. 19a. Berlin: Springer-Verlag; 1988. p. 24.

[14] Crangle J. The Magnetic Properties of Solids. Merseyside: Willmer Brothers Ltd.; 1977. p. 26.

[15] Krauss G. Principles of Heat Treatment of Steel. Ohio: American Society for Metals; 1980. p. 200.

[16] Jile D, Introduction to magnetism and magnetic materials. Suffolk: St Edmundsbury Press Ltd.; 1991. p. 259.

Conclusions

Conclusions

From the above theoretical and experimental studies, the following important conclusions have been reached:

Theoretical simulation of the effect of magnetic field on phase equilibrium in Fe-C binary system

The thermodynamic influence of magnetic field on phase equilibrium in Fe-C binary system has been studied theoretically. With regard to the calculation of magnetization of bcc phase, the Weiss molecular field model is extended by substituting the molecular field coefficient λ with a short-range ordering coefficient γ valid around and above *Tc*, therefore the accurate temperature variations of magnetization of ferrite phase are obtained. Analysis reveals that the short-range ordering coefficient γ can be expressed in an Arrhenius type relation analogous to the diffusion coefficient. The corresponding activation energy, as obtained by numerical analysis, takes the form of free energy. The calculated susceptibilities based on the corrected model are in good agreement with the measured ones at temperatures above T_C. This result successfully solves the problem of magnetization calculation around *Tc* that has long been harassing the study on this topic.

The magnetic susceptibility calculation of fcc phase is calculated on the basis of band model. The result that agrees well with the measured data has been obtained. In addition, the confusion in expressing the energy change due to the introduction of magnetic field has been clarified. The magnetic Gibbs free energy difference between austenite and ferrite then is calculated and on this basis, the phase equilibrium boundaries, ferrite/austenite and austenite/ferrite equilibrium in Fe-C diagram under magnetic field is simulated.

Results show that magnetic field can impose remarkable influence on phase equilibrium by enlarging the ferritic and shrinking the austenitic phase area, hence obviously enhance Ae_3 temperatures of steels and shift the eutectoid point to the high carbon and high temperature side. For hypoeutectoid steels, the Ae_3 temperatures are raised nearly 2~4°C per Tesla depending on the carbon content. For the pure iron the Ae_3 is increased by about 7°C under a magnetic field of 10 Teslas that is in fair agreement with the value measured by Ohtsuka et al. (ref. [15] in chapter 1)

Characteristics of Phase Transformation from Austenite to Ferrite in Magnetic field

The thermodynamic and kinetic influence of magnetic field is also experimentally investigated. Results show that magnetic field can considerably increase the amount of newly formed ferrite and accelerate the transformation rate from austenite to ferrite. Finally, a fine, randomly distributed ferritic and pearlitic microstructure, with equilibrium amount of ferrite is obtained under a fast cooling rate owing to the combination of the thermodynamic and kinetic effects of magnetic field. At the mean time, the possibility of the application of high magnetic field to practical heat treatment process has been evaluated theoretically and technically.

Based on the above results, an experiment of rapid annealing under high magnetic field has been designed and carried out on a hot-rolled 42CrMo. Results show that magnetic field can effectively prevent the formation of banded structure that happens commonly during conventional annealing in this material, and further improve the microstructure through refining and microstructure homogenizing. Meanwhile, magnetic field can greatly improve the practical heat treatment process by shortening the cooling time and leaving out the subsequent treatment to eliminate banded structure. On this basis, a new rapid annealing method under high magnetic field has been worked out and put forward. The method has been applied for an invention patent.

Due to the kinetic influence of the magnetic field on nucleation barrier and transformation rate as well as the influence of the previous hot rolling, the morphology of the newly formed ferrite during austenite to ferrite transformation can be greatly affected according to the cooling rate. When the cooling rate is relatively slow (10°C/min) and the magnetic field is applied in the same hot-rolling direction, ferrite grains and pearlite colonies align themselves alternately along the same direction, while without the magnetic field, the distribution of ferrite and pearlite are random. The reason for this is clarified as that the magnetic field can reduce the nucleation barrier of ferrite and accelerate the ferrite transformation so that ferrite nucleates at high temperature with low undercooling rate and mainly on austenite grain boundaries. As the deformation of previous hot rolling is inhomogeneous, fine-grained and coarse-grained zones are distributed alternately along the hot-rolling direction. Therefore, fine-grained zones offer more nucleation sites for ferrite. Meanwhile, the formation of ferrite needs the excessive carbon atoms to diffuse out. Then the coarse-grained zones with less ferrite nuclei receive more carbon atoms from the fine-grained zones and become rich in carbon, which makes the further formation of ferrite in these areas impossible. In addition, the dipolar interaction between neighboring ferrite grains along the

magnetic field direction can further lower the energy of the whole system and thus makes the ferrite chains more energetically stable. As a result, final aligned microstructure is obtained. But when cooling is increased to 46°C/min, no alignment of ferrite grains and pearlite colonies is found, instead, they distribute randomly with smaller average sizes. In such a case, nucleation occurs at low temperature. As the nucleation of ferrite occurs with high undercooling degree, more sites other than those causing alignment are available and thus the final randomly distributed microstructure is obtain.

Tempering Behaviors in High Magnetic Field

Magnetic field shows strong influence on the morphology of cementite when tempering is performed at high temperature (600°C and 650°C for 1 hour). It obviously prevents the directional growth of cementite along martensite plate boundaries and inner twin boundaries. The effect has been identified as to be due to the increased interfacial energy by magnetic field because of the magnetization difference between ferrite and cementite. In addition, the magnetostriction difference between the two phases can also result in the increase of strain energy. So the directional growth that enlarges the interfacial area and raises magnetostrictive strain energy is energetically impeded by the magnetic field. Thus the particle like cementite is obtained in the magnetic field. This indicates that magnetic field has a strong spheroidization effect on cementite. Based on this experimental investigation and theoretical analysis, a new influential factor has been proposed.

Magnetic field also has a retardation effect on recovery of the as-quenched matrix as was found in the deformed steels. As the magnetic field induced magnetic ordering may lower the mobility of the grain boundaries and the domain walls may act as barriers to grain boundary migration, the recovery process may be retarded. However, no <001> texture component along the direction of the magnetic field is detected in the 'distortion-free' regions as was found in the deformed steels. Instead, the crystallographic orientation distributions of the 'distortion-free' and the 'distorted' regions obtained with the magnetic field show obvious similarities. This indicates that although there exists magnetization anisotropy in different crystallographic directions, the magnetic free energy difference resulted from magnetization difference between different directions is not high enough to make those whose easy magnetization direction is parallel to the magnetic field direction to form and grow. In such a case, the driving force of the formation of the 'distortion-free' is mainly from the lattice distortion caused by the supersaturation of carbon atoms in the matrix.

Magnetic field can strongly affect the precipitation process of transition carbides during low temperature tempering. When tempered at 200°C for 1 hour without field, the usual orthorhombic η-Fe_2C carbides having an orientation relationship of $(110)\alpha''//(200)\eta$ and $[1\bar{1}\bar{3}]\alpha''//[0\bar{2}0]\eta$ are precipitated. However, when tempered under the same thermal conditions with a 14-Tesla field, a relatively high temperature carbide of monoclinic χ-Fe_5C_2 is precipitated with an orientation relationship of $(01\bar{1})\alpha''//(021)\chi$ and $[1\bar{3}\bar{3}]\alpha''//[5\bar{3}6]\chi$. The reason for this phenomenon is that χ-Fe_5C_2 has a higher magnetic moment compared with that of the η-Fe_2C, therefore its Gibbs free energy drops lower than that of η- Fe_2C under magnetic field and then it precipitates before η-Fe_2C. Under an increased driving force by magnetic field, the carbides are distributed more densely with smaller size. As a consequence, the toughness of the material is improved by 9% and no obvious drop of strengths or hardness is observed.

The investigation of the effects of the magnetic field on different diffusion-controlled solid phase transformations contributes to the establishment of the experimental and theoretical foundation for and development of the new EPM (Electromagnetic Processing of Materials) research.

Perspectives

So far, magnetic technique has been applied to many areas of materials science. Plenty of experimental phenomena of theoretical value and practical prospect have been explored. As a young science, it shows powerful impetus for development. But we should also clearly be aware that the application of magnetic field, especially high magnetic field, in materials science is still in its early stage. More physical phenomena are waiting to be revealed. Among existing results, many chemical and physical influential mechanisms with theoretical depths need to be worked out. In addition, the incomplete magnetic data of uncommon ferro-materials or even conventional ferro-materials, such as magnetic moment, *Tc* temperature, magnetic anisotropy, magnetostriction and their temperature variations, considerably hinder further development in this area. Therefore, future tendencies of application of magnetic field in materials science may be orientated in following directions:

1) Further probe new phenomena and new regulations in materials treatments and processing under high magnetic field in the existing areas, and then establish new theories and new techniques under magnetic field.

2) As more than 10 Teslas or even higher magnetic field is available owing to the progress in superconducting technique, influence of magnetic field is enhanced to obviously observable level in transformations happening in non-ferromagnetic materials. So research in solid state phase transformation will be extended from the conventional ferromagnetic materials to other non-ferromagnetic metallic or non-metallic materials. Meanwhile, more types of transformations other than martensitic, ferritic and bainitic transformations will be included.
3) To investigate effect of different types of magnetic field, such as static, alternative, pulsed field and probe the possible coupling between those types or changing from one type to another within one material treatment process to find new effects and phenomena.
4) To conduct in situ observation and physical properties measurement under field.
5) Setup a complete database on magnetic properties concerning various crystals and compounds through systematical measurement under high magnetic field. Establish a new high-field magnetism theory system that is more accurate and applicable to materials science research.
6) The existing research results will in turn drive the high magnetic generating equipment to be developed towards the direction of larger caliber, larger static area and more power.
7) To transfer existing experimental or theoretical results to production.

Appendix

SEM – X-ray Energy Dispersion Spectrometry (EDS)

The EDS chemical analysis has been performed with a LEICA 5440 SEM equipped with PGT (Princeton Gamma-Tech Inc.) to obtain the distribution homogeneity of Cr, Mo, Si, Mn and Fe in the hot-rolled 42CrMo. The SPIRIT γ system from PGT was used. The sample was cut from a hot-rolled rod along the rolling direction as shown in Fig. 1 and prepared by electrolytic polishing with 8% perchloric acid in ethanol at -10°C. The energy dispersion of the X-ray spectra of the above elements was obtained under 20kV accelerating voltage and 1 nA beam current. The detector dead time was between 20 to 30% and the acquisition time was 218 seconds. The quantitative spectrum analysis was achieved through the standard routines available in the PGT software. The X-ray images of Cr, Mo, Si, Mn and Fe in the material are shown in Fig. 2. It is seen that all the elements are distributed homogeneously within the analyzed sample section, which indicates that the bulk distribution of the elements are homogeneous. No segregation with respect to the hot-rolling direction is found for all these elements.

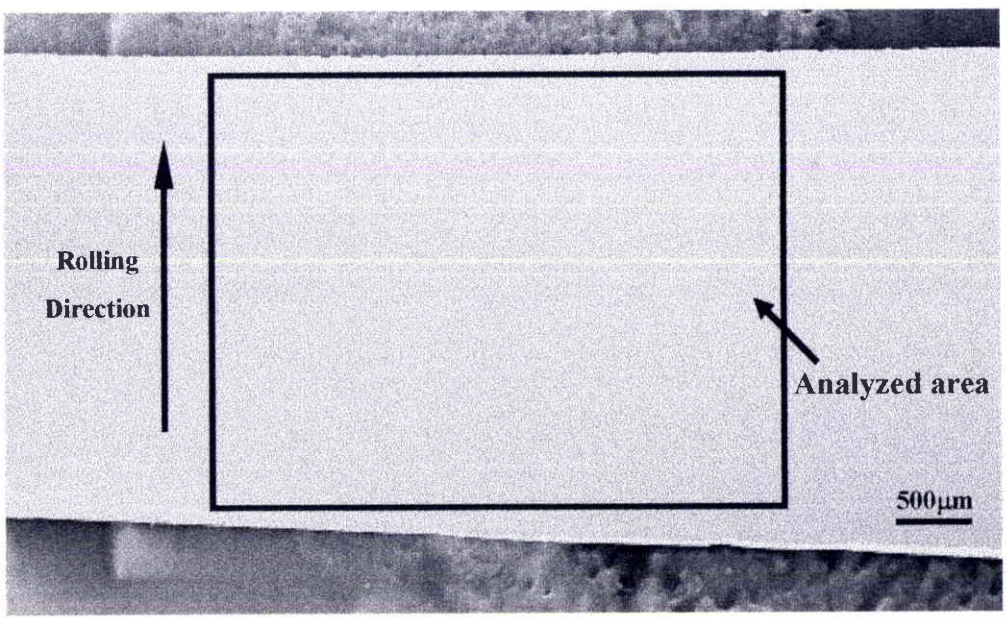

Figure 1 Hot-rolled 42CrMo sample: area analyzed by EDS

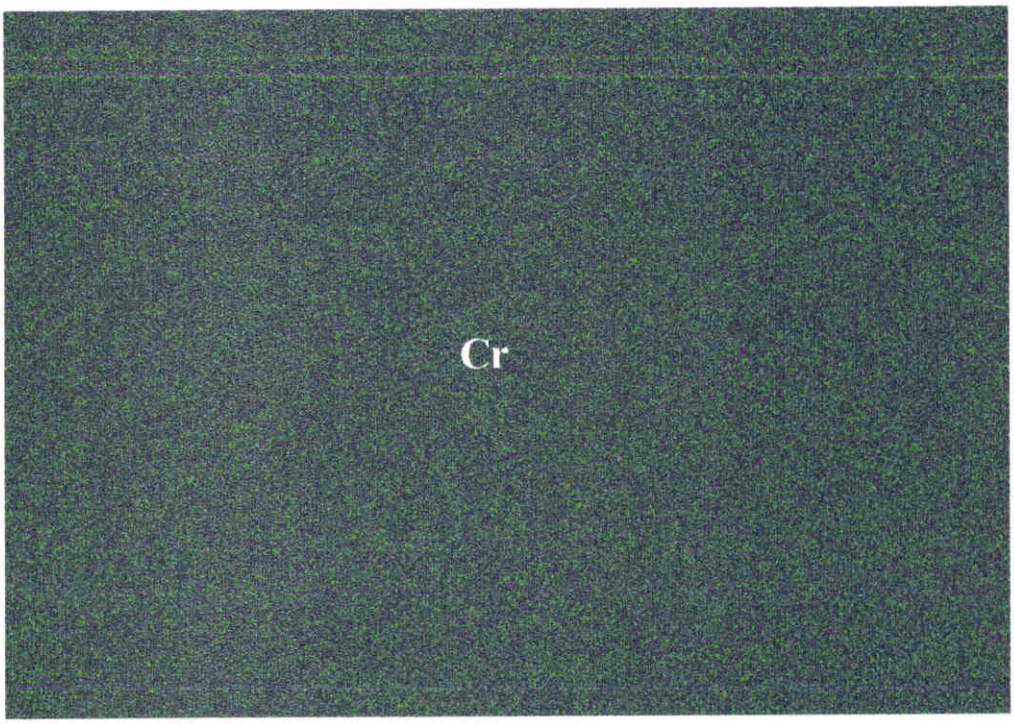
Cr

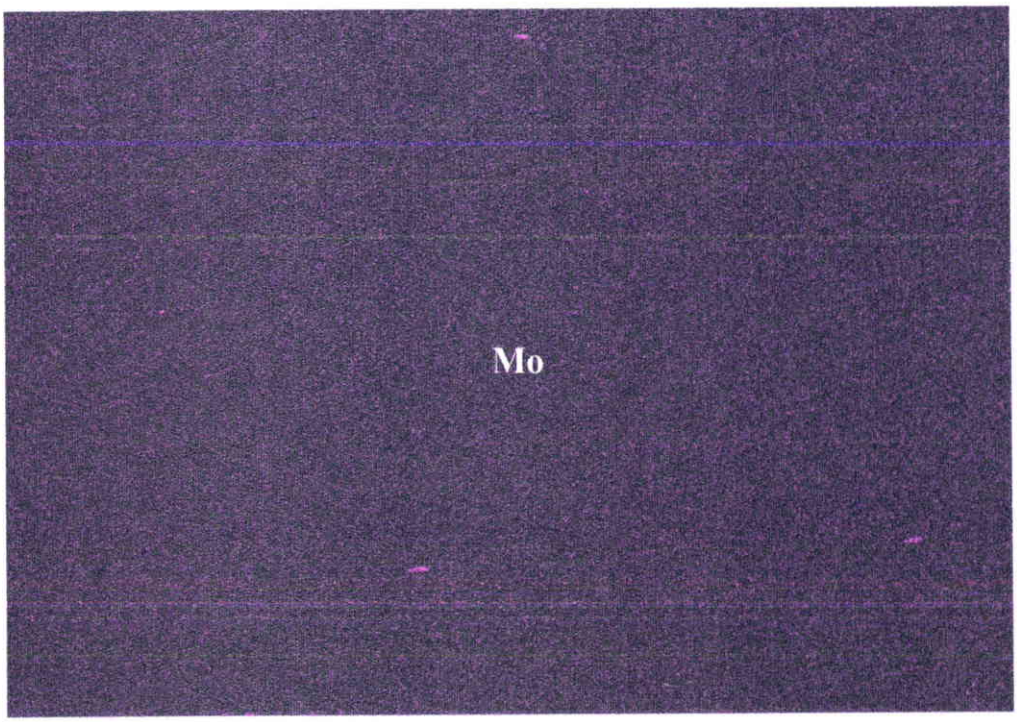
Mo

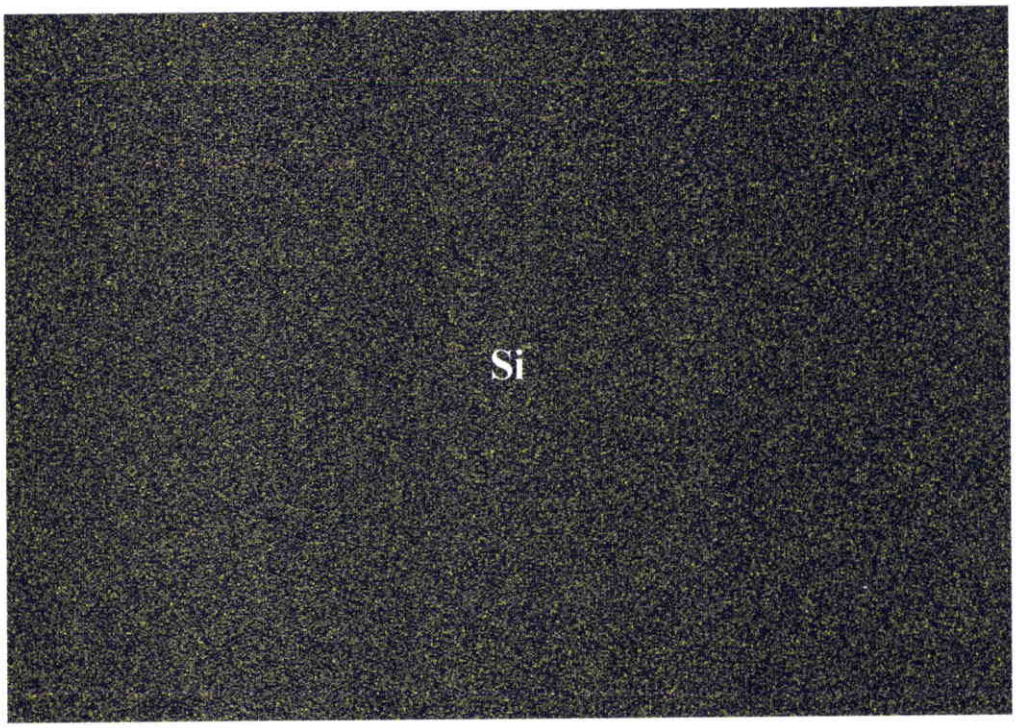
Si

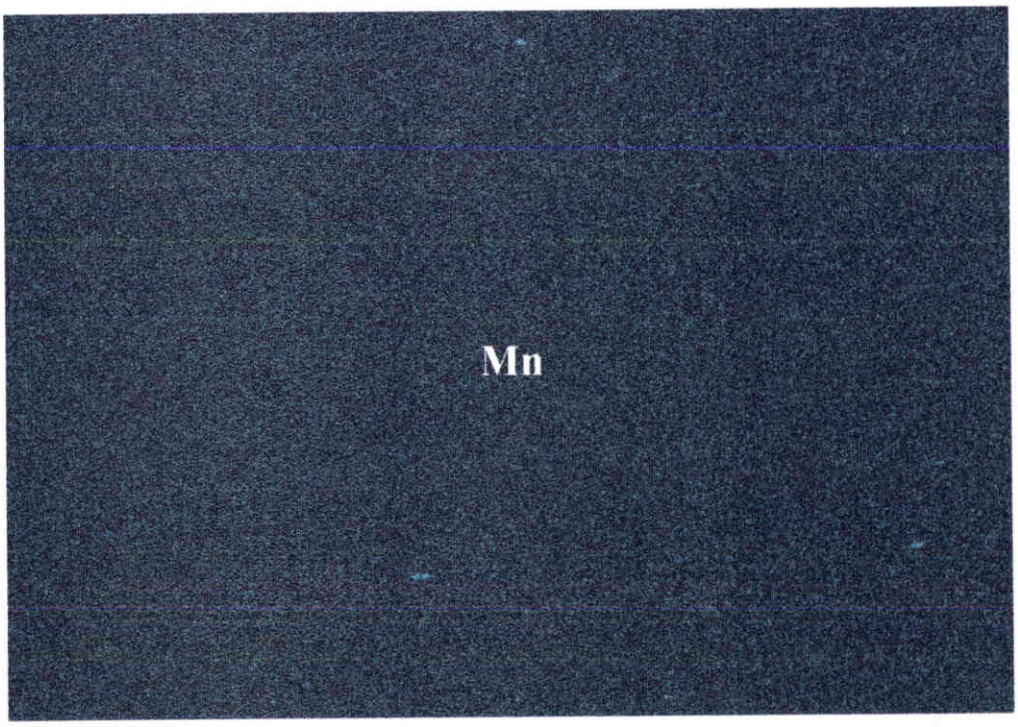
Mn

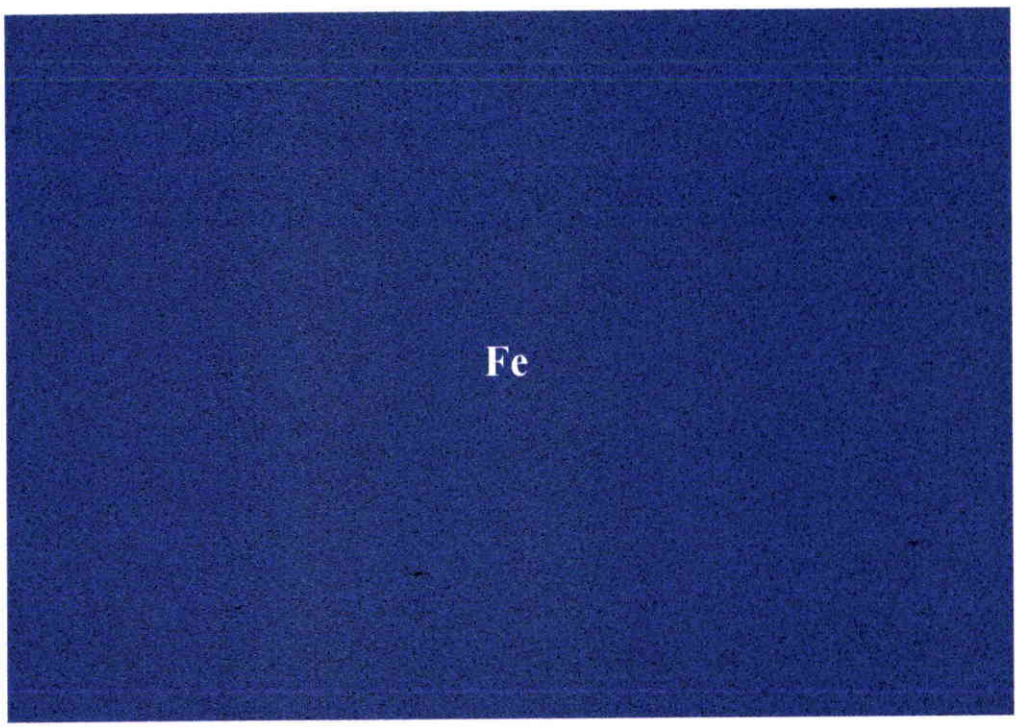

Figure 2 The X-ray images of Cr, Mo, Si, Mn and Fe (the hot-rolling direction is vertical in the pictures)